A NONLINEAR DYNAMIC ANALYSIS OF THE TRAFFIC SIGNAL CABLE SYSTEM

By

ADEOLA KEHINDE ADEDIRAN

A DISSERTATION PRESENTED TO THE GRADUATE SCHOOL
OF THE UNIVERSITY OF FLORIDA IN PARTIAL FULFILLMENT
OF THE REQUIREMENTS FOR THE DEGREE OF
DOCTOR OF PHILOSOPHY

UNIVERSITY OF FLORIDA

1997

To him who is, and who was and is to come the Almighty.

"For I know the plans I have for you," declares the Lord, "plans to prosper you and not to harm you, plans to give hope and a future."

Jeremiah 29:11

ACKNOWLEDGMENTS

The author would like to express profound gratitude to Dr. Marc Hoit and Dr. Ronald Cook for their unwavering support throughout the length of this doctoral program. Their affable personalities maintained an invaluable open door policy to students that has been most beneficial to this author. Special thanks also go to Dr. Fernando Fagundo, Dr. John Lybas and Dr. James Hobert for their various contributions to this dissertation and their professional guidance. It has indeed been an honor to have worked with such a distinguished caliber of lecturers. Other people that have proven to be a tremendous inspiration and support throughout this dissertation include Dr. Duane Ellifritt for, among other things, helping to obtain some needed reference articles; Petros Christou, for his help with programming; Dr. Glagola for all the friendly advice and Mrs. Clara Osinulu for the idea and encouragement to go for a doctorate degree.

The author will also like to thank fellow graduate students for the moral support, the Engineering Minority office and the American Association of University Women for financial aid at various times in the course of this doctoral program.

Finally and more important, the author would like to express gratitude to God, the author's mother, Adenihun, sisters, Adeoti and Bolaji and brother, Bayo for all their loving support.

TABLE OF CONTENTS

ACKNOWLEDGEMENT iii

LIST OF FIGURES vii

LIST OF TABLES ix

ABSTRACT xi

CHAPTERS

1. INTRODUCTION 1
    Problem Definition 1
        The Structure 1
        Theory 3
        The Computer Program 6
    Overview 6
        Content 7
        Scope 8

2. LITERATURE BACKGROUND 10
    Introduction 10
    Fundamentals of Cable Analysis 10
    Cable Dynamics 18
        Closed Form Solutions 19
    Finite Element Method 22
    Formulation of Element Properites 23
        Beam Properties 23
        Truss Element Properties 27
        Cable Element Properties 29
        Connector Element 36
        Transformation Matrix 46
        Damping Matrix 50
    Dynamic Solution Methods 53

Explicit Methods 54
Implicit Methods 55
Newmark Beta Method 56

3. THEORETICAL DEVELOPMENT 59
Introduction 59
Two Node Non-linear Cable Element 61
Equation of Motion 73
Modified Newmark Beta Method 77
Modified Newton - Raphson 81
Solution Algorithm 86
Solution Flowchart 89

4. LOADING 91
Introduction 91
Variable Area Wind Load 92
Variable Velocity Dynamic Wind Load 95
Autoregressive Filters 103
Test Data 107

5. PROGRAM VERIFICATION FOR STATIC LOADS 113
Static Problem Definition 113
Single Cable Structure Example 114
Static Test System Configuration 116
Loading Sequence of Tests Performed 120
Test Results and Predicted Values 123
Discussion of Results 130

6. PROGRAM VERIFICATION FOR DYNAMIC LOADS 144
The Structure's Configuration 144
Coordinates of Wind Load Test System 146
Wind Test Set-up 147
Description of Wind Load Test 148
Comparison of Results 149
Test Data 150
Wind Load Modeling 153

7. CONCLUSION 156
Summary 156

Review of Analysis Method Developed 157
Verification of Analysis Method 159
Advantages and Disadvantages of Solution Method 159
Recommendations for Further Research 160

APPENDICES

A. CABLE ELEMENT DERIVATION 162

B. USER'S MANUAL FOR DYNASS 179

LIST OF REFERENCES 221

BIOGRAPHICAL SKETCH 225

LIST OF FIGURES

Figure page

1.1 Traffic Signal System 2

1.2 Static load model 4

1.3 Mean and time varying components of wind Speed 5

2.1 Cartesian Coordinate 11

2.2 Displacement of a cable segment 12

2.3 Shape of cable due to self wt.. 14

2.4 Notations for Eqn. 2-12 21

2.5 Element degrees of freedom for a beam element 24

2.6 Degrees of freedom for a truss element 27

2.7 Truss element showing direction cosines 28

2.8 Straight nonlinear truss element used for cables 30

2.9 Deformed length due to displacements 31

2.10 Joint displacement and corresponding end forces 37

2.11 Relative deformation and associated forces 38

2.12 Rigid body and natural modes for large displacement beams 39

2.13 Rigid body rotations 41

2.14 Relative nodal rotations 43

2.15 Euler angles for transformation 48

3.1 Cable Element 61

3.2 Newton - Raphson Iteration 82

3.3 Flowchart of solution algorithm 90

4.1 Resolved wind load on signals 92

4.2 Lift and Drag coefficients 94

Figure page
4.3 Distribution of sample generated 98
4.4 Spectral density of fluctuating part of wind 101
4.5 Numerical filteration process 105
4.6 Wind speed generated using the spectral density function in Eqn. 4-10 . . 106
4.7 Wind load test systems with final cable tensions 108
4.8 Spectral Density (All wind speed ranges) 109
4.9 Spectral Density (Low wind speeds). 110
4.10 Spectral Density (Medium wind speeds). 111
4.11 Spectral Density (High wind speeds). 112
5.1 Single Cable Problem 114
5.2 Static Load Test System - Dimensions and Node Numbers 118
5.3 Cable tensions - Static Test # 1 133
5.4 Cable tensions - Static Test # 2 135
5.5 Cable tensions - Static Test # 3 137
5.6 Dynamic Structural Response at Catenary Node 6 (Test 1). 141
5.7 Dynamic Structural Response at Catenary Node 6 (Test 2). 142
5.8 Dynamic Structural Response at Catenary Node 6 (Test 3). 143
6.1 Wind Load Test System Dimension and Node Numbering 145

LIST OF TABLES

Table page

5-1 Displacement Comparison for Suspended Cable 115

5-2 Stress Comparison for Suspended Cable 115

5-3 Section Properties for Members shown in Fig. 5.2 117

5-4 Dimensions and node coordinate for Fig. 5.2 119

5-5 Loading Sequence for test # 1 120

5-6 Loading Sequence for test # 2 121

5-7 Loading Sequence for test # 3 122

5-8 Catenary Cable Results Comparison for Test # 1 124

5-9 Messenger Cable Results Comparison for Test # 1 125

5-10 Catenary Cable Results Comparison for Test # 2 126

5-11 Messenger Cable Results Comparison for Test # 2 127

5-12 Catenary Cable Results Comparison for Test # 3 128

5-13 Messenger Cable Results Comparison for Test # 3 129

5-14 Test 1 - Cable Tensions 132

5-15 Test 2 - Cable Tensions 134

5-16 Test 3 - Cable Tensions 136

5-17 Displacement Comparisons for Test 1 138

5-18 Displacement Comparisons for Test 2 139

5-19 Displacement Comparisons for Test 3 140

6-1 Dimensions and node coordinates for Fig. 6.1 146

6-2 Section Properties for Members shown in Fig 6.1 148
6-3 Wind Data for Low Wind Speed Test 150
6-4 Wind Data for MediumWind Speed Test 151
6-5 Wind Data for High Wind Speed Test 152
6-6 Wind Speeds and Resulting Drag Forces used in Dynamic Analysis. 153
6-7 Cable Tensions for Wind Load Test # 1 154

Abstract of Dissertation Presented to the Graduate School
of the University of Florida in Partial Fulfillment of the
Requirements for the Degree of Doctor of Philosophy

A NONLINEAR DYNAMIC ANALYSIS OF THE TRAFFIC SIGNAL CABLE SYSTEM

By

ADEOLA KEHINDE ADEDIRAN

May 1997

Chairperson: Marc I. Hoit
Cochairperson: Ronald A. Cook
Major Department: Civil Engineering Department

Finite element analysis of linear structures is an increasingly popular tool of choice for analysis by engineers. Only recently has this tool been applied to the case of nonlinear cable structures with a sufficient degree of veritable accuracy. Work in this dissertation provides a finite element approach to the analysis of cable structures with verification of the approach done for a traffic signal cable structure. There has been a preponderance of work done on the dynamic analysis of single cables and cable networks but very little is known about dynamic analysis of non-grid-like cable elements in conjunction with other elements such as beams and trusses. The approach of analysis presented in this dissertation provides a valuable bridge in available theories by creating a program that dynamically analyzes a cable in context of other types of elements also present within the structure. Using the principle of virtual work, the cable element developed in this dissertation is based upon a total Lagrangian formulation. The cable element models geometric nonlinear capability. Also modeled in the program developed is a nonlinear loading capability. A realistic wind load generation was accomplished by the use of auto-regressive numerical filters. With a complete finite element model sufficiently exhibiting the elastic and kinematic properties of the true structure, dynamic analysis was accomplished by numerical integration of the equation of motion. An incremental form of the general equation of motion is used because of a piecewise linear assumption. The numerical integration scheme presented in this dissertation is the Newmark's Beta method. The Newmark's Beta method reduces the equation of motion to a set of nonlinear algebraic equations. These equations are then solved using a modified Newton-Raphson. The finite element approach presented in this dissertation is programmed into a software, DYNASS. Verification of the program DYNASS and subsequently the solution approach is done by comparing predictions from DYNASS to test results obtained from recent traffic signal experiments performed at the Civil Engineering Department, University of Florida.

CHAPTER 1
INTRODUCTION

Problem Definition

The use of cables as load-carrying elements is common for structures such as bridges, cable reinforced membrane roofs, traffic signal systems, spatial cable nets and mooring lines. The set of forces seen in each cable application is different but there is a common trend in the behavior of these structural systems. This behavior is nonlinear. One source of nonlinearity is the large displacement the cables undergo. This type of nonlinear behavior is known as geometric nonlinearity. Several theories have been proposed to handle this problem. One such theory is presented in this report.

The Structure

The structure investigated here is the traffic signal system. The choice of this type of cable stayed structure was a result of the recent work done for the Florida Department of Transportation. The Civil Engineering Department at the

University of Florida developed the software program, ATLAS, to perform a static analysis of a two-point connection traffic signal system as shown in Fig. 1.1. The restrictions encountered during developing this program spurred the need for another analysis approach. The typical system considered consists of a catenary cable (slack cable configuration), a messenger cable (taut cable configuration), the signal heads and signs (points of dead and wind load application), and the prestressed concrete poles (as the support system).

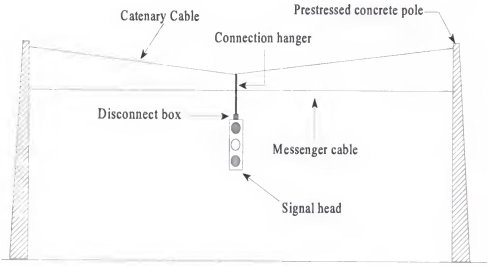

Fig. 1.1 Traffic Signal System

The traffic signal system considered includes that shown in Fig. 1.1 but is not limited to the two-point connection traffic signal system shown. The method presented in this research is capable of handling virtually any system of cables and frame elements, for example, the one-point connection traffic signal system and the suspended box system.

The Theory

The approach presented here uses the theories of structural dynamics to model the behavior of cables subjected to both dynamic wind loads and static loads. The static load case can be considered a special case of the general dynamic model. The static load is modeled as a constant load with duration equal to the full time of analysis. The structural response often of interest in the static load case is the damped out response, i.e. the stresses, moments, forces and deflections at *die-down.* For this response the initial rate of application of load is inconsequential. It is, however, good practice to maintain a slow ascent to full load in order to minimize impact effects of the load and to obtain a dynamic response more reflective of a stationary load.

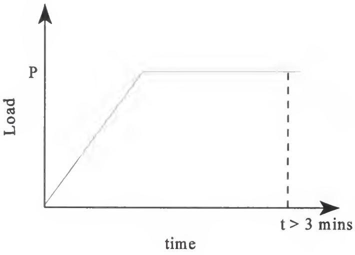

Fig. 1.2 - Static load model

The wind load is modeled as both static and dynamic. The equivalent static wind load as determined by AASHTO (American Association of State Highway Officials, "*Standard Specifications for Structural Supports for Highway Signs, Luminaries and Traffic signals*") is applied as a horizontal force (called the drag force) and a vertical force (called the lift force). An aspect of nonlinear behavior of traffic signal cable is the nonlinear wind loading. The research work presented provides a dynamic wind model comprising a steady wind pressure and a variable wind component. The variable wind component models wind gust effects. A wind gust is a short duration wind turbulence often characterized by its frequency content and its duration. Fig. 1.3 shows a typical wind gust representation.

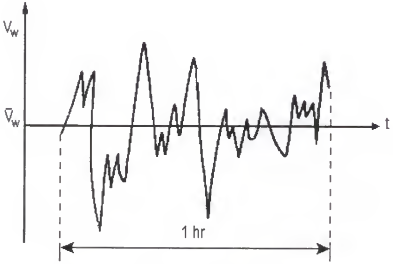

Fig. 1.3 - Mean and time varying components of wind speed

The dynamic theory presented uses geometric and time discretization. The geometric discretization or discrete element technique employed is the finite element method. Numerical integration is used in the solution of the equations of motion in the discrete time domain. Generally a nonlinear response analysis involves a significant amount of computation as it was in this case. Consequently, a computer program was written.

The Computer Program

The resulting program is called DYNASS. This program performs a nonlinear dynamic analysis of the traffic signal cable system. This program is written in Fortran with some wind generation routines in C. The results of this program are compared with results from other programs where possible and with test results from full size traffic signal system tests.

Overview

Each chapter in this report discusses topics or themes built upon in subsequent chapters. Topics discussed start from the theory proposed to the program written, to the comparison of the results from the program with test results and finally to the typical applications and conclusion. Figures and formulas are numbered consecutively throughout each chapter.

Content

Chapter two presents a literature background. This includes an overview of existing work done on this topic and an explanation of the fundamentals of structural dynamic theories and cable analysis theories.

Chapter three contains a detailed presentation of the theories and methods developed in this research. These include the various assumptions made and the equations derived. This chapter is essentially subdivided into two parts. The first part is the theoretical development just mentioned, and the second part discusses the algorithm used in the program, DYNASS.

Chapters four discusses the wind load models developed plus a general description of the other loads on the traffic signal system. There are two wind models formulated, the variable area wind load and the variable velocity wind load. Both models are discussed in some detail in chapter four. Finally, chapter four presents a brief discussion of the wind load data obtained from dynamic experiments performed. These experiments were conducted previously for a Florida Department of Transportation sponsored research.

Chapter five and six present comparisons of the results from DYNASS to other software, where available, and to test data obtained from experiments done. Chapter five compares results for static load cases only and chapter six deals with the comparison of results for dynamic wind load cases. Each chapter is concluded with a discussion of strengths and limitations of either the theory proposed and/or the program developed, for each load case.

The final chapter, chapter seven, deals with conclusions observed from the research and recommendations. Areas needing further research are also identified and noted.

Also included are Appendices A and B. Appendix A shows a detailed derivation of the 2-node cable element developed in this research. Appendix B gives a user's manual of the computer program developed. In appendix B, defaults assumed in the program are explained and for portions of the program not developed by the author, references are provided.

Scope

The scope of the research presented is limited by the inherent assumptions made in the cable analysis. The assumptions made, common to other types of cable analysis, are as follows:

- The cables are perfectly flexible and possess no bending stiffness, only axial stiffness.
- Cable materials are of hookean materials. Ferrous materials are commonly used for cables.
- Only small strains are involved, i.e. no yielding of cables ever reached.

By the nature of the type of structure investigated (traffic signal systems), the loads are essentially predefined. For this research, loads examined are restricted to the dead load from the weight of the signal heads and signs, and wind loads. Other assumptions discussed in chapter four further define the application of the theory and subsequently the program.

CHAPTER 2

LITERATURE BACKGROUND

Introduction

Several authors have dealt with the problem of the geometric nonlinearity of cables and have provided some solutions to the problem. A brief summary of pertinent results of their work is given in this chapter as they provide a foundation to the author's work. Also presented is a general theoretical background of cable analysis and dynamic analysis. The work covered here reflects only the solutions provided for cable dynamics. It is, however, congruent to consider the static cable problem as a special case of the cable dynamics problem hence extending these solutions to cover static cable analysis. Other methods strictly for static solutions include the force density method [1].

Fundamentals of Cable Analysis

Consider a uniform cable which hangs in static equilibrium in a vertical plane suspended between two supports. The forces acting on a differential element of the cable is dependent of the profile assumed by the cable at-rest position and the cable final deformed position. Let any point on this cable be described in the 3-D Cartesian coordinates shown in Fig. 2.1.

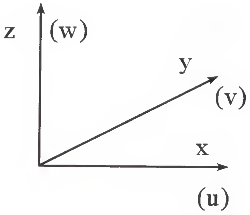

Fig. 2.1 Cartesian Coordinate

Let the cable ordinate after deformation be denoted $\bar{x}$, $\bar{y}$, $\bar{z}$ as shown in Fig. 2.2.

$\bar{x} = x + u$

$\bar{y} = y + v$

$\bar{z} = z + w$

The cable segment shown in Fig. 2.2 below can be described by a vector along the chord joining both ends of the cable segment.

$$\vec{L} = \frac{x_j - x_i}{ds} i + \frac{y_j - y_i}{ds} j + \frac{z_j - z_i}{ds} k$$

The terms $\frac{x_j - x_i}{ds}$ $\frac{y_j - y_i}{ds}$ and $\frac{z_j - z_i}{ds}$ are referred to as the direction cosines for the element.

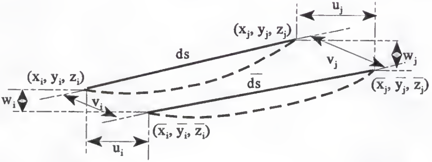

Fig. 2.2 Displacement of a cable segment

The relationship between the nodal forces and displacements at any point along the cable relative to the next is defined as follows,

$$u_j = u_i + \frac{\partial u}{\partial s} ds \qquad (2\text{-}1)$$

This says that the displacement at node *j* is the sum of the displacement at node *i* and the differential strain in the cable multiplied by the arc length of cable. Similarly for the displacements in the y and z direction, the relationship is

$$v_j = v_i + \frac{\partial v}{\partial s} ds \qquad (2\text{-}2)$$

$$w_j = w_i + \frac{\partial w}{\partial s} ds \qquad (2\text{-}3)$$

The above displacement-strain relationship is referred to as the linear strain - displacement relationship. The relationship between the forces at node *i* and *j* both along the cable can similarly be summarized as follows,

$$T_j = T_i + dT \qquad (2\text{-}4a)$$

$$F_{xj} = F_{xi} + dF_x \qquad (2\text{-}4b)$$

$$F_{yj} = F_{yi} + dF_y \qquad (2\text{-}4c)$$

$$F_{zj} = F_{zi} + dF_z \qquad (2\text{-}4d)$$

For static analysis the forces acting on a finite length of a cable are

T = Cable tension

F_x, F_y, F_z= equivalent nodal loads due to for example dead weight of cable and/or cladding or applied nodal load. In the "unloaded configuration" otherwise referred to as the *null* state, the applied load is taken as zero.

The tension in the undeformed slack cable is computed from the cable profile. The basic shape of a slack cable subjected to its own weight is a catenary profile. However, if the slope of the cable is everywhere small, the profile adopted by the cable can be accurately described by a parabola. It is advantageous as a means of simplification to describe cable shape in two dimensions. Here the x-z plane is used.

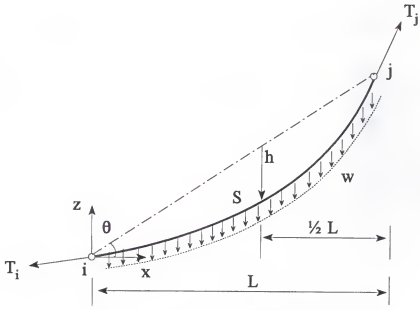

Fig. 2.3 Shape of cable due to self wt.

According to Ref. [2] the parabolic profile is given by Eqn. 2-5.

$$z(x) = x\tan(\theta) - \frac{4hx}{L^2}(L - x) \tag{2-5}$$

The tension in the cable at any point x along the span of the cable is as given in Eqn. 2-6.

$$T(x) = \frac{wL^2}{8h}\left[1 + \left(\tan(\theta) - \frac{4h}{L} + \frac{8hx}{L^2}\right)^2\right]^{1/2} \tag{2-6}$$

S = length of the cable along the sag (Fig 2.3).

z (x) = vertical distance of any point along the cable relative the starting node.

tan (θ) = slope of the chord joining both ends of the cable.

h = distance from the chord at mid-span of the cable. This is used to define cable sag.

w = weight of the cable per horizontal distance.

L = span of the cable.

T (x) = tension in the cable (null state) at any point along the cable.

$sag = h/L$

Comparing the above profile with the catenary profile in Ref. [3], the following equations form the catenary profile equivalent of Eqns 2-5 and 2-6 above. Note that the catenary shape is more difficult to define and indeed is only defined by an iterative process of trial and error.

$$z(x) = \frac{H}{w}\left[\cosh(\varepsilon) - \cosh\left(2\phi\frac{x}{L} - \varepsilon\right)\right] \tag{2-7}$$

$$\varepsilon = \sinh^{-1}\left[\frac{\phi\tan(\theta)}{\sinh(\phi)}\right] + \phi \tag{2-8}$$

$$\phi = \frac{wL}{2H} \tag{2-9}$$

$$T(x) = H\sqrt{1 + \sinh\left[\sinh\left(\frac{\frac{wL}{2H}\tan(\theta)}{\sinh\left(\frac{wL}{2H}\right)}\right) + \frac{wL}{2H} - \frac{wx}{H}\right]^2} \tag{2-10}$$

H = horizontal component of the tension in the cable. This is invariant along the cable.

The other variables retain their definitions given on previous page.

There are two unknowns in the above equations, z(x) and H. The value of H is often obtained by approximately setting z(x) to sag × span (L) at x = L/2. The rest of the configuration is obtained by using the H computed. It is apparent that it is more convenient to use the parabolic approximation. The error introduced by the approximation is of the order of 1% - 2% for slack cables with small sag. For example, if the tension at the first third point and the z coordinate were required of the cable with the following properties:

sag = 10%, w = 0.12 plf, L = 3500 ft, take tan(θ) as zero i.e. both cable ends are on the same level. The results will be the following.

Assuming the cable shape is parabolic -

z (x = ⅓L) = 311.111 ft. And T (x = ⅓L) = 529.646 lbf.

Using the catenary equations above the results -

z (x = ⅓L) = 311.557 ft. And T (x = ⅓L) = 536.839 lbf.

An error of just 1.4%. For the remainder of this dissertation, the parabolic (null) profile will serve as the reference state for the slack catenary cable. The null state shape is important in the derivation of the stiffness matrix of the cables as well as in determining the initial tensions in the cable. Any assumption about this initial configuration could significantly influence analysis results.

Cables, like trusses, are idealized as not having any bending stiffness (in reality they possess some bending stiffness). This introduces equation of conditions in the equilibrium analysis of cables making them inherently unstable.

In addition, they can undergo large displacements and cannot resist compression. These complexities invalidate the more conventional linear theories often based on the assumption of small displacements and unconditional stability. To solve the problem of inherent cable instability it is necessary to introduce additional resisting forces that can keep the cable in equilibrium. The problem of large displacement is best dealt with by applying the load in small enough increments as to achieve small enough displacements in each increment. Lastly, the inability of cables to sustain compression can be taken into account by solving the problem in steps and keeping track of the stresses in the cable. The cable elements are rendered inactive when in compression and active when in tension. A very logical method of solving a cable problem, therefore, is to use the theories of structural dynamics. It is advantageous to use this technique because it introduces inertia and damping forces that can be used to stabilize the cable and it provides a time step solution which allows the application of load in small increments and supplies a framework for keeping track of cable stresses.

Cable Dynamics

The solutions to the cable dynamics problem can be discussed in two major categories, closed form solutions otherwise referred to as the "exact" solution, and the finite element solutions i.e. explicit solutions such as the Euler's method, Central Difference method and Runge-Kutta method and the more common implicit methods such as the Wilson Theta method and the Newmark's Beta method.

Closed Form Solutions

Most closed form solutions, for taut cables and cables with small sag to span ratios, are based on a linear theory (i.e. small displacement theory). Irvine and Caughey [4], Uwe Starossek [5] and Veletsos and Darbre [6] have all presented semi-empirical solutions based on this linear theory. Of importance is the experimental results of Irvine and Caughey [4]. Their work revealed the observed dynamic behavior of cables with small sag subjected to free vibration. When a cable vibrates it does so in two major motions. The transverse horizontal motion and the in-plane motion. Both motions are observed to be uncoupled. The transverse motion is essentially a swinging motion as the cable rocks in and out of its at-rest plane. The in-plane motion consists of two components, the symmetric and anti-symmetric components. The anti-symmetric components consist of in-line motion similar to a wave traveling along the length of the cable and in-plane transverse motions which are unsymmetrical in-plane deflections of the cable. The symmetrical components are analogous to simple harmonic motions occurring along the cable. For small sag to span ratios (< 1:8) these components of motion constitute the modal shapes that could then be analyzed. The results of most of the aforementioned authors establish the mode shapes of cable vibration and their corresponding frequencies. The limitation of the linear theory is that for catenary cables with large sag the theory ceases to be accurate The theory also becomes problematic when the cable is considered as part of a structure and not standing alone.

The equation of motion from linear theory is given in Eqn. 2-12.

From Uwe Starossek [6],

$$H = \frac{m\ g\ l^2}{8\ f} \tag{2-11}$$

H = Horizontal component of the cable tension

m = mass of the cable per unit length

g = acceleration due to gravity

l = cable span

f = sag of the cable

The in-plane equation of motion is for sag ≤ 1/20;

$$H\frac{\partial^2 w}{\partial x^2} + h_\tau \frac{d^2 z}{d x} = m\frac{\partial^2 w}{\partial t^2} + c\frac{\partial w}{\partial t} \tag{2-12}$$

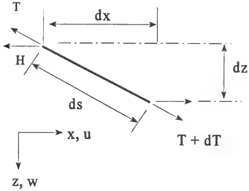

Fig. 2.4 Notations For Eqn. 2-12 for a cable segment

c = damping force per unit length

u, w = displacement in the x, z directions respectively.

$$h_\tau = \tau \frac{dx}{ds}$$

τ = dynamic part of the total cable tension. This is invariant along the cable.

An alternative to the exact solution is the discrete idealization of the continuum. There are two major techniques of discrete idealization of a structural continuum, the lumped mass method and the finite element method. The finite element method is more commonly used because, among other reasons, the numerical modeling has a clearer physical interpretation. With the finite method, the dynamic solution for cable vibrations are either explicit solutions or implicit solutions.

Finite Element Method

Due to the nonlinear behavior of cable systems, direct superposition of loads and displacements as would be necessary with the typical modal superposition analysis is not strictly valid. However, according to Leonard [7] and others, if an incremental load approach is adopted and the load increment is small enough, then within each step it is reasonable to assume linearity of the superposed dynamic response. An additional condition for a linearized solution is that the prestressed cable configuration prior to load application be known and that the cable system possess a significant stiffness. Using finite element analysis the traffic signal system is idealized as follows; the strain poles as beam elements, the cables as nonlinear cable elements and the connectors as large displacement beam elements. A common practice is the use of steel bracing for the poles. These braces could be modeled as linear truss elements.

Formulation of Element Properties

The properties of the linear beam elements are given below, their derivations can be found in most structural analysis books. The typical geometrically nonlinear truss element often used for cable analysis is also given in this chapter. The cable element adopted for this dissertation, however, is derived in chapter 3.

Beam Properties

According to Ref. [8] the stiffness matrix for the 3-D beam element is given in Eqn. 2-13.

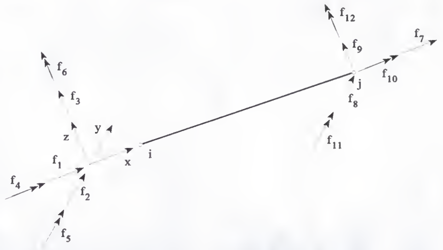

Fig. 2.5 Element degrees of freedom for a beam element.

$$[K]=\begin{bmatrix}
EA_x/l & 0 & 0 & 0 & 0 & 0 & -EA_x/l & 0 & 0 & 0 & 0 & 0 \\
0 & 12EI_3/l^3 & 0 & 0 & 0 & 6EI_3/l^2 & 0 & -12EI_3/l^3 & 0 & 0 & 0 & 6EI_3/l^2 \\
0 & 0 & 12EI_2/l^3 & 0 & -6EI_2/l^2 & 0 & 0 & 0 & -12EI_2/l^3 & 0 & -6EI_2/l^2 & 0 \\
0 & 0 & 0 & GJ/l & 0 & 0 & 0 & 0 & 0 & -GJ/l & 0 & 0 \\
0 & 0 & -6EI_2/l^2 & 0 & 4EI_2/l & 0 & 0 & 0 & 6EI_2/l^2 & 0 & 2EI_2/l & 0 \\
0 & 6EI_3/l^2 & 0 & 0 & 0 & 4EI_3/l & 0 & -6EI_3/l^2 & 0 & 0 & 0 & 2EI_3/l \\
-EA_x/l & 0 & 0 & 0 & 0 & 0 & EA_x/l & 0 & 0 & 0 & 0 & 0 \\
0 & -12EI_3/l^3 & 0 & 0 & 0 & -6EI_3/l^2 & 0 & 12EI_3/l^3 & 0 & 0 & 0 & -6EI_3/l^2 \\
0 & 0 & -12EI_2/l^3 & 0 & 6EI_2/l^2 & 0 & 0 & 0 & 12EI_2/l^3 & 0 & 6EI_2/l^2 & 0 \\
0 & 0 & 0 & -GJ/l & 0 & 0 & 0 & 0 & 0 & GJ/l & 0 & 0 \\
0 & 0 & -6EI_2/l^2 & 0 & 2EI_2/l & 0 & 0 & 0 & 6EI_2/l^2 & 0 & 4EI_2/l & 0 \\
0 & 6EI_3/l^2 & 0 & 0 & 0 & 2EI_3/l & 0 & -6EI_3/l^2 & 0 & 0 & 0 & 4EI_3/l
\end{bmatrix}$$

(2-13)

E = Elastic Modulus (Young's Modulus)

I_2 = Moment of inertia about the strong axis

I_3 = Moment of inertia about the weak axis

l = Length of the beam element

The consistent mass matrix for the above 3-D beam element is as follows [9]:

$$[M]=\frac{\rho AL}{420g}\begin{bmatrix} 140 & 0 & 0 & 0 & 0 & 0 & 70 & 0 & 0 & 0 & 0 & 0 \\ 0 & 156 & 0 & 0 & 0 & -22L & 0 & 54 & 0 & 0 & 0 & 13L \\ 0 & 0 & 156 & 0 & 22L & 0 & 0 & 0 & 54 & 0 & -13L & 0 \\ 0 & 0 & 0 & {}^{140J}\!/\!_{A} & 0 & 0 & 0 & 0 & 0 & {}^{70J}\!/\!_{A} & 0 & 0 \\ 0 & 0 & 22L & 0 & 4L^2 & 0 & 0 & 0 & 13L & 0 & -3L^2 & 0 \\ 0 & -22L & 0 & 0 & 0 & 4L^2 & 0 & -13L & 0 & 0 & 0 & -3L^2 \\ 70 & 0 & 0 & 0 & 0 & 0 & 140 & 0 & 0 & 0 & 0 & 0 \\ 0 & 54 & 0 & 0 & 0 & -13L & 0 & 156 & 0 & 0 & 0 & 22L \\ 0 & 0 & 54 & 0 & 13L & 0 & 0 & 0 & 156 & 0 & -22L & 0 \\ 0 & 0 & 0 & {}^{70J}\!/\!_{A} & 0 & 0 & 0 & 0 & 0 & {}^{140J}\!/\!_{A} & 0 & 0 \\ 0 & 0 & -13L & 0 & -3L^2 & 0 & 0 & 0 & -22L & 0 & 4L^2 & 0 \\ 0 & 13L & 0 & 0 & 0 & -3L^2 & 0 & 22L & 0 & 0 & 0 & 4L^2 \end{bmatrix} \tag{2-14}$$

J = Polar moment of inertia

A = Cross sectional area

ρ = Density of beam material (lb/ft^3)

g = Acceleration due to gravity (32.2 ft/sec^2)

Truss Element Properties

The degree of freedom for a typical truss element is shown in Fig. 2.6.

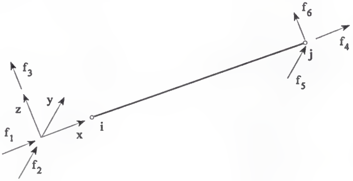

Fig. 2.6 Degrees of freedom for a truss element

The stiffness matrix for the truss is given in Eqn 2-15 [10]. This stiffness matrix is in the element local coordinate.

$$[K] = \frac{E\,A_x}{l}\begin{bmatrix} 1 & 0 & 0 & -1 & 0 & 0 \\ 0 & 0 & 0 & 0 & 0 & 0 \\ 0 & 0 & 0 & 0 & 0 & 0 \\ -1 & 0 & 0 & 1 & 0 & 0 \\ 0 & 0 & 0 & 0 & 0 & 0 \\ 0 & 0 & 0 & 0 & 0 & 0 \end{bmatrix} \qquad (2\text{-}15)$$

In the structure's global coordinate, the stiffness matrix is given in Eqn. 2-16.

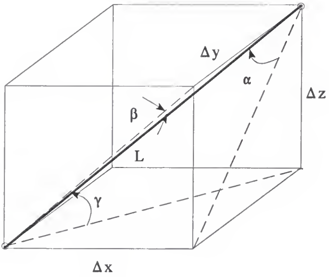

Fig. 2.7 - Truss element showing direction cosines

$$[K] = \frac{AE}{L}\begin{bmatrix} C_\alpha^2 & C_\beta C_\alpha & C_\gamma C_\alpha & -C_\alpha^2 & -C_\beta C_\alpha & -C_\gamma C_\alpha \\ C_\alpha C_\beta & C_\beta^2 & C_\gamma C_\beta & -C_\alpha C_\beta & -C_\beta^2 & -C_\gamma C_\beta \\ C_\alpha C_\gamma & C_\beta C_\gamma & C_\gamma^2 & -C_\alpha C_\gamma & -C_\beta C_\gamma & -C_\gamma^2 \\ -C_\alpha^2 & -C_\beta C_\alpha & -C_\gamma C_\alpha & C_\alpha^2 & C_\beta C_\alpha & C_\gamma C_\alpha \\ -C_\alpha C_\beta & -C_\beta^2 & -C_\gamma C_\beta & C_\alpha C_\beta & C_\beta^2 & C_\gamma C_\beta \\ -C_\alpha C_\gamma & -C_\beta C_\gamma & -C_\gamma^2 & C_\alpha C_\gamma & C_\beta C_\gamma & C_\gamma^2 \end{bmatrix} \quad (2\text{-}16)$$

$$C_\alpha = \frac{\Delta x}{L} \quad C_\beta = \frac{\Delta y}{L} \quad C_\gamma = \frac{\Delta z}{L} \tag{2-17}$$

$$L = \sqrt{(\Delta x)^2 + (\Delta y)^2 + (\Delta z)^2} \tag{2-18}$$

The mass matrix in global coordinates is also given below [9].

$$[M] = \frac{m\,l}{6}\begin{bmatrix} 2 & 0 & 0 & -1 & 0 & 0 \\ 0 & 2 & 0 & 0 & -1 & 0 \\ 0 & 0 & 2 & 0 & 0 & -1 \\ -1 & 0 & 0 & 2 & 0 & 0 \\ 0 & -1 & 0 & 0 & 2 & 0 \\ 0 & 0 & -1 & 0 & 0 & 2 \end{bmatrix} \tag{2-19}$$

m = mass per unit length for the element

l = length of the element

Cable Element Properties

A straight truss element capable of large displacement is commonly used for cables. The derivation [3] of the stiffness matrix for this element is briefly discussed here so as to be differentiated from that in chapter 3. Fig. 2.8 presents the straight element nonlinear truss in its local axis.

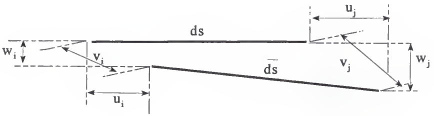

Fig. 2.8 Straight nonlinear truss element used for cables

From Eqn. 2-1, the component of horizontal displacement is,

$$u_i + \frac{\partial u}{\partial s}ds - u_i \quad = \quad \frac{\partial u}{\partial s}ds \tag{2-20}$$

Similarly, the component of displacements in the y and z directions are

$$v_i + \frac{\partial v}{\partial s}ds - v_i \quad = \quad \frac{\partial v}{\partial s}ds \tag{2-21}$$

$$w_i + \frac{\partial w}{\partial s}ds - w_i \quad = \quad \frac{\partial w}{\partial s}ds \tag{2-22}$$

The resultant axial strain along the member due to the above displacements can be computed by determining the deformed element length $\overline{ds}$. The deformed length due to displacement in the x direction is simply,

$$d\bar{s}_x = ds + \frac{\partial u}{\partial s} ds \tag{2-23}$$

The deformed length due to displacements in the y and z directions are shown in Fig. 2.9.

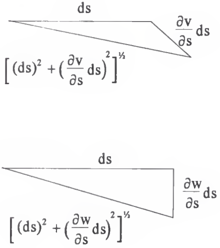
ds
$\frac{\partial v}{\partial s} ds$
$\left[(ds)^2 + \left(\frac{\partial v}{\partial s} ds \right)^2 \right]^{1/2}$
ds
$\frac{\partial w}{\partial s} ds$
$\left[(ds)^2 + \left(\frac{\partial w}{\partial s} ds \right)^2 \right]^{1/2}$

Fig. 2.9 Deformed length due to displacements

The axial strain from the above in the x, y and z directions is given in Eqns 2-24, 2-25 and 2-26.

$$\bar{\varepsilon}_x = \frac{ds + \frac{\partial u}{\partial s}ds - ds}{ds} = \frac{\partial u}{\partial s} \tag{2-24}$$

$$\bar{\varepsilon}_y = \frac{\left(ds^2 + \left(\frac{\partial v}{\partial s}ds\right)^2\right)^{1/2} - ds}{ds} = \left(1 + \left(\frac{\partial v}{\partial s}\right)^2\right)^{1/2} - 1 \tag{2-25}$$

$$\bar{\varepsilon}_z = \frac{\left(ds^2 + \left(\frac{\partial w}{\partial s}ds\right)^2\right)^{1/2} - ds}{ds} = \left(1 + \left(\frac{\partial w}{\partial s}\right)^2\right)^{1/2} - 1 \tag{2-26}$$

Applying the binomial expansion

$$\sqrt{1 + a^2} = 1 + \frac{1}{2}a^2 - \frac{1}{8}a^4 + \ldots$$

and neglecting the higher order terms Eqns 2-25 and 2-26 become

$$\bar{\varepsilon}_y = 1 + \frac{1}{2}\left(\frac{\partial v}{\partial s}\right)^2 - 1 = \frac{1}{2}\left(\frac{\partial v}{\partial s}\right)^2 \tag{2-27}$$

$$\bar{\varepsilon}_z = 1 + \frac{1}{2}\left(\frac{\partial w}{\partial s}\right)^2 - 1 = \frac{1}{2}\left(\frac{\partial w}{\partial s}\right)^2 \qquad (2\text{-}28)$$

The total axial strain in the element is the summation of the strain expressions in Eqns 2-26, 2-27 and 2-28. This summation is referred to as the large deflection strain-displacement equation.

$$\bar{\varepsilon} = \frac{\partial u}{\partial s} + \frac{1}{2}\left(\frac{\partial v}{\partial s}\right)^2 + \frac{1}{2}\left(\frac{\partial w}{\partial s}\right)^2 \qquad (2\text{-}29)$$

If the nodal displacements are known for a finite length L of the nonlinear truss element, Eqn 2-29 becomes,

$$\bar{\varepsilon} = \frac{u_j - u_i}{L} + \frac{1}{2}\left(\frac{v_j - v_i}{L}\right)^2 + \frac{1}{2}\left(\frac{w_j - w_i}{L}\right)^2 \qquad (2\text{-}30)$$

Using Castigliano’s theorem for the force-displacement relationship, the expression for the strain energy in the element is given in Eqn 2-31.

$$U = \frac{1}{2}\int T \,\Delta = \frac{AE}{2}\int \bar{\varepsilon}^2 \, ds \qquad (2\text{-}31)$$

Substituting the expression for strain and expanding the brackets we obtain

$$U = \frac{AE}{2}\int\left(\frac{\partial u}{\partial s}\right)^2 + \frac{\partial u}{\partial s}\left(\frac{\partial v}{\partial s}\right)^2 + \frac{\partial u}{\partial s}\left(\frac{\partial w}{\partial s}\right)^2 + \frac{1}{4}\left(\frac{\partial v}{\partial s}\right)^4 + \frac{1}{2}\left(\frac{\partial v}{\partial s}\right)^2\left(\frac{\partial w}{\partial s}\right)^2 + \frac{1}{4}\left(\frac{\partial w}{\partial s}\right)^4 ds$$

(2-32)

Ignoring the fourth order terms and substituting the notation used in Eqn 2-30, we obtain a new expression for U.

$$U = \frac{AE}{2}\int\left(\frac{u_j - u_i}{L}\right)^2 + \frac{u_j - u_i}{L}\left(\frac{v_j - v_i}{L}\right)^2 + \frac{u_j - u_i}{L}\left(\frac{w_j - w_i}{L}\right)^2 ds \qquad (2\text{-}33)$$

Note that,

$$T = \frac{AE}{L}\left(u_j - u_i\right) \qquad (2\text{-}34)$$

Where T is the tension force in the truss element. Solving the integral we get Eqn 2-35.

$$U = \frac{AE}{2L}\left(u_j - u_i\right)^2 + \frac{AE}{2L^2}\left(u_j - u_i\right)\left(v_j - v_i\right)^2 + \frac{AE}{2L^2}\left(u_j - u_i\right)\left(w_j - w_i\right)^2 \qquad (2\text{-}35)$$

Differentiating the Eqn 2-35 with respect to the nodal displacements gives the stiffness coefficient associated with that displacement. The expression for tension, from Eqn 2-34 above is substituted into Eqn 2-35. The assumption is made that the tension in the cable is approximately a constant.

$$\frac{\partial U}{\partial u_i} = \frac{AE}{L}\left(u_i - u_j\right) \qquad (2\text{-}36)$$

$$\frac{\partial U}{\partial v_i} = \frac{T}{L}\left(v_i - v_j\right) \qquad (2\text{-}37)$$

$$\frac{\partial U}{\partial w_i} = \frac{T}{L}\left(w_i - w_j\right) \tag{2-38}$$

$$\frac{\partial U}{\partial u_j} = \frac{AE}{L}\left(u_j - u_i\right) \tag{2-39}$$

$$\frac{\partial U}{\partial v_j} = \frac{T}{L}\left(v_j - v_i\right) \tag{2-40}$$

$$\frac{\partial U}{\partial w_j} = \frac{T}{L}\left(w_j - w_i\right) \tag{2-41}$$

In matrix form, the geometric stiffness of a nonlinear truss can be written as given in Eqn 2-42. The first matrix term below is the conventional elastic stiffness of a truss element. The second term is referred to as the geometric stiffness term. This geometric stiffness accounts only for initial cable stress and not for nonlinear strain - displacement relationship.

$$[K] = \frac{EA}{L}\begin{bmatrix} 1 & 0 & 0 & -1 & 0 & 0 \\ 0 & 0 & 0 & 0 & 0 & 0 \\ 0 & 0 & 0 & 0 & 0 & 0 \\ -1 & 0 & 0 & 1 & 0 & 0 \\ 0 & 0 & 0 & 0 & 0 & 0 \\ 0 & 0 & 0 & 0 & 0 & 0 \end{bmatrix} + \frac{T}{L}\begin{bmatrix} 0 & 0 & 0 & 0 & 0 & 0 \\ 0 & 1 & 0 & 0 & -1 & 0 \\ 0 & 0 & 1 & 0 & 0 & -1 \\ 0 & 0 & 0 & 0 & 0 & 0 \\ 0 & -1 & 0 & 0 & 1 & 0 \\ 0 & 0 & -1 & 0 & 0 & 1 \end{bmatrix}$$

(2-42)

Connector Element

The load on the traffic signal system is applied by the traffic signal heads and the traffic signs. These are attached to the system via connectors. The connectors have translational and rotational degrees of freedom. In this they are identical to the beam element discussed previously. The connectors, however, undergo large displacements. These displacements affect how the stiffness of the connector is added to the structure's overall stiffness. The connector stiffness matrix presented next is a beam element stiffness accounting for large displacements. The element presented here and adopted for this dissertation was derived by Chen and Agar [11]. The element stiffness is broken into the elastic component and the geometric component. The elastic stiffness is as given in the earlier described beam element, the geometric stiffness is set up in terms of the natural displacements (deformation) of the beam shown in Fig 2.11. The derivation of the geometric stiffness is given in detail in Ref. [11]. The derivation presented in Ref. [11] rely predominantly on work done by Bathe and Bolourchi [12]. In this dissertation, only the definition of the coefficients of the geometric stiffness and its application is described. The degrees of freedom for the large displacement beam element used as connectors is identical to that of regular beams. The resulting beam end forces corresponding to these degrees of freedom are shown in Fig. 2.10. To accurately determine the end forces another set of forces referred to as the natural forces or basic beam forces must be defined. The natural beam forces are the forces developed in the beam due to relative deformation of the beam ignoring rigid body motions. These forces are shown in Fig. 2.11.

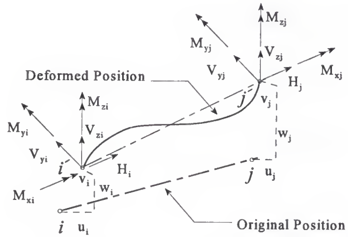

Fig. 2.10 Joint displacements and corresponding end forces

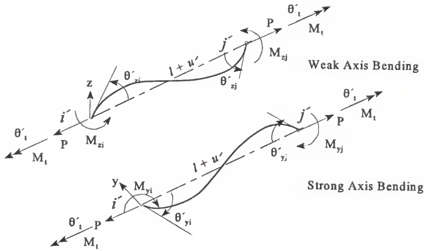

Fig. 2.11 Relative deformations and associated forces

From Fig. 2.10, the nodal degrees of freedom are,

$$\{d_n\}^T = \{u_i \ v_i \ w_i \ \theta_{xi} \ \theta_{yi} \ \theta_{zi} \ u_j \ v_j \ w_j \ \theta_{xj} \ \theta_{yj} \ \theta_{zj}\} \quad (2\text{-}43)$$

The nodal displacements in Eqn 2-43 consist of the two major components the rigid body component and the natural displacements (i.e. relative deformation) component. From Ref. [13] six rigid body modes and six natural displacement modes completely defines any displacement that may be seen in a large displacement beam. The identified modes are as given in Fig 2.12.

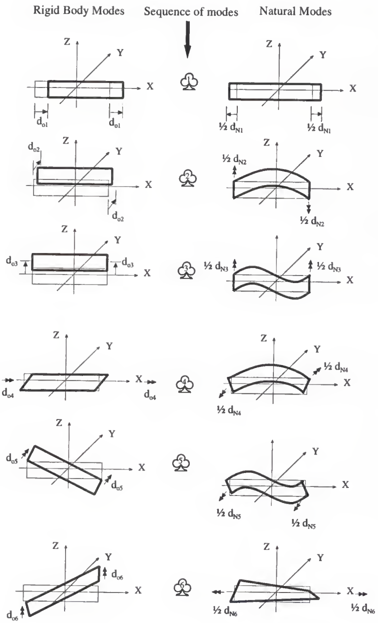

Fig. 2.12 Rigid body and natural modes for large displacement beams

From Fig. 2-12 it can be seen that natural mode 1 can be defined by the change in length of the member i.e. axial deformation. The rest of the modes of deformation are bending deformations. These can be defined by the end rotations. The natural displacements (i.e. relative deformations) that are necessary for the computation of the end forces can therefore, be summarized as given in Eqn 2-44. Notations are shown in Fig. 2.11.

$$\{d_N\} = \begin{Bmatrix} \bar{u} \\ \theta'_{yi} \\ \theta'_{yj} \\ \theta'_{zi} \\ \theta'_{zj} \\ \theta'_t \end{Bmatrix} \qquad (2\text{-}44)$$

The computation of $\{d_N\}$ in Eqn. 2-44 is not intuitively obvious. For illustration of the process of computing the relative rotations, an assumption is made here that the connector is initially straight as shown in Fig. 2.13. The relative rotational angles are the total nodal rotations obtained from analysis, i.e. static or dynamic analysis minus any member rigid body chord rotations. In Fig. 2.13, it can be seen that the rigid body rotations about the y, x and z global axes are as follows:

$$\phi_x = \sin^{-1}\frac{|dy|}{\sqrt{dy^2+dz^2}} \qquad \phi_y = \sin^{-1}\frac{|dx|}{\sqrt{dx^2+dz^2}}$$

$$\phi_z = 0$$

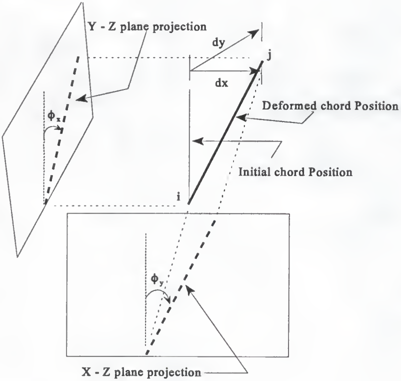

Fig. 2.13 Rigid Body Rotations

$$dx = x_j - x_i$$
$$dy = y_j - y_i$$
$$dz = z_j - z_i$$
$$l' = \sqrt{dx^2 + dy^2 + dz^2}$$

Using the cartesian coordinate system shown in Fig 2.1, clockwise rotation about the y axis is considered positive and counter-clockwise rotation about the x axis is positive. Therefore when dx is positive ϕ_y gets a positive sign but when dy is positive ϕ_x must be assigned a negative sign. The relative rotational deformation is then computed as shown in Eqn. 2-45 below.

$$\begin{Bmatrix} \overline{u} \\ \theta'_{yi} \\ \theta'_{yj} \\ \theta'_{zi} \\ \theta'_{zj} \\ \theta'_{t} \end{Bmatrix} = \begin{Bmatrix} l' - l \\ \theta_{yi} - \phi_y \\ \theta_{yj} - \phi_y \\ \theta_{zi} - \phi_x \\ \theta_{zj} - \phi_x \\ \theta_{xi} - \theta_{xj} \end{Bmatrix} \qquad (2\text{-}45)$$

Eqn 2-45 above assumes that the nodal rotational displacements (with the nodal designation *i* or *j*) have been resolved to the local coordinate system but the chord rotations (ϕ) are in global reference. Nodal rotations are measured relative to the original orientation of the beam. Relative rotations are measured relative to the chord of the beam. l' is the deformed length of the beam and l is the original length of the beam. To check the validity of Eqn. 2-45, consider the chord rotation and bending deformation of the next connector example. In Fig. 2.14, for ease of illustration the assumption is made that deformation exist only in the 2 -

dimensional, x - z plane.

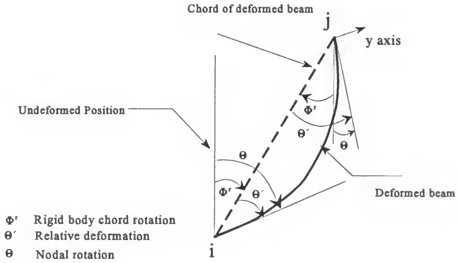

Fig. 2.14 Relative Nodal Rotations

Note that the nodal rotation at node (*i*) is clockwise hence positive, at node (*j*) the nodal rotation is counter-clockwise hence negative. The chord rotation is positive at both ends. The resultant relative rotation at node (*i*) is smaller in magnitude but with the same sign as the nodal rotation, i.e. clockwise. The resultant relative rotation at node (*j*) is bigger in magnitude but with the same sign as the nodal rotation, i.e. counter-clockwise. This conforms with results from applying Eqn. 2-45. The natural end forces of the beam element, as shown in Fig 2-11, can be obtained by multiplying the above relative deformation vector by the basic beam stiffness, [k$_{NE}$].

$$\{P_N\} = [k_{NE}]\{d_N\} \tag{2-46}$$

Substituting the matrix terms into Eqn. 2-46, Eqn 2-47 is obtained.

$$\{P_N\} = \begin{bmatrix} \frac{AE}{L} & 0 & 0 & 0 & 0 & 0 \\ 0 & \frac{4EI_y}{L} & \frac{2EI_y}{L} & 0 & 0 & 0 \\ 0 & \frac{2EI_y}{L} & \frac{4EI_y}{L} & 0 & 0 & 0 \\ 0 & 0 & 0 & \frac{4EI_z}{L} & \frac{2EI_z}{L} & 0 \\ 0 & 0 & 0 & \frac{2EI_z}{L} & \frac{4EI_z}{L} & 0 \\ 0 & 0 & 0 & 0 & 0 & \frac{GJ}{L} \end{bmatrix} \begin{Bmatrix} \bar{u} \\ \theta'_{yi} \\ \theta'_{yj} \\ \theta'_{zi} \\ \theta'_{zj} \\ \theta'_t \end{Bmatrix} \tag{2-47}$$

The end force vector computed from Eqn 2-47 can be seen in Fig. 2.11.

$$\{P_N\} = \begin{Bmatrix} P \\ M_{yi} \\ M_{yj} \\ M_{zi} \\ M_{zj} \\ M_t \end{Bmatrix} \tag{2-48}$$

The coefficients of geometric stiffness are obtained from the basic end forces. The geometric stiffness matrix for a large displacement beam according to Chen and Agar [11] is shown in Eqn. 2-49 below.

$$
\left[k_g\right] = \begin{bmatrix}
0 & 0 & 0 & 0 & 0 & 0 & 0 & 0 & 0 & 0 & 0 & 0 \\
 & a & 0 & b & e & f & 0 & -a & 0 & k & -e & f \\
 & & a & c & -f & e & 0 & 0 & -a & -\hat{l} & -f & -e \\
 & & & d & g & -h & 0 & -b & -c & -d & -g & h \\
 & & & & i & j & 0 & -e & f & -g & -n & m \\
 & & & & & i & 0 & -f & -e & -h & -m & -n \\
 & & & & & & 0 & 0 & 0 & 0 & 0 & 0 \\
 & & & & & & & a & 0 & -k & e & -f \\
 & & & & & & & & a & -\hat{l} & f & e \\
 & & & & & SYMM. & & & & d & g & -h \\
 & & & & & & & & & & i & -j \\
 & & & & & & & & & & & i
\end{bmatrix}
$$

(2-49)

The terms in the matrix above are as follows:

$$
a = 6P/5l, \quad b = M_{yi}/l, \quad c = M_{zi}/l, \quad d = P\left(I_y + I_z\right)/A_x, \quad e = M_t/l, \quad f = P/10
$$

$$
g = \left(M_{zi} + M_{zj}\right)/6, \quad h = \left(M_{yi} + M_{yj}\right)/6, \quad i = 2Pl/15, \quad j = \frac{M_t}{2}\frac{\left(I_z - I_y\right)}{\left(I_z + I_y\right)}, \quad k = M_{yj}/l,
$$

$$
\hat{l} = M_{zi}/l, \quad m = M_t/2, \quad n = Pl/30,
$$

(2-50)

Note that l is the length of the beam and the other variables are as defined in Eqn 2-48. The final expression for the stiffness of the connector element with reference to the element local axes is,

$$[k_T] = [k_e] + [k_g] \tag{2-51}$$

The above stiffness in global coordinates can be obtained by applying the standard coordinate transformation.

Transformation Matrix

The translational transformation matrix can be obtained by using the k - node method. This method is used in the SSTAN program developed at the civil engineering department, University of Florida. The transformation matrix is a 3×3 matrix. The terms of the transformation matrix [T] is obtained as follows. The first 1 × 3 row entries represent a unit vector lying along the member local axis,

$$\left\{ \frac{dx}{l}, \frac{dy}{l}, \frac{dz}{l} \right\}$$

l = length of the member

dx, dy and dz are similar to Δx, Δy, Δz in Fig. 2.7 and similar to those given on page 40. Another unit vector must be defined along a node in the plane of the element but not along the member. This node is referred to as the k-node.

$$\left\{\frac{dx_k}{l_k}, \frac{dy_k}{l_k}, \frac{dz_k}{l_k}\right\}$$

The second 1 x 3 row in the transformation matrix is obtained from the cross product of the k-node unit vector and the member unit vector. The third 1 x 3 row is obtained by getting the cross product of the previous member unit vector (in the first row of the transformation matrix) and the unit vector gotten in the first cross product (now in the second row of the transformation matrix). The resultant 3 x 3 matrix [T] is used to transform nodal displacements from global to local coordinate systems.

For the case of the beam with large displacement, in addition to the initial transformation matrix [T] described above, it is often advantageous to use another transformation matrix [R] based on Euler angles. This is because this transformation matrix formulation can better keep track of the twisting of the element than the former. A combination of both transformation matrices could be adopted with the first transformation [T] used to transform element properties from the local coordinate system to the initial member global position. The second transformation [R] can then be used to transform from the initial global position to the member's deformed position. The transformation matrix, [R], used in the context just described is described next. The Euler transformation matrix [R] is also explained in the context of a numerical time step solution, which is reflective of its usage in chapter 3.

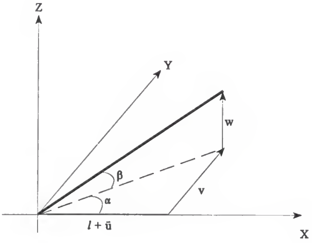

Fig. 2.15 Euler angles for transformation

l = original length of the beam.

$\bar{u}$ = axial relative displacement.

v = relative displacement in the y direction.

w = relative displacement in the z direction.

The Euler angles in Fig. 2.15 can be computed as shown in Eqn. 2-52 and Eqn. 2-53. Note that u, v and w above are computed using the cumulative nodal displacements in the case of dynamic time step solution.

$$\alpha = \tan^{-1}\frac{v}{l + \bar{u}} \tag{2-52}$$

$$\beta = \tan^{-1}\frac{w}{\sqrt{(l + \bar{u})^2 + v^2}} \tag{2-53}$$

The final Euler angle that is needed is the angle of twist, γ. The angle of twist can be obtained from the rotational displacement about the local x axis. It is assumed that the nodal incremental displacements have been transformed to the element's initial local coordinate system using just the initial k-node transformation [T]. The angle of twist is cumulated at each iteration using the change in nodal rotations.

$$\gamma^{t} = \gamma^{t-\Delta t} + \frac{1}{2}\left\{\cos\beta\cos\alpha\left(\Delta\theta_{xi} + \Delta\theta_{xj}\right) + \cos\beta\sin\alpha\left(\Delta\theta_{yi} + \Delta\theta_{yj}\right) + \sin\beta\left(\Delta\theta_{zi} + \Delta\theta_{zj}\right)\right\}$$

(2-54)

γ^{t} = the angle of twist at time t

$\gamma^{t+\Delta t}$ = the angle of twist at time t + Δt

$\Delta\theta_{\{axis\}\{node\}}$ = change in nodal rotation about the axis {x, y or z} at node {i or j}.

α and β are as computed from Eqn. 2-52 and Eqn. 2-53.

The final transformation matrix [R] is presented in Eqn. 2-55.

$$[R] = \begin{bmatrix} \cos(\beta)\cos(\alpha) & \cos(\beta)\sin(\alpha) & \sin(\beta) \\ -\cos(\gamma)\sin(\alpha) - \sin(\gamma)\sin(\beta)\cos(\alpha) & \cos(\gamma)\cos(\alpha) - \sin(\gamma)\sin(\beta)\sin(\alpha) & \sin(\gamma)\cos(\beta) \\ \sin(\gamma)\sin(\alpha) - \cos(\gamma)\sin(\beta)\cos(\alpha) & -\sin(\gamma)\cos(\alpha) - \cos(\gamma)\sin(\beta)\sin(\alpha) & \cos(\gamma)\cos(\beta) \end{bmatrix}$$

(2-55)

The final transformation matrix for the large displacement beam is therefore:

$[A] = [R][T]$

[A] = final transformation.

Applying the transformation matrix, the stiffness of the member in terms of the global nodal displacements is

$$\left[K_T\right]_G = \begin{bmatrix} A & & O & \\ & A & & \\ & & A & \\ & O & & A \end{bmatrix}^T \left[k_e + k_g\right] \begin{bmatrix} A & & O & \\ & A & & \\ & & A & \\ & O & & A \end{bmatrix} \qquad (2\text{-}56)$$

Damping Matrix

The last property that needs to be defined is the damping matrix. The damping matrix for a structural system is easier defined proportional to either the mass, the stiffness or both. There are two classical damping matrices. The

Rayleigh damping and the Caughey damping [14]. The Rayleigh damping matrix is described below. With Rayleigh damping, the damping matrix is defined as follows.

$$[C] = a_0[M] + a_1[K] \tag{2-57}$$

a_0 and a_1 are damping constants depending on the controlling modal frequencies and the corresponding specified modal damping ratio.

$$a_0 = \xi \frac{2\varpi_i \varpi_j}{\varpi_i + \varpi_j} \qquad a_1 = \xi \frac{2}{\varpi_i + \varpi_j} \tag{2-58}$$

ξ = modal damping ratio

ϖ_i = modal frequency corresponding to mode *i*.

ϖ_j = modal frequency corresponding to mode *j*.

Controlling modes are often the higher modes corresponding to the number of degrees of freedom for the system.

For nonlinear analysis the eigenvalues are never obtained as part of the solution. There needs to be a way to estimate the natural frequency of the system prior to a rigorous nonlinear analysis. For the structural system defined, an estimate of the natural frequency of the system can be taken as either the natural frequency of the cables on infinitely rigid supports or the natural frequency of the poles without the cables. Both estimates are given below.

For the catenary cable subjected to self weight, no initial pre-tension and a specified sag, the natural frequency [3] is

$$\varpi_n = n\pi\sqrt{\frac{g}{8f}} \qquad n = 1, 2, 3, \ldots \tag{2-59}$$

n = modes to investigate

g = acceleration due to gravity

f = sag at mid-span of the cable

l = span of the cable

For cables where the sag is assumed to be zero the above equation ceases to be a good estimate. Therefore for a messenger cable with initial pre-tension and a near zero sag , the natural frequency can be estimated as

$$\varpi_n = \frac{n\pi}{l}\sqrt{\frac{Tg}{m}} \tag{2-60}$$

For the poles, taken as cantilever beams, the natural frequency can be estimated as follows [9]:

$$\varpi_n = \frac{n^2\pi^2}{l^2}\sqrt{EIg/m} \tag{2-61}$$

Matrix representation of the element properties have now been developed. The solution techniques that will be used to determine the time history response of the discretized structure is considered next.

Dynamic Solution Methods

The equation of motion [14] for a typical structure is

$$[M]\{\ddot{d}\} + [C]\{\dot{d}\} + [K]\{d\} = \{P\} \tag{2-62}$$

$[M]$ = assembled mass matrix of the structure.

$[C]$ = assembled damping matrix of the structure.

$[K]$ = assembled stiffness matrix.

$\{\ddot{d}\}$ = acceleration vector.

$\{\dot{d}\}$ = velocity vector.

$\{d\}$ = displacement vector.

$\{P\}$ = applied load vector.

For nonlinear analysis direct time integration is used. This means that the solution to the equation of motion is determined at discrete times (t_i i=0,1,2...). The initial conditions at the beginning of the time steps are always known and it is assumed that some variation in, and self consistent relationship between, the displacements, velocities and accelerations occur during the time step. The methods of solution available for dynamic analysis vary depending on the assumptions made for the variation in displacements, velocities and accelerations within the time step. As earlier mentioned these methods are classified as either explicit or implicit.

Explicit Methods

A disadvantage of using explicit method is that they are conditionally stable. The more common explicit solutions are Central Difference method and Runge-Kunta method. In explicit methods it is assumed that the displacement and velocity at time $t + \Delta t$ are independent of the acceleration at $t + \Delta t$. Consequently, the displacement at the end of the time step is projected from the equation of motion at the beginning of the time step. In particular, the elastic forces and damping forces within the time step are computed using displacements and velocities at the beginning of the current time step and the beginning of the previous time step. For details of the available explicit methods, the writer recommends Ref. [7], [9], [14]. For the cable analysis it is important to apply the load in small increments, it is, therefore, more convenient to perform an incremental analysis. Implicit methods of analysis allows us to rewrite the equation of motion in terms of the change in the displacement, velocity and acceleration.

Implicit Methods

The incremental steps are measured relative to a reference state at the beginning of the time step. The equation of motion given in Eqn 2-62 can then be rewritten.

$$[M]\left\{\Delta \ddot{d}(t)\right\} + [C]\left\{\Delta \dot{d}\,(t)\right\} + [K]\{\Delta d(t)\} = \{\Delta P(t)\} \tag{2-63}$$

The new shape of the cable at any time (t) can be obtained as follows

$$d(t + \Delta t) = d(t) + \Delta d(t) \tag{2-64}$$

The solution of Equation 2-63 above can be obtained by a number of different implicit methods. The more common methods are the Adam-Stoermer method, Newmark's Beta method and Wilson Theta method. These methods actually all have the same form and can be easily inter-changed with a manipulation of the parameters associated with each method. The Newmark's Beta is used by the writer and is discussed next.

Newmark Beta Method

Newmark Beta method [14] is based on the following equations written in terms of incremental parameters.

$$\{\Delta d\} = \Delta t\left\{\dot{d}(t)\right\} + \left[\left(\frac{1}{2} - \beta\right)\left\{\ddot{d}(t)\right\} + \beta\left\{\ddot{d}(t + \Delta t)\right\}\right]^2 \qquad (2\text{-}65)$$

$$\left\{\Delta \dot{d}\right\} = \frac{\Delta t}{2}\left[\left\{\ddot{d}(t) + \ddot{d}(t + \Delta t)\right\}\right] \qquad (2\text{-}66)$$

Solve Eqn. 2-65 for $\left\{\ddot{d}(t + \Delta t)\right\}$ and Eqn. 2-67 is obtained.

$$\left\{\ddot{d}(t + \Delta t)\right\} = \frac{1}{\beta \Delta t^2}\{\Delta d\} - \frac{1}{\beta \Delta t}\left\{\dot{d}(t)\right\} - \frac{\frac{1}{2} - \beta}{\beta}\left\{\ddot{d}(t)\right\} \qquad (2\text{-}67)$$

From Eqn. 2-67 the change in acceleration within the time step can be expressed as follows:

$$\left\{\Delta \ddot{d}\right\} = \left\{\ddot{d}(t + \Delta t)\right\} - \left\{\ddot{d}(t)\right\} = \frac{1}{\beta \Delta t^2}\{\Delta d\} - \frac{1}{\beta \Delta t}\left\{\dot{d}(t)\right\} - \frac{1}{2\beta}\left\{\ddot{d}(t)\right\} \qquad (2\text{-}68)$$

Substituting Eqn. 2-67 into Eqn. 2-66 and the expression for the change in velocity can be rewritten as,

$$\left\{\Delta \dot{d}\right\} = \frac{1}{2\beta \Delta t}\{\Delta d\} - \frac{1}{2\beta}\left\{\dot{d}(t)\right\} - \frac{\frac{1}{2} - 2\beta}{2\beta}\Delta t\left\{\ddot{d}(t)\right\} \qquad (2\text{-}69)$$

Substituting Eqn. 2-65, 2-66 and 2-68 into 2-63 and rearranging terms we have the final equations for the Newmark's Beta method.

$$\left[\tilde{K}(t)\right]\{\Delta d\} = \left\{\Delta \tilde{P}(t)\right\} \qquad (2\text{-}70)$$

$$\left[\tilde{K}(t)\right] = \frac{1}{\beta \Delta t^2}[M] + \frac{1}{2\beta \Delta t}[C(t)] + [K(t)] \qquad (2\text{-}71)$$

$$\left\{\Delta \tilde{P}(t)\right\} = \{\Delta P(t)\} + [M]\left[\frac{1}{\beta \Delta t}\left\{\dot{d}(t)\right\} + \frac{1}{2\beta}\left\{\ddot{d}(t)\right\}\right] + [C(t)]\left[\frac{1}{2\beta}\left\{\dot{d}(t)\right\} + \frac{\frac{1}{2} - 2\beta}{2\beta}\Delta t \left\{\ddot{d}(t)\right\}\right]$$

(2-72)

The solution procedure using Newmark's Beta method may then be summarized as follows:

- From initial conditions, calculate effective stiffness (Eqn. 2-71) and effective incremental load vector (Eqn. 2-72).
- Solve for incremental displacement (Eqn. 2-70) and cumulative displacement (Eqn. 2-64).
- Solve for incremental velocity (Eqn. 2-69) and velocity at t + Δt.
- Impose total equilibrium at the end of the time step to obtain the acceleration at the end of the time step.

$$\left\{\ddot{d}(t + \Delta t)\right\} = \frac{\{P(t + \Delta t)\} - \{f_d(t + \Delta t)\} - \{f_e(t + \Delta t)\}}{[M]} \qquad (2\text{-}73)$$

f_d = damping force vector

f_e = elastic force vector.

- Repeat the process for the next time step.

The parameter β reflects the variation of the acceleration within the time step. There are various values that could be used for β. For $\beta = 1/6$ we have the linear acceleration method. For $\beta = 1/4$ we have the constant acceleration method. And finally for $\beta = 1/8$, the acceleration is constant, equal to the beginning value over the first half of the time step and constant, equal to the ending value over the last half of the time step. When β is taken as zero the Newmark's Beta method degenerates to the Euler integration scheme. Similarly if β is taken as ½ Newmark's method becomes identical to the central difference integration and to backward difference when β is unity. The constant acceleration method is unconditionally stable . This means that the solution will not become unbounded as the integration progresses. With the numerical integration, there are inaccuracies due to round-off or due to time increment being too large to represent the forcing function or the structural response. The errors can be redistributed at each time step by using the Newton-Raphson method.

CHAPTER 3

THEORETICAL DEVELOPMENT

Introduction

In chapter 2, the typical cable element commonly found in literature was discussed. The formulation of a different 2 node straight cable element adopted for this dissertation is presented in this chapter. This formulation includes the equation of motion and solution to the equation for the traffic signal system.

The equations derived in this chapter are based on the Cartesian coordinate system shown in Fig. 2.1. The deformation parameters *u* in the x direction, *v* in the y direction and *w* in the z direction are deformations relative to the initial (*null*) state. The initial states for the cables are taken as either *taut* or *slack*. The taut cable has an initial pretensioned cable state. The load acting on this cable at the initial configuration (time t = 0) is the self weight of the cable and the initial tension. The cable with this null state (condition of zero deformation), in the case of the traffic signal system, is referred to as the *messenger* cable. The messenger cable null state has an initial axial strain but an assumed zero *sag*. The catenary cable, in the case of the traffic signal system, has a slack null state. The catenary cable in this case is presumed to have zero pretension (except for tension from self weight) and a specified sag. The default sag if none is specified is 5 %. Two additional reference configurations are of importance. These are the present configuration at time t and the next configuration at time t + Δt. The incremental displacement at the nodes, therefore is the difference between the coordinates of the nodes at time t and at time t + Δt. The cumulative displacement at the beginning of the time step is the difference between the coordinates at time t and the null state. Similarly the cumulative displacement at the end of the time step is the difference between the coordinates at time t + Δt and the null state. The null configuration is the base reference configuration. Both the messenger and catenary cable are idealized by the 2-node non-linear cable element derived in the following section. The main difference between this cable element and that derived in chapter 2 is the inherent assumption in the strain - displacement relationship.

Two Node Nonlinear Cable Element

The shape function of the element adopted is given in Eqn. 3-2.

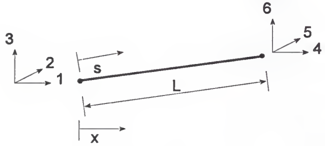

Fig. 3.1 Cable Element

The element properties for this cable element are derived directly in the global coordinate system. An explicit derivation of a 2 node cable element from first principles using some novel manipulations of typical energy expression is presented next. The derivation presented is based on the work presented by Henghold and Russell [16] and Haritos and He [17]. Ref. [17] presented a total

Lagrangian formulation of the incremental equation of motion for cable movement. This writer has adopted this approach with a deviation in that the cable tension used for the geometric stiffness is cumulated in each time step in an updated Lagrangian fashion. This is observed to be more convenient in terms of numerical implementation of the element. Ref. [16], however, uses the method of perturbation of the virtual work expression for a cable element to derive the equation of motion of the cable. Though this is very different from the approach adopted in this dissertation, the writer has chosen to adopt the reference's approach of defining the element's displacement field (shape function) in such a way as to derive the element stiffness directly in terms of the deformed global coordinates as opposed to the more classical approach of using a local coordinate system with a local to global transformation. The shape function is defined to relate the coordinates of any generic point along the cable element to the nodal coordinates.

$$\begin{Bmatrix} x \\ y \\ z \end{Bmatrix} = [N] \begin{Bmatrix} x_1 \\ y_2 \\ z_3 \\ x_4 \\ y_5 \\ z_6 \end{Bmatrix} \tag{3-1}$$

In terms of a convenient notation Eqn. 3-1 can be rewritten as shown in Eqn. 3-2.

$$\{d_s\} = [N]\{d_n\} \tag{3-2}$$

d_s = coordinate of an arbitrary point s along the cable

d_n = coordinates of the nodal points. n is the degrees of freedom shown in Fig. 3.1.

N = shape function

The interpolation function for a linear displacement field is given below [18].

$$[N]^T = \begin{bmatrix} 1-\frac{s}{L} & 0 & 0 \\ 0 & 1-\frac{s}{L} & 0 \\ 0 & 0 & 1-\frac{s}{L} \\ \frac{s}{L} & 0 & 0 \\ 0 & \frac{s}{L} & 0 \\ 0 & 0 & \frac{s}{L} \end{bmatrix} \tag{3-3}$$

Applying the principle of virtual work, the expression for total work done for a single element at the time t + Δt is as follows.

$$\delta \overline{W} = \int_0^L \delta \overline{d_s}^T \overline{q_s}\, ds + \sum_{j=1}^{n} \delta \overline{d_s}^T \overline{F_j} - \int_0^L \delta \overline{d_s}^T \overline{f_d}\, ds - \int_0^L A\, \overline{\delta\varepsilon}^T \overline{\sigma}\, ds = 0$$

(3-4)

$\delta\overline{W}$ = sum of the internal and external virtual work done on the element.

$\overline{q}_s$ = gravity and inertia forces acting along the arc of the cable.

$\overline{F}_j$ = applied nodal load - j is the degrees of freedom. (j = 1...n).

$\overline{f}_d$ = damping force vector.

$\delta\overline{d}_s$ = vector of small virtual variations in coordinates.

Note that, though for convenience the writer has chosen to omit the brackets { } used as vector notation, the displacement and forces in Eqn. 3-4 and subsequent equations are vectors. Note also that the straight line overstrike ,¯, indicate values or properties at time t + Δt. The superscript , ^{T}, indicate the transpose of the vector.

The last term in the Eqn. 3-4 is the equivalent internal virtual work due to stress σ at time t + Δt. This is referred to as the virtual strain energy. The variation in the coordinate at time t + Δt is equivalent to the variation in the difference between the coordinates at time t and time t + Δt. It is, therefore useful to express the coordinate at time, t + Δt, as follows.

$$\{d_s\}_{t+\Delta t} = \{d_s\}_t + \{\Delta d_s\} \qquad (3\text{-}5)$$

$$\{\Delta d_s\} = [N]\{\Delta d_n\} \qquad (3\text{-}6)$$

Δd_n = change in nodal displacement vector.

Δd_s = change in displacement vector of any generic point along the cable.

Substituting Eqn. 3-2 into Eqn. 3-4 yields Eqn. 3-7.

$$\delta W = \int_0^L [N]^T \delta\Delta d_n{}^T q_s \, ds + \sum^{n} [N]^T \delta\Delta d_n{}^T F_j - \int_0^L [N]^T \delta\Delta d_n{}^T f_d \, ds - \int_0^L A \, \overline{\delta\varepsilon}^T \, \overline{\sigma} \, ds$$

(3-7)

σ = Kirchhoff stress.

ε = Lagrangian strain of deformed cable.

A nonlinear strain-displacement relationship is adopted, therefore the strain is as given in Eqn. 3-8.

$$\varepsilon_s = \frac{1}{2}\left\{\left(\frac{\partial \bar{s}}{\partial s_o}\right)^2 - 1\right\} \qquad (3\text{-}8)$$

$\partial \bar{s}$ = stretched length of a cable segment at time $t + \Delta t$

∂s_o = unstressed length of a cable segment at time $t = 0$

In terms of the shape function expression in Eqn. 3-3, Eqn. 3-8 may be rewritten as,

$$\varepsilon_s = \frac{1}{2}\left\{ \frac{\partial d_s}{\partial s}^T \frac{\partial d_s}{\partial s} - 1 \right\} \tag{3-9}$$

$$\varepsilon_s = \frac{1}{2}\left\{ \{d_n\}^T [N']^T [N']\{d_n\} - 1 \right\} \tag{3-10}$$

$$[N']^T = \begin{bmatrix} -\frac{1}{L} & 0 & 0 \\ 0 & -\frac{1}{L} & 0 \\ 0 & 0 & -\frac{1}{L} \\ \frac{1}{L} & 0 & 0 \\ 0 & \frac{1}{L} & 0 \\ 0 & 0 & \frac{1}{L} \end{bmatrix} \tag{3-11}$$

Note that N′ is the differential of the shape function with respect to the generic distance, s, along the cable. The analysis approach described in chapter 2 is that of incremental displacement. It is therefore important to define the corresponding incremental strain. Subtracting the nodal coordinates at time t from the corresponding coordinates at time t + Δt, the incremental nodal displacement is obtained. Similarly, subtracting the expression for strain (Eqn. 3-8) at time, t, from a corresponding expression at time t + Δt yields the change in strain.

$$\Delta\varepsilon = \frac{1}{2}\left\{ \left(\frac{\partial \overline{d_s}}{\partial s}\right)^T \left(\frac{\partial \overline{d_s}}{\partial s}\right) - 1 \right\} - \frac{1}{2}\left\{ \left(\frac{\partial d_s}{\partial s}\right)^T \left(\frac{\partial d_s}{\partial s}\right) - 1 \right\} \tag{3-12}$$

$\overline{d}_s$ = coordinate of an arbitrary point s along the cable at time t + Δt

$$\Delta d_s = \overline{d_s} - d_s \tag{3-13}$$

Solving for $\overline{d}_s$ in Eqn. 3-13 and substitute into Eqn. 3-12 results in Eqn. 3-14.

$$\Delta\varepsilon = \frac{1}{2}\left\{\left(\frac{\partial\Delta d_s}{\partial s}\right)^T\left(\frac{\partial\Delta d_s}{\partial s}\right) + \left(\frac{\partial d_s}{\partial s}\right)^T\left(\frac{\partial\Delta d_s}{\partial s}\right) + \left(\frac{\partial\Delta d_s}{\partial s}\right)^T\left(\frac{\partial d_s}{\partial s}\right)\right\} \tag{3-14}$$

Substituting the notation used in Eqn. 3-10 into 3-14, Eqn. 3-15 is obtained.

$$\Delta\varepsilon = \frac{1}{2}\left\{\Delta d_n{}^T[N']^T[N']\,\Delta d_n + d_n{}^T[N']^T[N']\,\Delta d_n + \Delta d_n{}^T[N']^T[N']\,d_n\right\} \tag{3-15}$$

The last two terms in Eqn. 3-15 are equal, therefore the above equation can be simplified further as shown in Eqn. 3-16.

$$\Delta\varepsilon = \frac{1}{2}\left\{\Delta d_n{}^T[N']^T[N']\,\Delta d_n\right\} + d_n{}^T[N']^T[N']\,\Delta d_n \tag{3-16}$$

The virtual work of internal forces as given by the last term of Eqn. 3-4 is given below.

$$\delta U = A\int_0^L \delta\bar{\varepsilon}^T \bar{\sigma}\, ds \tag{3-17}$$

Applying the unit-load method [19], the virtual strain energy expression in Eqn. 3-17 can be rearranged to be in terms of the stiffness for the cable element.

$$\delta U = AE\int_0^L \delta\varepsilon^T \bar{\varepsilon}\, ds \tag{3-18}$$

The strain in the cable element at time t + Δt is equivalent to the strain at time t plus the change in strain given in Eqn. 3-16. The variation in strain at time t + Δt is equivalent to the variation of the change in strain.

$$\delta\bar{\varepsilon}^T = \delta\Delta\varepsilon^T \tag{3-19}$$

Substituting Eqn. 3-16 into 3-19 and then into 3-18 the equation given in Eqn. 3-20 is obtained.

$$\delta U = AE\int_0^L\left(\frac{1}{2}\left\{\Delta d_n{}^T[N']^T[N']\right\}\delta\Delta d_n + \frac{1}{2}\left\{\delta\Delta d_n{}^T[N']^T[N']\right\}\Delta d_n + d_n{}^T[N']^T[N']\delta\Delta d_n\right)^T \bar{\varepsilon}\, ds \tag{3-20}$$

$\delta\Delta d_n$ = variation of incremental nodal displacement vector.

Again, note that the first two terms in Eqn. 3-20 are equivalent.

$$\delta U = AE\int_0^L\left(\left\{\Delta d_n{}^T[N']^T[N']\right\}\delta\Delta d_n + d_n{}^T[N']^T[N']\delta\Delta d_n\right)^T \bar{\varepsilon}\, ds \tag{3-21}$$

From Eqn. 3-21, it can be noted that the term, $\delta\Delta d_n$, is common to all the terms of Eqn. 3-4, and hence cancels out. Substituting the term for strain, $\bar{\varepsilon}$, Eqn. 3-21 reduces to an expression in terms of stiffness.

$$\bar{\varepsilon} = \varepsilon + \Delta\varepsilon \qquad (3\text{-}22)$$

$$\{f_s\} = AE\int_0^L \Bigl(\Bigl\{ \Delta d_n{}^T [N']^T [N'] \Bigr\} + d_n{}^T [N']^T [N'] \Bigr)^T \times$$
$$\Bigl(\varepsilon + \Bigl(\tfrac{1}{2} \Bigl\{ \Delta d_n{}^T [N']^T [N'] \Delta d_n \Bigr\} + d_n{}^T [N']^T [N'] \Delta d_n \Bigr) \Bigr) \, ds$$
$$(3\text{-}23)$$

Rearranging and collecting sub-expressions in Eqn. 3-23, Eqn. 3-24 is obtained.

$$f_s = K_E \Delta d_n + K_L \Delta d_n + R_E \qquad (3\text{-}24)$$

$$K_E = AE \int_0^L \varepsilon \, [N']^T [N'] \, ds \qquad (3\text{-}25)$$

$$K_L = AE\int_0^L \Bigl(\Bigl\{ \Delta d_n{}^T [N']^T [N'] \Bigr\} + \Bigl\{ d_n{}^T [N']^T [N'] \Bigr\} \Bigr)^T \times \Bigl(\tfrac{1}{2} \Bigl\{ \Delta d_n{}^T [N']^T [N'] \Bigr\} + \Bigl\{ d_n{}^T [N']^T [N'] \Bigr\} \Bigr) \, ds$$
$$(3\text{-}26)$$

$$R_E = AE \int_0^L [N']^T [N'] \, \varepsilon \, d_n \, ds \qquad (3\text{-}27)$$

K_E is the referred to as the initial stress matrix and R_E is the force vector due initial stress. Note that the term AEε is equivalent to tension in the cable at the beginning of the time step. For $t = 0$, this term is the pretension in the element. For subsequent time steps the tension term can be computed as follows,

$$T_t = T_{t-\Delta t} + AE\{\Delta\varepsilon\}_{t-\Delta t} \qquad (3\text{-}28)$$

Note that K_L is dependent on unknown displacements. This is the non-linear component of the element stiffness, [K]. This can not be computed at the start of analysis and must be substituted by an initial approximate stiffness. Let this approximation be

$$K_A = AE\int^{L} \left\{d_n{}^T [N']^T [N']\right\}^T \times \left\{d_n{}^T [N']^T [N']\right\} ds \tag{3-29}$$

The expression in Eqn. 3-29 was achieved by simply setting Δd_n in Eqn. 3-26 to zero. If the shape functions for the 2-node element is substituted into the Eqn. 3-25, 3-26, 3-27 and 3-29, the following expressions for K_E, K_L and K_A on the next page are obtained. See Appendix A for complete derivation of the expression. The following notations are used.

$$d_n = \left\{\begin{matrix} x_i \\ y_i \\ z_i \\ x_j \\ y_j \\ z_j \end{matrix}\right\} \qquad \begin{matrix} i & = & 1\ldots3 \\ j & = & 4\ldots6 \end{matrix} \qquad \Delta d_n = \left\{\begin{matrix} u_i \\ v_i \\ w_i \\ u_j \\ v_j \\ w_j \end{matrix}\right\} \qquad \begin{matrix} i & = & 1\ldots3 \\ j & = & 4\ldots6 \end{matrix}$$

$$\left\{\begin{matrix} dx \\ dy \\ dz \end{matrix}\right\} = \left\{\begin{matrix} x_j - x_i \\ y_j - y_i \\ z_j - z_i \end{matrix}\right\} \qquad \left\{\begin{matrix} du \\ dv \\ dw \end{matrix}\right\} = \left\{\begin{matrix} u_j - u_i \\ v_j - v_i \\ w_j - w_i \end{matrix}\right\}$$

The expression for K_E is as follows:

$$\left[K_E \right] = \frac{T_{t-\Delta t} + A\,E\,\Delta\varepsilon}{L} \begin{bmatrix} 1 & 0 & 0 & -1 & 0 & 0 \\ 0 & 1 & 0 & 0 & -1 & 0 \\ 0 & 0 & 1 & 0 & 0 & -1 \\ -1 & 0 & 0 & 1 & 0 & 0 \\ 0 & -1 & 0 & 0 & 1 & 0 \\ 0 & 0 & -1 & 0 & 0 & 1 \end{bmatrix}$$

(3-30)

L = initial cable element length.

$$[K_A] = \frac{AE}{L^3}\begin{bmatrix} dx^2 & dx\,dy & dx\,dz & -dx^2 & -dy\,dx & -dz\,dx \\ dx\,dy & dy^2 & dy\,dz & -dy\,dx & -dy^2 & -dy\,dz \\ dx\,dz & dy\,dz & dz^2 & -dz\,dx & -dy\,dz & -dz^2 \\ -dx^2 & -dy\,dx & -dz\,dx & dx^2 & dx\,dy & dx\,dz \\ -dy\,dx & -dy^2 & -dy\,dz & dx\,dy & dy^2 & dy\,dz \\ -dz\,dx & -dv\,dz & -dz^2 & dx\,dz & dv\,dz & dz^2 \end{bmatrix} \qquad (3\text{-}31)$$

$$[K_L] = \frac{AE}{2L^3}\begin{bmatrix} (dx+du)(2dx+du) & (dx+du)(2dy+dv) & (dx+du)(2dz+dw) & -(dx+du)(2dx+du) & -(dx+du)(2dy+dv) & -(dx+du)(2dz+dw) \\ (dy+dv)(2dx+du) & (dy+dv)(2dy+dv) & (dy+dv)(2dz+dw) & -(dy+dv)(2dx+du) & -(dy+dv)(2dy+dv) & -(dy+dv)(2dz+dw) \\ (dz+dw)(2dx+du) & (dz+dw)(2dy+dv) & (dz+dw)(2dz+dw) & -(dz+dw)(2dx+du) & -(dz+dw)(2dy+dv) & -(dz+dw)(2dz+dw) \\ -(dx+du)(2dx+du) & -(dx+du)(2dy+dv) & -(dx+du)(2dz+dw) & (dx+du)(2dx+du) & (dx+du)(2dy+dv) & (dx+du)(2dz+dw) \\ -(dy+dv)(2dx+du) & -(dy+dv)(2dy+dv) & -(dy+dv)(2dz+dw) & (dy+dv)(2dx+du) & (dy+dv)(2dy+dv) & (dy+dv)(2dz+dw) \\ -(dz+dw)(2dx+du) & -(dz+dw)(2dy+dv) & -(dz+dw)(2dz+dw) & (dz+dw)(2dx+du) & (dz+dw)(2dy+dv) & (dz+dw)(2dz+dw) \end{bmatrix}$$

$$(3\text{-}32)$$

Eqn. 3-33 can be deduced from Eqns. 3-25 and 3-27.

$$\{R_E\} = [K_E]\{d_n\} \tag{3-33}$$

$$\{R_E\} = \frac{T_{t-\Delta t} + AE\Delta\varepsilon}{L}\begin{Bmatrix} -dx \\ -dy \\ -dz \\ dx \\ dy \\ dz \end{Bmatrix} \tag{3-34}$$

Equation of Motion

The above portion calculated the strain energy portion of Eqn. 3-4. It is now necessary to consider the other terms in Eqn. 3-4. The kinetic energy term is the first term in Eqn. 3-4. This is in terms of the variable q_s defined in Eqn. 3-35 below.

$$q_s = g_s + f_i \tag{3-35}$$

q_s = distributed load along the element.

g_s = gravity load due to self weight.

f_i = inertial forces.

Rewriting the first term in Eqn. 3-7 yields Eqn. 3-36.

$$g_s - \delta K = \int_0^L w_s [N]^T h_1 \, ds - \int_0^L m_s [N]^T [N] \{\ddot{d}_n\} ds \qquad (3\text{-}36)$$

w_s = cable self weight per unit length.

m_s = cable mass per unit length.

δK = kinetic energy due to inertia forces.

$\{\ddot{d}_n\}$ = nodal acceleration.

h_1 is an index array based on the coordinate system adopted. It is used to determine how the weight of the element is added to the structure.

The self weight acts in the negative z direction.

$h_1^T = \{0 \quad 0 \quad -1\}$

$$\delta K = \frac{w_s L}{6g} \begin{bmatrix} 2 & 0 & 0 & -1 & 0 & 0 \\ 0 & 2 & 0 & 0 & -1 & 0 \\ 0 & 0 & 2 & 0 & 0 & -1 \\ -1 & 0 & 0 & 2 & 0 & 0 \\ 0 & -1 & 0 & 0 & 2 & 0 \\ 0 & 0 & -1 & 0 & 0 & 2 \end{bmatrix} \begin{Bmatrix} \ddot{u}_i \\ \ddot{v}_i \\ \ddot{w}_i \\ \ddot{u}_j \\ \ddot{v}_j \\ \ddot{w}_j \end{Bmatrix} \qquad (3\text{-}37)$$

g = acceleration due to gravity.

$$g_s = \frac{w_s L}{2} \begin{Bmatrix} 0 \\ 0 \\ -1 \\ 0 \\ 0 \\ -1 \end{Bmatrix} \tag{3-38}$$

The second term in Eqn. 3-7 and Eqn. 3-4 is the applied nodal load.

$$\left\{F_j\right\} = \begin{Bmatrix} f_1 \\ f_2 \\ f_3 \\ f_4 \\ f_5 \\ f_6 \end{Bmatrix} \tag{3-39}$$

This is the computed nodal load due to dead weight of cladding and/or traffic signal heads and/or wind load. Since the cable element is a two node element, the nodal distribution of a body load is an even split between the two adjacent nodes. The third term in Eqn. 3-7 is the damping term. This is obtained as discussed in chapter 2. The equation of motion for the cable element is therefore given as shown in Eqn. 3-40.

$$[M]\{\ddot{d}_n\}+[C]\{\dot{d}_n\}+[K]\{\Delta d_n\} = \{F_j\}+\{g_s\}-\{R_E\} \qquad (3\text{-}40)$$

The solution to Eqn. 3-40 above can be obtained by a myriad of numerical integration schemes mentioned in chapter 2. When the cable element is assembled with the other element types, i.e. beams and connectors The R_E term in Eqn. 3-40 above can be replaced by a similar term F_E. Where F_E is the initial stress vector for all the elements in the structure.

$$[M]\{\ddot{d}_n\}+[C]\{\dot{d}_n\}+[K]\{\Delta d_n\} = \{F_j\}+\{g_s\}-\{F_E\} \qquad (3\text{-}41)$$

It should be noted that the self weight vector remains the same at the beginning of the time and at the end. The change in force due to the self weight is zero. When the wind load is considered the nodal force vector would include the wind force. At the beginning of each time step the incremental displacement vector is zero and the velocity and acceleration vector are as obtained from the previous time step analysis. The initial conditions of the dynamic analysis is obtained from setting both the displacement and velocity vectors to zero and obtaining the acceleration from equilibrium of the structure.

$$\{\ddot{d}_n\} = \frac{\{F_j\}+\{g_s\}-\{F_E\}}{[M]} \qquad (3\text{-}42)$$

The use of the incremental displacement facilitates the use of implicit numerical integration schemes for solution to Eqn. 3-41. Chapter 2 discusses the Newmark Beta method. This method in its modified form was adopted by the writer. The modification adopted is presented in the following section. This modification is referred to as the alpha modification.

Modified Newmark Beta Method

Due to the inherent problem of "blow up" in the analytically unstable traffic signal cable system and the fact that the unconditionally stable Newmark Beta method possesses no intrinsic numerical damping, Wood et al [20] proposed the use of an alpha factor. This factor introduces a positive artificial damping. This modified Newmark's method with positive artificial damping of higher vibrational modes is observed not only to reduce the "blow up" effect but also reduce the cumulative error which inevitably occurs in a numerical integration procedure.

Applying the alpha modification to Eqn. 3-40 results in an averaging effect of the inertia forces at the beginning and at the end of the time step.

$$(1-\alpha)[M]\{\ddot{d}_n\}_{t+\Delta t} + (\alpha)[M]\{\ddot{d}_n\}_t + [C]\{\dot{d}_n\}_{t+\Delta t} + [K]\{\Delta d_n\}_t = \{P_n\}_{t+\Delta t} \tag{3-43}$$

$$\left\{P_n\right\}_{t+\Delta t} = \left\{F_j\right\}_{t+\Delta t} + \left\{g_s\right\}_{t+\Delta t} - \left\{F_E\right\}_{t+\Delta t} \tag{3-44}$$

Note that if α is zero Eqn. 3-43 reduces to Eqn. 3-40. Apply Newmark's method based on Eqns. 3-45 and 3-46 to Eqn. 3-44. For convenience the nodal designation is dropped for Eqn. 3-45 to Eqn 3-50. It should however be understood that these are nodal displacement, velocity and acceleration.

$$\dot{d}_{t+\Delta t} = \dot{d}_t + \left[(1-\gamma)\Delta t\right]\ddot{d}_t + (\gamma\,\Delta t)\ddot{d}_{t+\Delta t} \tag{3-45}$$

$$d_{t+\Delta t} = d_t + (\Delta t)\dot{d}_t + \left[\left(\tfrac{1}{2}-\beta\right)(\Delta t)^2\right]\ddot{d}_t + \left[\beta(\Delta t)^2\right]\ddot{d}_{t+\Delta t} \tag{3-46}$$

Solving Eqn. 3-46 for acceleration at time t + Δt yields Eqn. 3-47.

$$\ddot{d}_{t+\Delta t} = \frac{1}{\beta\Delta t^2}\Delta d_t - \frac{1}{\beta\Delta t}\dot{d}_t - \left(\frac{1}{2\beta}-1\right)\ddot{d}_t \tag{3-47}$$

Substituting Eqn. 3-47 into 3-45 yields Eqn. 3-48.

$$\dot{d}_{t+\Delta t} = \frac{\gamma}{\beta\Delta t}\Delta d_t - \left(\frac{\gamma}{\beta}-1\right)\dot{d}_t + \Delta t\left(1-\frac{\gamma}{2\beta}\right)\ddot{d}_t \tag{3-48}$$

Following the steps described in chapter 2 and substituting Eqn. 3-47 and 3-48 into Eqn. 3-43, the final expressions for the effective stiffness and load vectors are obtained.

$$(1-\alpha)[M]\left\{\frac{1}{\beta\Delta t^2}\Delta d_t - \frac{1}{\beta\Delta t}\dot{d}_t - \left(\frac{1}{2\beta}-1\right)\ddot{d}_t\right\} + \alpha[M]\ddot{d}_t + [C]\left\{\frac{\gamma}{\beta\Delta t}\Delta d_t - \left(\frac{\gamma}{\beta}-1\right)\dot{d}_t + \Delta t\left(1-\frac{\gamma}{2\beta}\right)\ddot{d}_t\right\}$$
$$+ \; [K]\{\Delta d_t\} \; = \; \{P_{t+\Delta t}\}$$

(3-49)

Note that

$$\{\Delta d_t\} = \{d_{t+\Delta t}\} - \{d_t\} \tag{3-50}$$

Collecting terms and rearranging Eqn. 3-49 gives Eqn. 3-51.

$$[\hat{K}]\{\Delta d_n\}_t \;=\; [\Delta \hat{P}] \tag{3-51}$$

$$[\hat{K}] \;=\; (1-\alpha)[M]\left(\frac{1}{\beta\Delta t^2}\right) \;+\; [C]\left(\frac{\gamma}{\beta\Delta t}\right) \;+\; [K] \tag{3-52}$$

$$\{\hat{P}_n\} \;=\; \{P_n\}_{t+\Delta t} + [M]\left\{\frac{(1-\alpha)}{\beta\Delta t}\{\dot{d}_n\}_t + \left(\frac{1}{2\beta}-1\right)(1-\alpha)\{\ddot{d}_n\}_t - \alpha\{\ddot{d}_n\}_t\right\} + [C]\left\{\left(\frac{\gamma}{\beta}-1\right)\{\dot{d}_n\}_t + \Delta t\left(\frac{\gamma}{2\beta}-1\right)\{\ddot{d}_n\}_t\right\}$$

(3-53)

When α is zero the above described Newmark's method reduces to that described in chapter 2. The values of β and γ are as described in chapter 2. If the alpha modification is to be used, the values of the constants are given below.

When β = ¼ and γ = ½ for the regular Newmark's method, the constant acceleration method is obtained. This method is a second order solution with zero artificial damping and unconditional stability. The intent of the alpha factor is to insert positive artificial damping while keeping the property of unconditional stability. For a second order method with positive artificial damping and unconditional stability the following condition must be satisfied.

$$\beta \geq \frac{\gamma}{2} \geq \frac{1}{4} \quad \& \quad \alpha \leq \frac{1}{2} \quad \& \quad \alpha + \gamma \geq \frac{1}{2} \tag{3-54}$$

Wood et al [18] in their paper suggest the use of the following as giving the best results.

$\alpha = 0.1 \qquad \beta = 0.3025 \qquad \gamma = 0.6$

$\alpha = -0.1 \qquad \beta = 0.5 \qquad \gamma = 0.6$

$\alpha = -0.1 \qquad \beta = 0.3025 \qquad \gamma = 0.6$

The writer suggests the use of $\alpha = 0.1 \quad \beta = 0.3025 \quad \gamma = 0.6$ for the traffic signal cable system as it yields the best artificial damping effect for the system. When the incremental displacement is obtained from Eqn. 3-51, in order to maintain dynamic equilibrium, this computed incremental displacement needs to be refined. The reasons for the need of refinement are as follows;

a) The stiffness matrix at time t + Δt is dependent on the recently computed displacements values.

b) The $\{F_E\}$ term in the equation of motion contain values dependent on the nonlinear cable stiffness and nonlinear connector stiffness.

The Newton-Raphson method is adopted to refine the computed incremental displacements. Application of the Newton - Raphson is discussed next.

Modified Newton Raphson Method

A graphical representation of the steps involved in the modified Newton Raphson method is given in Fig. 3.2. There are two additional modifications made to the regular non-recursive Newton - Raphson procedure [9], [14]. One has to do with the nonlinear loading and the other the nonlinear stiffness of the cable elements. Note that both the loading and the stiffness are dependent on the incremental displacements being computed. The writer has taken these into account in modifying the Newton - Raphson procedure adopted.

Recall from Eqn. 3-41 that,

$$\{P\} = \{F_j\} - \{R_E\} \qquad (3\text{-}55)$$

$\{F_j\}$ = Applied nodal loads. These consist of dead weight of cladding and/or wind loads applied at the nodal points. Discussion of loading on the traffic signal cable system is presented in chapter 4.

$\{R_E\}$ = Equivalent nodal force vector for member stress at time t. This accounts for the stresses in the structure at the beginning of the time step.

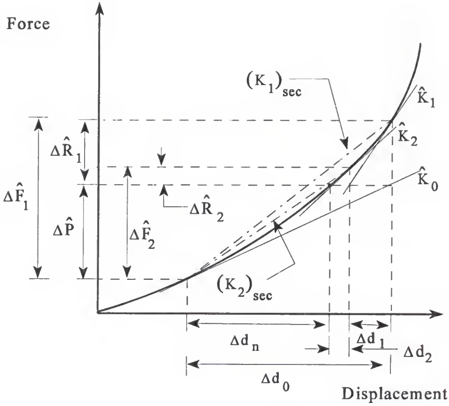

Fig. 3.2 Newton - Raphson Iteration

The complete procedure to refine Δd_o shown in Fig. 3.2 on the previous page is given to illustrate the modified Newton-Raphson method :

1. Initialize data.

$$\hat{K}_o = [\hat{K}] \quad \textit{From Eqn}\,(3-52)$$
$$\hat{P} = \{\hat{P}_n\} \quad \textit{From Eqn}\,(3-53)$$
$$\Delta\hat{R}_o = \hat{P}$$
$$\Delta d_o = \hat{K}_o^{-1}\,\Delta R \quad \textit{From Eqn}\,(3-51)$$

In computing the above initial values, ΔP is assumed to be zero in Eqn. 3-53. It is assumed that if Δt is taken small enough the approximation error introduced by this assumption is negligible.

2. Compute the instantaneous cable stiffness at a displacement Δd_o and set it equal to $\hat{K}_1$.

3. The incremental resisting force:

$$\Delta\hat{F}_1 = (K_1)_{\sec}\,\Delta d_o \tag{3-56}$$

Where the secant stiffness $(K_1)_{sec}$ can be approximated by Eqn. 3-57.

$$(K_i)_{\sec} = \frac{\hat{K}_0 + \hat{K}_i}{2} \tag{3-57}$$

$$\therefore \quad \Delta F_1 = \frac{\Delta \hat{R}_o + \hat{K}_1 \, \Delta d_o}{2} \tag{3-58}$$

4. The residual force at the end of the first iteration is as shown in Eqn. 3-59

$$\Delta \hat{R}_1 = \hat{P} - \Delta F_1 \tag{3-59}$$

5. Δd_1 is computed as in step 1.

$$\Delta d_1 = \hat{K}_1^{-1} \, \Delta \hat{R}_1 \tag{3-60}$$

The sign of the displacement computed in Eqn. 3-60 is negative because the residual force is negative.

6. Repeat step 2, compute $\hat{K}_2$.

7. Repeat step 3, compute new resisting force.

$$\therefore \quad \Delta F_2 = \frac{\hat{K}_0 \left(\Delta d_0 + \Delta d_1\right) + \hat{K}_2 \left(\Delta d_0 + \Delta d_1\right)}{2} \tag{3-61}$$

8. Repeat step 4, compute the residual force.

$$\Delta \hat{R}_2 = \hat{P} - \Delta F_2$$

9. Using Eqn. 3-60 above compute Δd_2. The whole procedure is continued until the residual force is smaller than some tolerance value. The true

displacement, therefore, is as given in Eqn. 3-62.

$$\Delta d_n = \Delta d_o + \Delta d_1 + \Delta d_2 \tag{3-62}$$

There are many convergence checks that could be used. Some authors suggest a check on subsequent displacement computations; that is

$$\frac{\Delta d_i}{\Delta d_n} \leq \xi \qquad i = 0,1,2 \ldots \tag{3-63}$$

where ξ is a prescribed tolerance. The problem faced when convergence is strictly based on the convergence of the nodal displacement is that of different rates of convergence for rotational displacements and translational displacements. The units and range of values for rotations differ greatly compared to translations. As a result the translational displacements may converge while the rotational displacements may not simultaneously converge. The writer has chosen a convergence criterion based on the work done by the residual forces.

$$\left| \frac{\left\{\Delta \hat{R}_i\right\}^T \Delta d_i}{\left\{\Delta \hat{P}\right\}^T \Delta d_n} \right| \leq \xi \qquad i = 0,1,2 \ldots \tag{3-64}$$

The use of the modified Newmark's method and the above described Newton-Raphson method in the entire solution procedure is described next.

Solution Algorithm

Based on the theory developed in the previous sections of this chapter the solution to the equation of motion given in Eqn. 3-40 was obtained as follows.

1. Compute the effective load vector as given in Eqn. 3-53. Note that ΔP is given by the right hand side of Eqn. 3-41. For the first time step analysis ΔP is taken to be zero. At the end of each time step $P_{t+\Delta t}$ is computed and the actual change in load, ΔP, for that time step is obtained. This change in load is used as the estimate for the next time step analysis. The acceleration at the beginning of each time step is, however, obtained by imposing total equilibrium at the end of the previous time step and using the true load in the equilibrium equation.

2. Compute the effective stiffness matrix using Eqn. 3-52. The initial effective stiffness matrix at time $t = 0$, uses $[K] = [K_E] + [K_A]$, where $[K_E]$ and $[K_A]$ are as defined in Eqn. 3-25 and 3-28. At subsequent times, the effective stiffness matrix uses $[K] = [K_E] + [K_L]$. The nonlinear stiffness $[K_L]$ is computed as given in Eqn. 3-26.

3. Solve for change in displacements.

$$\{\Delta d_n\} = [\hat{K}]_t^{-1}\{\hat{P}\}_t \tag{3-65}$$

4. The Newton Raphson iteration scheme is used to refine the incremental displacement obtained in Eqn. 3-65. The Newton-Raphson procedure gives a better estimate of $\{\Delta d_n\}$. This is done as shown in steps 1 - 9 on pages 83 - 85.

5. Compute the final condition at the end of the time step.

$$\{d_n\}_{t+\Delta t} = \{d_n\}_t + \{\Delta d_n\} \tag{3-66}$$

$$\{\dot{d}_n\}_{t+\Delta t} = \frac{\gamma}{\beta\,\Delta t}\Delta d_n + \left(1-\frac{\gamma}{\beta}\right)\{\dot{d}_n\}_t + \Delta t\left(1-\frac{\gamma}{2\beta}\right)\{\ddot{d}_n\}_t$$

(3-67)

$$\{\ddot{d}_n\}_{t+\Delta t} = \frac{\{P\}_{t+\Delta t} - \alpha[M]\{\ddot{d}_n\}_t - [C]\{\dot{d}_n\}_{t+\Delta t} - [K]\{\Delta d_n\}_t}{(1-\alpha)[M]}$$

(3-68)

6. Set the incremental displacement of the next time step as follows and repeat the above steps

$$\{\Delta d_n\} = \{0\}$$

The dynamic time step analysis is concluded when the free-vibration response dies down. The complete analysis gives the full dynamic response history for the transient dynamic loads applied and/or the equivalent static solution of the dead load applied. For the static equivalent solution the "die-down" criteria is as follows.

$$\frac{\left|\sum_{l}^{p}[K]\{\Delta d_n\}^2\right|}{p-l} - \frac{\left|\sum_{p}^{q}[K]\{\Delta d_n\}^2\right|}{q-p} \leq \xi \tag{3-69}$$

This means that the strain energy of the structure is averaged over several time steps and compared to the average of the next several time steps. When the difference between the two strain energies computed is negligible, die-down is achieved.

l, p and *q* are beginning and ending time step cycles for strain energy computation.

Solution Flowchart

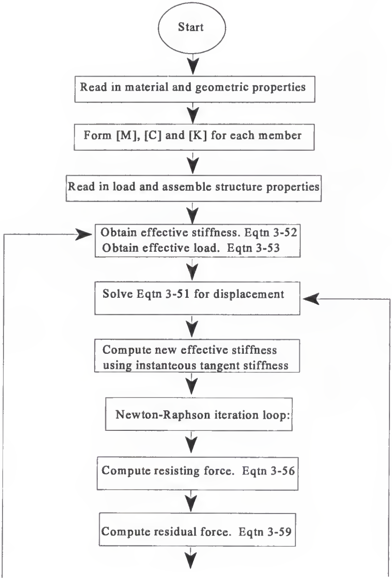
Start
Read in material and geometric properties
Form [M], [C] and [K] for each member
Read in load and assemble structure properties
Obtain effective stiffness. Eqtn 3-52
Obtain effective load. Eqtn 3-53
Solve Eqtn 3-51 for displacement
Compute new effective stiffness
using instanteous tangent stiffness
Newton-Raphson iteration loop:
Compute resisting force. Eqtn 3-56
Compute residual force. Eqtn 3-59

Continued on next page

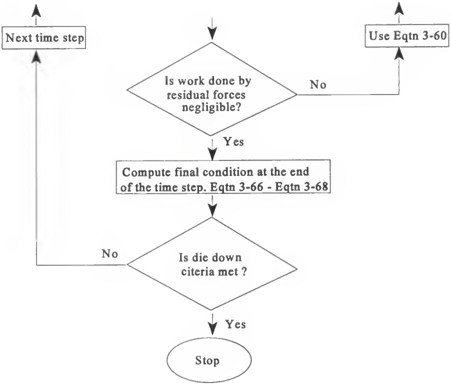
Next time step
Use Eqtn 3-60
Is work done by residual forces negligible?
No
Yes
Compute final condition at the end of the time step. Eqtn 3-66 - Eqtn 3-68
No
Is die down citeria met ?
Yes
Stop

Fig 3.3 Flowchart of Solution Algorithm

CHAPTER 4
LOADING

Introduction

The loads on the traffic signal system can be split into two categories. The dead load and the wind load. The dead load is the summation of the weight of the cable, weight of the signal.heads. The dead load assumed to be acting on the traffic light system is as given in Ref. [21]. The wind load acting on the structure is discussed in this chapter.

Two models of wind loading were developed. The variable area wind load model and the variable velocity dynamic wind load model. The variable wind load area model was largely developed in Ref. [21]. The application of this model is slightly different in this research. The variable velocity model is a simplified true wind simulation. Both models and their applications are discussed.

Variable Area Wind Load

The wind speed is assumed to be a constant for this model. The wind load is taken to act at the centroid of the traffic signal heads and the traffic signs. As the wind impacts the surfaces of these objects the wind pressure is taken to act normal to the these surfaces. The resultant normal force is resolved into the vertical uplift force and the horizontal drag force.

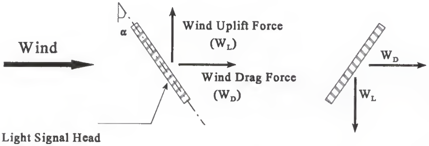

Fig. 4.1 Resolved Wind Load on Signals

The wind pressure is obtained directly from Bernoulli's general law for an ideal fluid.

$$p = \frac{\rho V^2}{2} = 0.002558 V^2 \quad lbs/ft^2 \tag{4-1}$$

ρ = mass density of air.

V = along-wind velocity. (ft/sec)

p = wind pressure (lbs/ft).

If wind gust is to be taken into account we introduce a factor F_z. The gust factor varies with height. The gust factor at any height is given by Eqn. 4-2 [24].

$$F_z = F_{30}\left(\frac{30}{z}\right)^{0.0625} \tag{4-2}$$

F_{30} = gust factor at 30 ft, recommended to be 1.30.

z = height of the centroid of the signal heads above ground.

For the structures being investigated, the gust factor is approximately 1.3 for height, z, of 17 ft. The final pressure equation becomes,

$$p = 0.002558(1.3V)^2 \tag{4-3}$$

The resolved forces are computed from Eqns. 4-4 and 4-5 respectively. These Eqns. introduces two coefficients, the lift and drag factors. These are used to account for the aspect ratio and orientation of the wind surface.

$$W_D = C_D\, p\, A \tag{4-4}$$

$$W_L = C_L\, p\, A \tag{4-5}$$

C_D = drag coefficient

C_L = lift coefficient

A = area of the wind surface

The drag and lift factors account for the reduction in the area impacted by wind as the signal head rotates. The drag and lift coefficients in Eqns 4-4 and 4-5 are given in Ref. [21] and [22] and are shown in Fig. 4.2.

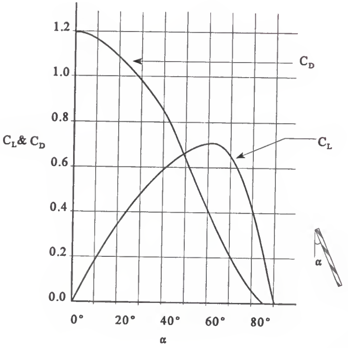

Fig. 4.2 Lift and Drag Coefficients

The expressions for the drag and lift coefficients shown in Fig. 4.2 is given by Eqns 4-7 and 4-8 [23].

$$C_D = 1.2 - 1.08\times10^{-2}\,\alpha - 4.16\times10^{-5}\,\alpha^2 \tag{4-7}$$

$$C_L = 2.32\times10^{-2}\alpha - 1.87\times10^{-4}\alpha^2 - 2.23\times10^{-6}\alpha^3 + 8.61\times10^{-8}\alpha^4 - 7.79\times10^{-10}\alpha^5 \tag{4-8}$$

Due to the fact that the signal heads are free swinging, the surface area impacted by the wind at any given time is dependent on the tensions in the cables and the corresponding deformations in the cables. For dynamic analysis, the time step method facilitates the computation of the angle α at every time step and hence the calculation of the new area impacted by the wind in each time step.

Variable Velocity Dynamic Wind Load

The wind speed in this model is taken to be the summation of a mean wind speed value and a fluctuating (or gust) component.

$$V(t) = \overline{V} + v(t) \tag{4-9}$$

The mean wind speed value is the same as in the previous wind load model. The fluctuating component can be obtained from experimental data or be artificially generated. The generation of artificial wind gust data is often the easier choice. A vast body of literature exists on the methods of artificially generating the gust component of wind. Only a brief presentation of the method adopted for this research is made. Further information can be obtained from the following references; Davenport [24], Chen and Ahamdi [25], Iannuzzi and Spinelli [26], Solari [27] [28] and Haritos [29].

The gust component of wind can be represented by a random process with a substantially Gaussian distribution. This means that the process has zero mean and a unit variance. The process is taken as stationary (i.e. invariant with time) and ergodic (i.e. the statistics of the sample are the same as that for the ensemble). These assumptions are important because the theoretical derivation of the power spectrum from time records is only possible for a stationary process and for the wind sample generated to be realistic, the ensemble of random wind signals must be assumed spatially homogenous.

The longitudinal field of turbulence for a wind trace must conform to the following spectral density suggested by Davenport [24]:

$$S_v(\omega) = \frac{4\kappa {V_{10}}^2}{\omega} \frac{X^2}{\left(1+X^2\right)^{4/3}} \tag{4-10}$$

S_v = power spectrum density of horizontal gustiness at height z_{10}.

z_{10} is standard reference height and is set equal to 10 m. (33 ft.).

V_{10} = mean hourly wind velocity at the reference height (ft/sec).

ω = frequency (cycles/sec.).

κ = drag coefficient for ground disturbance at reference height.

See table from Ref. [24] below.

$$X = \frac{4000\,\omega}{V_{10}} \quad \left(\frac{\omega}{V_{10}} = \textit{wave number in cycles/ ft} \right)$$

Type of surface	*Drag coefficient (κ)*
Open terrain with very few obstacles: open grass or farmland with few trees, hedgerows etc.	*0.005*
Terrain uniformly covered with obstacles 30-50 ft in height : residential suburbs, small towns, small fields.	*0.015*
Terrain with large and irregular obstacles e.g. large cities, very broken country with many tall trees.	*0.050*

There are two methods of simulating the necessary random fields required, one is based on the superposition of sine and cosine functions. This is known as the wave superposition method [26] and the other is based on the use of numerical filters on sequences of random numbers, this is commonly referred to as linear filtering. For this research the later method is adopted. The random number sample generated must have a normal distribution given in Eqn 4-11 and shown in Fig. 4.3.

$$f(x) = \frac{1}{\sqrt{2\pi}} e^{-\frac{1}{2}x^2} \tag{4-11}$$

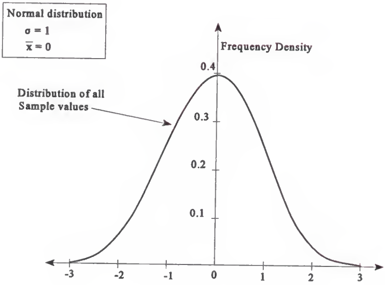

Fig 4.3 Distribution of sample generated

The random number generator similar to that proposed by Leva [30] is utilized here. This is a *normal* pseudorandom number generator. The numbers are generated using an acceptance-rejection technique. Each number generated is checked to see if it lies within an acceptable Gaussian distribution field.

The input for the normal random number generator is another random number generator, usually a flat spectral random number generator. The random number routine used could be the implicit rand() routine in Fortran 77 library or any other random number generator. The writer has chosen to use a random number generator provided in the standard C library. This random number routines generate numbers in the range [0,1] with a flat spectral density distribution. The routine, drand(), generates a sequence of 48-bit integer values, X_i, according to the linear congruential formula.

$$X_{i+1} = \left(a\,X_i + c\right) \bmod m$$

The default values for the Unix Sun system for the constants a, c, and m are

a = 5DEECE66D16 = 2736731631558

c = B16 = 138

m = 248

The routine drand must be initialized with a seed value, X_i. A default value exists for this but it is often advised not to use this. The seed value is provided to the computer by the user with the routine srand (*long seedval*). This routine is called once. Subsequent calls of drand uses the value last number returned as seed. This ensures the data is truly random and no seed is used twice.

The random data generated represents white noise. This must be filtered to conform to the spectral density function given in Eqn. 4-10. To do this another property of the spectral density, the covariance function must be considered. Iannuzzi and Spinelli [26] defined the covariance function using the Weiner-Khinchin co-spectrum equation. Their formulation accounted for certain along-wind fluctuations as would be evident if two objects in the path of the along-wind turbulence were separated by some distance. For the purpose of this research one object in the stream of the wind is considered, hence wind analysis of one signal process is sufficient as opposed to the correlation of two signal processes provided in Ref. [26]. The covariance function, in this case becomes the auto-covariance function (Eqn. 4-12). For the purpose of applying numerical filters the auto-covariance function shall be evaluated at five different lag times (τ). Values of τ chosen are given in Eqn. 4-13.

$$C_{XX}(\tau) = \int_0^\infty S(\omega) e^{-i 2\pi \omega \tau}\, d\omega = \int_0^\infty S(\omega) \cos(2\pi \omega \tau)\, d\omega \qquad (4\text{-}12)$$

$$\tau = n\,\Delta t \qquad n = -2, -1, 0, 1, 2 \qquad (4\text{-}13)$$

To be able to evaluate the integral given in Eqn. 4-12 it is important to understand another property of the spectral density function given in Eqn 4-10. This has to do with the frequency content of a typical gust wind. Using as an example a mean wind velocity of 60 mph and a drag coefficient of 0.05, the spectral density using Eqn. 4-10 yields Fig. 4.4 shown below.

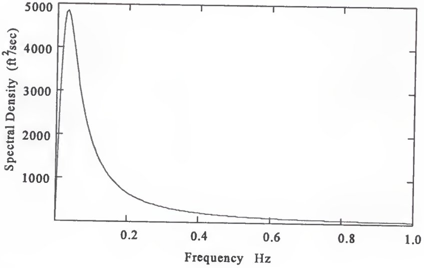

Fig. 4.4 Spectral density of fluctuating part of wind (V=60 mph)

It is observed that the spectral amplitude increases rapidly at small frequencies reaching a maximum at about 0.03 Hz. After which there is a rapid decay of spectral energy. By 0.2 Hz, 90% of the spectral energy is passed and by 1 Hz, the percentage is 99% . Therefore, for the integral given in Eqn. 4-12 a frequency integration limit of 0 - 1 Hz, in this case, represents the entirety of the spectrum. The expression, Eqn 4-12, could be solved exactly by using the theory of complex contour integration. However for this research numerical integration was chosen to solve the integral. Simpson's method is used. The largest positive frequency that would be the limit of integration is determined from the length of record of wind speed to be generated and the time interval of the wind record required. The smallest frequency that can be detected, referred to as the frequency resolution (or spectral resolution) f_o, is called the fundamental frequency. The largest frequency, f_q, is called the Nyquist frequency or the folding frequency.

$$f_o = \frac{1}{T_l} \tag{4-14}$$

$$f_q = \frac{N f_o}{2} \tag{4-15}$$

T_l = Length of record (sec)

N = Number of wind speed data (Must be an even number).

With the definition of the auto-covariance it is now possible to make the white noise generated by the random generators conform to the spectral density function of given in Eqn. 4-12. Several numerical filters have been used in the available body of literature to do this. Auto-regressive filters were chosen for this study because these have been proven to need the least computational time [26]. The only caveat is that the series generated using a time step of less than 0.1 sec tend to be divergent. For situations where the time step for structural response is smaller than 0.1 sec (as is often the case), linear interpolation schemes with wind data generated for a time step of 0.1 sec should be used.

Auto-regressive Filters

An auto-regressive filter of order p is given in Eqn. 4-16

$$v(t) = \sum_{m=1}^{p} a_m v(t - m\Delta t) + \varepsilon(t) \qquad (4\text{-}16)$$

$v(t)$ = new stream of filtered data with the spectral distribution in Eqn. 4-12. This represents the fluctuating portion of the wind.

a_m = auto-regressive parameters computed from the covariance functions.

$t, \Delta t$ = time and time increment of wind history.

p = order of regression. For this research p = 3 was chosen.

$$\varepsilon(t) = \sigma_x x(t) \qquad (4\text{-}17)$$

σ_x = standard deviation of the filtered random process. This can be computed from Eqn. 4-19.

The regression parameters can be computed from the system of linear equations obtained from Eqn. 4-18.

$$C_{XX}(j\Delta t) = \sum_{m=1}^{p} C_{XX}\left[(j-m)\Delta t\right] a_m \qquad j = 1, \dots p \tag{4-18}$$

$$\sigma_x^{\,2} \;=\; C_{XX}(0) + \sum_{m=1}^{p} a_m\, C_{XX}(m\Delta t) \tag{4-19}$$

Substituting the previously selected value of p equal to 3 into Eqn. 4-16 we obtain the following set of linear equations.

$$C_{XX}(\Delta t) = \quad C_{XX}(0)a_1 + C_{XX}(-\Delta t)a_2 + C_{XX}(-2\Delta t)a_3 \tag{4-20}$$

$$C_{XX}(2\Delta t) = \quad C_{XX}(\Delta t)a_1 + C_{XX}(0)a_2 + C_{XX}(-\Delta t)a_3 \tag{4-21}$$

$$C_{XX}(3\Delta t) = \quad C_{XX}(2\Delta t)a_1 + C_{XX}(\Delta t)a_2 + C_{XX}(0)a_3 \tag{4-22}$$

The parameters a_1, a_2, a_3 can be evaluated form Eqns 4-20, 4-21 and 4-22.

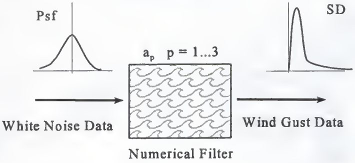

Psf - Probablity density function

SD - Spectral density function

Fig. 4.5 Numerical filtering Process

This procedure should result in a realistic variable wind trace. The final step is to check if the spectral density function of the variable wind speeds generated in Eqn. 4-16 is the same as that given in Eqn. 4-12. This is accomplished by computing the variance of the filtered data and compare this with the variance of the spectral density function in Eqn. 4-12. Both variances should be identical.

Since dynamic wind generated accounts for gust, the velocity computed in Eqn 4-9 is used in Eqn 4-1 instead of 4-3. The variable wind model equation, therefore, becomes

$$p = 0.002558\left(\overline{V} + v(t)\right)^2 \qquad (4\text{-}22)$$

The pressure value computed from Eqn. 4-22 is therefore used in the lift force and drag force equations as in the previous wind load model. A sample of an actual wind trace generated from the above method is shown in Fig. 4.6. The wind spectrum used for Fig. 4.6 is the same as that given in Fig.4.4.

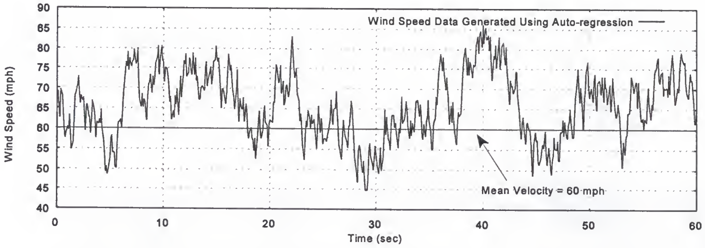

Fig. 4.6 Wind speed generated using the Spectral Density Function in Eqn 4-10

Test Data

A wind load test was performed on a traffic signal system. Details of the tests are given in Ref. [31]. The results from these experiments are compared with predictions from the program developed in this dissertation. Most of the comparisons of results are discussed in chapter 6. One comparison germane to this chapter is the comparison of the statistics of the raw wind velocities measured during these experiments to the spectral density function given in Eqn. 4-12. Before comparison can be made it should be noted that random data obtained were measured using low frequency anemometers of which examples are pitot static tubes, propellers and vane anemometers. In this case, Gill 3-Cup anemometers, Model 12102, were used. The readings obtained are biased by the response time of the instrument used. In addition, wind loading recorded were not natural wind events but were generated by propellers of air boats. The wind gusts generated by the air boats were therefore, atypical of the natural wind gusts in terms of randomness and duration of the events. Three different tests set-ups were considered (Fig. 4.7). The two-point connection signal system, the one-point connection signal system and another two-point connection signal system with near zero catenary sag. Only results from the first test set-up are considered in chapter 6 to verify the theories presented in this dissertation.

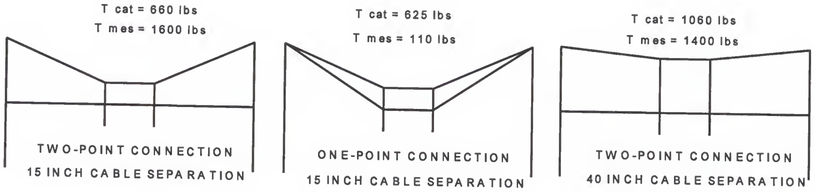

Fig. 4-7: Wind Load Test Systems with final cable tensions

The Results for test set-up # 3 are used in this chapter. The essence of comparisons in this chapter is to determine if the wind loads from the air boat wind simulation could be generated by the numerical wind simulation presented in this chapter.

Wind load was simulated in stages. The first stage is the low wind speed range, then a medium wind range and finally a high wind speed range. When the wind speed ensemble is taken the spectral density distribution is reflective of that given in Eqn. 4-10 as is apparent in Fig. 4-8 below.

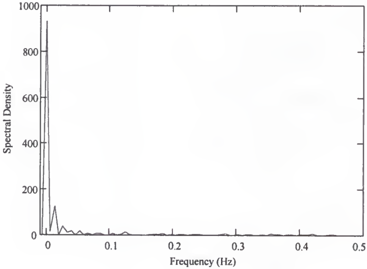

Fig. 4-8 Spectral Density (All wind speed ranges)

The wind samples collected, however, were observed not to be ergodic. This is as to be expected because wind mean velocity was forced to be varying in such a way as to allow for the partitioning of the data into the wind speed ranges mentioned above. The spectral density plots for the ranges are shown in Fig. 4.9 to Fig.4.11.

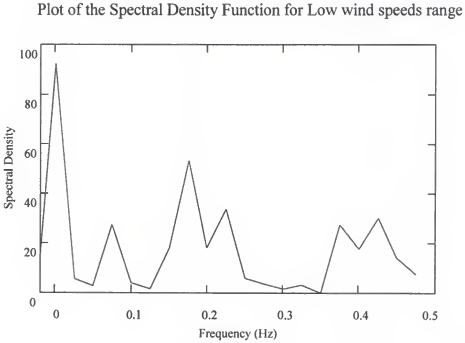

Fig. 4.9 Spectral Density (Low Wind Speeds)

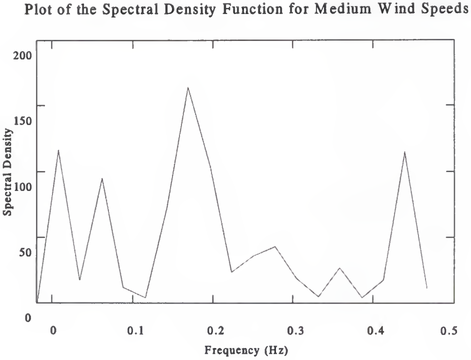

Fig. 4.10 Spectral Density (Medium Wind Speeds)

The wind speed trace generated by the air boats in the low and medium wind speed range obviously does not conform to the spectral distribution of the Fig. 4.4. This would have to be taken into consideration when comparing the results in chapter 6, since the results are compared in ranges. For the high wind speeds some correlation was observed with the spectral density distribution given in Fig. 4.4 as can be seen in Fig. 4.11.

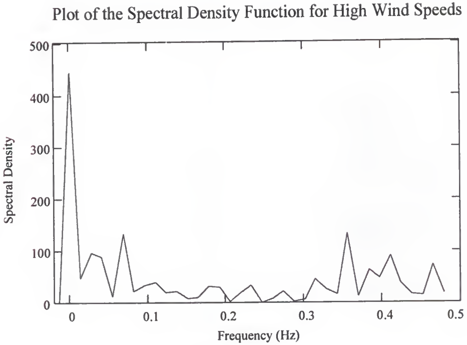

Fig. 4.11 Spectral Density (High Wind Speeds)

There apparent conclusion therefore is that numerical simulation can be used with some certainty of accuracy to predict the air boat wind fields for the entire wind speed ensemble but would not simulate the gradation in wind speed.

CHAPTER 5
PROGRAM VERIFICATION FOR STATIC LOADS

Static Problem Definition

Full scale static load tests were conducted on a Two-point traffic signal system. These tests, performed at the University of Florida Structural Laboratory, are used to verify the theories presented in this dissertation. Details of actual testing and instrumentation can be seen in Ref. [31]. For the purpose of subsequent discussion only the test system configuration, the sequence of load application and the pertinent test results are of importance. Prior to the static load test discussion a simpler single cable structure is used to verify the cable element developed.

This single cable structure was presented in a paper [32] by Baron and Vendatesan. The results from this paper was compared in Ref. [7, pg 113] to verify another method of analysis. Results from both references are compared here with results from DYNASS, the program developed in this dissertation.

Single Cable Structure Example

The single cable example is shown in Fig. 5.1 below. The area of the cable is 0.227 in^2 and E = 12 000 ksi. The corresponding self weight is 0.7945 lb/ft. Though the self weight was not considered in the static methods of analysis presented in Ref. [7] and [32], the weight is required for dynamic analysis and is hence included in DYNASS.

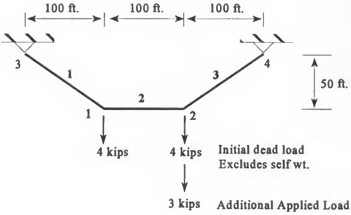

Fig 5.1 Single Cable Problem

For comparison in DYNASS, analysis is started from a slack no load state. The 4 kip loads are then applied for the prestressed state. Finally, the additional 3 kip load is added. The comparison of results is only done for the additional deflections due to the added 3 kip load and the stresses in the cable at final equilibrium. Deflection is compared only at nodes 1 and 2.

Table 5-1 Displacement Comparison for Suspended Cable

Node #	Component	Ref. [7] inches	Ref. [32] inches	DYNASS inches	% of diff. DYNAS-Ref. [7]	% of diff. DYNAS-Ref. [32]
1	x	26.00	26.28	25.47	-2.04	-3.08
	z	52.36	52.08	49.86	-4.77	-4.26
2	x	23.80	23.40	22.93	-3.66	-2.01
	z	-49.11	-48.48	-47.22	-3.85	-2.60

Table 5-2 Stress Comparison for Suspended Cable

Member #	Ref. [7] ksi	Ref. [32] ksi	DYNASS ksi	% of diff. DYNAS-Ref. [7]	% of diff. DYNAS-Ref. [32]
1	52.96	53.32	53.50	0.65	0.34
2	48.52	48.91	49.04	1.06	0.27
3	55.18	55.52	55.93	1.34	0.73

The cable element in DYNASS appears to be slightly stiffer than that assumed in the Ref. [7] and [32]. It should however, be noted that inherent in the assumptions in static solutions in Ref. [7] and [32] is the principle of superposition. This principle, according to some schools of thought, has been observed to overestimate structural response for non-linear problems. The analysis in DYNASS applies all load concurrently, hence does not use the principle of superposition. In addition, initial pre-tensioning of the cable due to its self weight is accounted for in DYNASS and not in the Ref. [7] and Ref. [32].

Static Test System Configuration

The traffic signal system tested is given in Fig. 5.2 also available in Ref. [31 - p 16]. The poles were made of 2 - W12×26 each braced in the plane of loading by a two double angle section (2L - 3½×3½×¼) and also in the out-of-plane, by a single angle section (L - 3×4×¼). A ¼ inch zinc coated steel wire was used for the messenger cable and a ⅜ inch zinc coated steel wire, for the catenary cable. The hanger/connectors were steel pipes 1½ inch in diameter. Actual signal heads were not used but the weight of a typical 3 light (12" lens), polycarbonate material plus disconnect box signal head was simulated. Properties of each member of the set-up is given in Table 5-3.

Table 5-3 Section Properties for Members shown Fig. 5-2

Member	**A** (in^2)	**I2** (in^4)	**I3** (in^4)	**J** (in^4)
Strain Pole (W12×26)	7.65	204	17.3	0.300
In-plane bracing (2L - 3½×3½×¼)	3.38	4.02	1.59	0.0386
Out-of-plane bracing (L - 3×4×¼)	1.69	2.77	1.36	0.0386
Pipe Connector (1½ ⌀)	0.799	0.31	0.31	0.620

The modulus of elasticity (E) used for all sections except for cables was 29000 ksi. For both cables, a young's modulus of 23000 ksi was deemed appropriate. The coordinates for each node fed into the program is as given in Table 5-4.

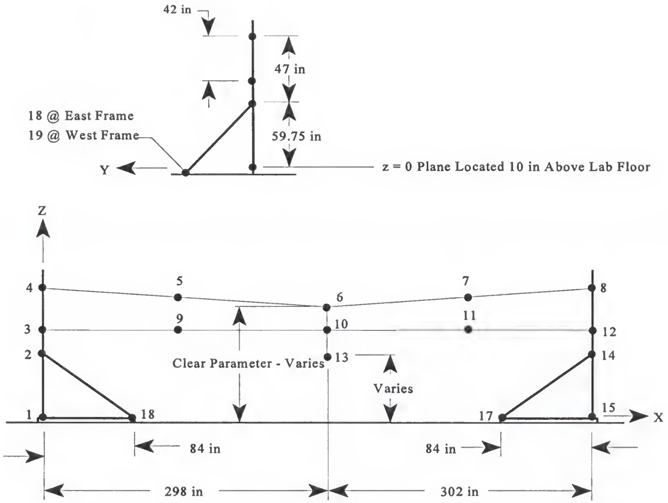

Fig. 5-2: Static Load Test System Dimensions and Node Numbers

Table 5-4 Dimensions and node coordinates for Fig. 5.2

Node	X (in)	Y (in)	Z (in)
1	0	0	0
2	0	0	59.75
3	0	0	80.75
4	0	0	122.75
5	149	0	c=1*
6	298	0	c=1*
7	449	0	c=1*
8	600	0	122.75
9	149	0	80.75
10	298	0	80.75
11	449	0	80.75
12	600	0	80.75
13	298	0	varies**
14	600	0	59.75
15	600	0	0
16	96	0	0
17	504	0	0
18	0	72	-10
19	600	72	-10

* This initial coordinate is computed by the program.

** Load was applied at varying heights for different tests.

Loading Sequence of Tests Performed

There were in all 3 static tests performed. The loading sequence and initial stress conditions for each test are given in Tables 5-5, 5-6 and 5-7.

Table 5-5 Loading Sequence for Test # 1

Test # 1			
Load Stages	Load Applied (lbs)		Comments
	Vertical	Lateral	
Initial conditions			Initial messenger cable tension was 1.141 kips. Initial catenary cable tension was 0.165 kips after the hanger weight alone was applied.
Stage 1	50.4	0	Hanger weight plus concentrated load. Sag in catenary cable was 3.633% after dead load application. Messenger cable was attached after dead had been applied.
Stage 2	50.4	29.0	Point of application of load was 46.375 in. from node 6.
Stage 3	50.4	56.3	
Stage 4	50.4	83.6	
Stage 5	50.4	101.2	Last load sequence.

Table 5-6 Loading Sequence for Test # 2

Test # 2			
Load Stages	Load Applied (lbs)		Comments
	Vertical	Lateral	
Initial conditions			Initial messenger cable tension was 1.127 kips. Initial catenary cable tension was 0.167 kips after hanger weight only.
Stage 1	60.4	0	Hanger weight plus concentrated load. Sag in catenary cable was 3.743% after the dead load application. Messenger cable was attached after dead load was applied.
Stage 2	60.4	29.0	Point of application of load was 46.375 in. from node 6.
Stage 3	60.4	56.3	
Stage 4	60.4	83.6	
Stage 5	60.4	119.6	Last load sequence.

Table 5-7 Loading Sequence for Test # 3

Test # 3			
Load Stages	Load Applied (lbs)		Comments
	Vertical	Lateral	
Initial conditions			Initial messenger cable tension was 1.046 kips. Initial catenary cable tension was 0.522 kips after hanger weight only.
Stage 1	70.4	0	The messenger cable was attached before application of the concentrated load. Sag in catenary cable was 1.112% after dead load application.
Stage 2	70.4	29.0	Point of application of load was 63.94 in. from node 6.
Stage 3	70.4	56.3	
Stage 4	70.4	83.6	
Stage 5	70.4	110.9	Last load sequence.

For test 3 the effect of sag was being investigated hence the drastic change in sag. The results from the above tests and their comparison to the predicted values from DYNASS is presented next.

Test Results and Predicted Values

The test results from the tests are tabulated against the values predicted from the DYNASS program. Results compared are displacements of nodes 6 (catenary cable) and 10 (messenger cable) and tension in the cables Since a dynamic theory has been used to approximate a static load case, plots showing the complete structural response including die-down is included for the dead load cases.

Table 5-8 Catenary Cable Results comparison for Test # 1

Loading	Test # 1 Result for Catenary Cable Node 6			Calculated Results for Catenary Cable Node 6		
	Tension (lbs)	Horizontal displ. (in.)	Vertical displ. (in.)	Tension (lbs)	Horizontal displ. (in.)	Vertical displ. (in.)
15.0 lb hanger hung from catenary cable	165	0	0	163.5	0	0
35.4 lb vertical load applied to hanger.	405	0.000	-1.125	406.1	0	-1.087
29.0 lb horizontal load applied to hanger.	454	1.668	-0.938	435.4	1.285	-1.513
Horizontal load increased to 56.3 lbs	528	2.532	-1.563	505.6	1.992	-1.683
Horizontal Load increased to 83.6 lbs	632	2.916	-1.938	590.6	2.257	-1.915
Horizontal load increased to 101.2 lbs	696	2.700	-2.000	644.4	2.275	-2.072

Table 5-9 Messenger Cable Results comparison for Test # 1

Loading	**Test # 1 Result for Messenger Cable Node 10**			**Calculated Results for Messenger Cable Node 10**		
	Tension (lbs)	Horizontal displ. (in.)	Vertical displ. (in.)	Tension (lbs)	Horizontal displ. (in.)	Vertical displ. (in.)
15.0 lb hanger hung from catenary cable	1141	0	0	1141.0	0	0
35.4 lb vertical load applied to hanger.	1129	0.000	0.000	1134	0	-0.002
29.0 lb horizontal load applied to hanger.	1227	-4.140	0.825	1183	-4.149	0.296
Horizontal load increased to 56.3 lbs	1388	-6.900	2.063	1335	-7.080	1.881
Horizontal Load increased to 83.6 lbs	1610	-9.300	3.156	1507	-9.209	3.011
Horizontal load increased to 101.2 lbs	1718	-10.368	4.375	1616	-10.306	3.644

Table 5-10 Catenary Cable Results comparison for Test # 2

Loading	**Test # 2 Result for Catenary Cable Node 6**			**Calculated Results for Catenary Cable Node 6**		
	Tension (lbs)	Horizontal displ. (in.)	Vertical displ. (in.)	Tension (lbs)	Horizontal displ. (in.)	Vertical displ. (in.)
15.0 lb hanger hung from catenary cable	167	0	0	168	0	0
45.0 lb vertical load applied to hanger.	460	0.000	-1.000	486.2	0	-1.304
29.0 lb horizontal load applied to hanger.	495	1.092	-0.875	502.3	0.763	-1.762
Horizontal load increased to 56.3 lbs	567	1.920	-1.031	556.1	1.320	-1.912
Horizontal Load increased to 83.6 lbs	639	2.364	-1.281	634.5	1.609	-2.131
Horizontal load increased to 119.6 lbs	747	2.484	-1.500	736.1	1.664	-2.437

Table 5-11 Messenger Cable Results comparison for Test # 2

Loading	**Test # 2 Result for Messenger Cable Node 10**			**Calculated Results for Messenger Cable Node 10**		
	Tension (lbs)	Horizontal displ. (in.)	Vertical displ. (in.)	Tension (lbs)	Horizontal displ. (in.)	Vertical displ. (in.)
15.0 lb hanger hung from catenary cable	1127	0	0	1127	0	0
45.0 lb vertical load applied to hanger.	1112	0.000	0.000	1118	0	-0.007
29.0 lb horizontal load applied to hanger.	1200	-3.936	0.596	1162	-4.073	0.500
Horizontal load increased to 56.3 lbs	1387	-6.996	1.737	1309	-7.011	1.503
Horizontal Load increased to 83.6 lbs	1566	-9.000	2.858	1477	-9.182	2.530
Horizontal load increased to 119.6 lbs	1808	-11.100	4.070	1695	-11.309	3.709

Table 5-12 Catenary Cable Results comparison for Test # 3

Loading	**Test # 3 Result for Catenary Cable Node 6**			**Calculated Results for Catenary Cable Node 6**		
	Tension (lbs)	Horizontal displ. (in.)	Vertical displ. (in.)	Tension (lbs)	Horizontal displ. (in.)	Vertical displ. (in.)
15.0 lb hanger hung from catenary cable	522	0	0	522.2	0	0
55.0 lb vertical load applied to hanger.	916	0.000	-2.875	843.2	0	-3.545
29.0 lb horizontal load applied to hanger.	942	1.020	-2.750	856.3	1.055	-3.594
Horizontal load increased to 56.3 lbs	993	2.628	-2.875	900.2	2.093	-3.747
Horizontal Load increased to 83.6 lbs	1078	3.564	-3.125	970.5	2.985	-3.993
Horizontal load increased to 110.9 lbs	1167	4.596	-3.250	1054	3.668	-4.302

Table 5-13 Messenger Cable Results comparison for Test # 3

Loading	**Test # 3 Result for Messenger Cable Node 10**			**Calculated Results for Messenger Cable Node 10**		
	Tension (lbs)	Horizontal displ. (in.)	Vertical displ. (in.)	Tension (lbs)	Horizontal displ. (in.)	Vertical displ. (in.)
15.0 lb hanger hung from catenary cable	1046	0	0	1046	0	0
55.0 lb vertical load applied to hanger.	1100	0.000	-2.50	1063	0.000	-3.126
29.0 lb horizontal load applied to hanger.	1222	-4.920	-1.875	1144	-4.591	-2.726
Horizontal load increased to 56.3 lbs	1388	-7.932	-1.000	1306	-7.910	-1.900
Horizontal Load increased to 83.6 lbs	1584	-10.308	-0.250	1488	-10.376	-0.984
Horizontal load increased to 110.9 lbs	1800	-12.408	0.625	1670	-12.285	-0.127

Discussion of Results

To best model the actual testing procedure as presented in Ref. [31]. The following analysis steps were adopted by the writer. For Test 1 and 2 the hanger was attached to the catenary cable alone prior the additional gravity load being attached. Both the hanger and the catenary cable were then attached to the messenger cable. In the analysis of the Test 1 and 2 set-up. The hanger self weight was applied to the catenary cable. The stresses and displacements for this load case was obtained and served as the base reference point. When the additional gravity load is applied the change in the configuration from the reference configuration is compared with what was measured. For the application of the lateral loads the prestressed configuration from the gravity load case served as input. A pre-tensioning of the connector element is done to ensure that the gravity load pick-up by the messenger cable is minimized. This procedure is observed to follow the actual testing procedure within limits of experimental error.

Comparing tension computations for the static tests, a good match is observed for tests 1 and 2 with the maximum percent difference of 3.82%. For test 3, however, there is a larger difference with a percent difference of 7.67%. It should be noted that loading procedure for test 3 was changed in the middle of testing. The hanger was connected before the additional gravity load was applied. This caused some relaxation in the catenary cable. The near zero sag for test 3 could also be a factor in the resulting difference between the measured and the computed tensions, this is because absolute zero sag in the catenary cable causes numerical floating errors in the analysis method adopted. Fig. 5.3 to Fig. 5.5 show graphically the change in tension relative to the change in lateral load.

The differences in displacements measured to that computed was more varied and less consistent than with the tension differences. This is probably due to the fact that the relative difference in displacement is an average of half an inch. The readings in the lab were observed to fluctuate more than half an inch. Hence, the difficulty in establishing if the variations are due to non-conforming results or experimental errors. The results, nevertheless validate the theories espoused by this research. Displacement comparisons are seen shown in Tables 5-17 to Table 5-19. The dynamic response of the structure is best seen with a plot of a nodal displacement with time. The structural response of the starting configuration, i.e. hanger weight load case, is shown in Fig. 5.6 to Fig. 5.8. The regions of structural instability are identified in each plot for test 1 and 2. The behavior of the test 3 was decisively different but is included for completeness. The regions identified are points where the structural response had been observed to diverge when a larger time step is used in the analysis.

Table 5-14 Test 1 - Cable Tensions

Comments	Loads	Measured	Data	Computed	Data	% difference	
Test #1		Catenary	Messenger	Catenary	Messenger	Catenary	Messenger
	(lbs)	(lbs)	(lbs)	(lbs)	(lbs)		
Gravity	15	165	1141	163.5	1141	0.91%	0.00%
	50.4	405	1129	406.1	1134	-0.27%	-0.44%
Lateral	29	454	1227	435.4	1183	4.10%	3.59%
	56.3	528	1388	505.6	1335	4.24%	3.82%
	83.6	632	1610	590.6	1507	6.55%	6.40%
	101.2	696	1718	644.4	1616	7.41%	5.94%
					Mean =	**3.82%**	**3.22%**
				Standard	**Deviation =**	**0.0302792**	**0.028899**

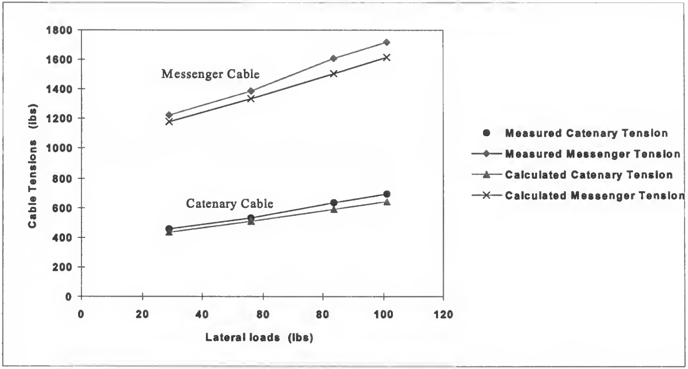

Fig. 5.3 Cable tensions Static Test #1

Table 5-15 Test 2 - Cable Tensions

Comments	**Loads**	**Measured**	**Data**	**Computed**	**Data**	**% difference**	
Test #2		Catenary	Messenger	Catenary	Messenger	Catenary	Messenger
	(lbs)	(lbs)	(lbs)	(lbs)	(lbs)		
Gravity	15	167	1127	168	1127	-0.60%	0.00%
	50.4	460	1112	486.2	1118	-5.70%	-0.54%
Lateral	29	495	1200	502.3	1162	-1.47%	3.17%
	56.3	567	1387	556.1	1309	1.92%	5.62%
	83.6	639	1566	634.5	1477	0.70%	5.68%
	119.6	747	1808	736.1	1695	1.46%	6.25%
					Mean =	**-0.61%**	**3.36%**
				Standard	**Deviation =**	**0.0279404**	**0.030135**

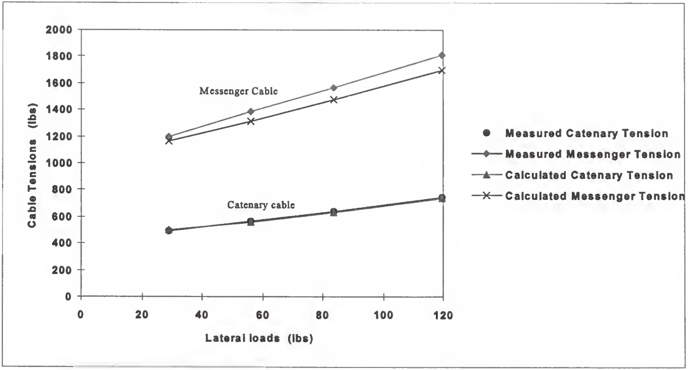

Fig. 5.4 Cable Tensions - Static Test 2

Table 5-16 Test 3 - Cable Tensions

Comments	Loads	Measured Data		Computed Data		% difference	
Test #3		Catenary	Messenger	Catenary	Messenger	Catenary	Messenger
	(lbs)	(lbs)	(lbs)	(lbs)	(lbs)		
Gravity	15	522	1046	522.2	1046	-0.04%	0.00%
	50.4	916	1100	843.2	1063	7.95%	3.36%
Lateral	29	942	1222	856.3	1144	9.10%	6.38%
	56.3	993	1388	900.2	1306	9.35%	5.91%
	83.6	1078	1584	970.5	1488	9.97%	6.06%
	119.6	1167	1800	1054	1670	9.68%	7.22%
					Mean =	**7.67%**	**4.82%**
				Standard	**Deviation =**	**0.04**	**0.03**

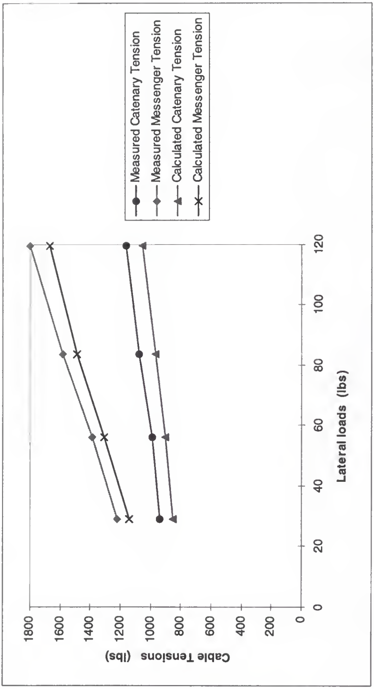

Fig. 5.5 Cable Tensions - Static Test 3

Table 5-17 Displacement Comparisons for Test 1

Comments	Loads	Measured	Data	Computed	Data	Absolute	difference
Test #1		Lateral	Vertical	Lateral	Vertical	Lateral	Vertical
Catenary	(lbs)	(in.)	(in.)	(in.)	(in.)	(in.)	(in.)
Gravity	15	0	0	0	0	0.00	0.00
	50.4	0	-1.125	0	-1.087	0.00	0.03
Lateral	29	1.668	-0.938	1.285	-1.513	0.23	-0.38
	56.3	2.532	-1.563	1.992	-1.683	0.21	-0.08
	83.6	2.916	-1.938	2.257	-1.915	0.23	0.01
	101.2	2.7	-2	2.275	-2.072	0.16	-0.04
					Mean =	**0.14**	**-0.07**
				Standard	**Deviation =**	**0.11**	**0.15**

Comments	Loads	Measured	Data	Computed	Data	Absolute	difference
Test #1		Lateral	Vertical	Lateral	Vertical	Lateral	Vertical
Messenger	(lbs)	(in.)	(in.)	(in.)	(in.)	(in.)	(in.)
Gravity	15	0	0	0	0	0.00	0.00
	50.4	0	0	0	0	0.00	0.00
Lateral	29	-4.14	0.825	-4.149	0.296	0.00	0.64
	56.3	-6.9	2.063	-7.08	1.881	-0.03	0.09
	83.6	-9.3	3.156	-9.209	3.011	0.01	0.05
	101.2	-10.368	4.375	-10.306	3.644	0.01	0.17
					Mean =	**0.00**	**0.16**
				Standard	**Deviation =**	**0.01**	**0.25**

Table 5-18 Displacement Comparisons for Test 2

Comments	Loads	Measured	Data	Computed	Data	Absolute	difference
Test #2		Lateral	Vertical	Lateral	Vertical	Lateral	Vertical
Catenary	(lbs)	(in.)	(in.)	(in.)	(in.)		
Gravity	15	0	0	0	0	0.00	0.00
	50.4	0	-1	0	-1.304	0.00	0.30
Lateral	29	1.092	-0.875	0.763	-1.762	0.33	0.89
	56.3	1.92	-1.031	1.32	-1.912	0.60	0.88
	83.6	2.364	-1.281	1.609	-2.131	0.76	0.85
	110.9	2.484	-1.5	1.664	-2.437	0.82	0.94
					Mean =	**0.42**	**0.64**
				Standard	**Deviation =**	**0.36**	**0.39**

Comments	Loads	Measured	Data	Computed	Data	Absolute	difference
Test #2		Lateral	Vertical	Lateral	Vertical	Lateral	Vertical
Messenger	(lbs)	(in.)	(in.)	(in.)	(in.)		
Gravity	15	0	0	0	0	0.00	0.00
	50.4	0	0	0	-0.007	0.00	0.01
Lateral	29	-3.936	0.596	-4.073	0.5	0.14	0.10
	56.3	-6.996	1.737	-7.011	1.503	0.01	0.23
	83.6	-9	2.858	-9.182	2.53	0.18	0.33
	110.9	-11.1	4.07	-11.309	3.709	0.21	0.36
					Mean =	**0.09**	**0.17**
				Standard	**Deviation =**	**0.10**	**0.16**

Table 5-19 Displacement Comparison for Test 3

Comments	Loads	Measured	Data	Computed	Data	Absolute	difference
Test #3		Lateral	Vertical	Lateral	Vertical	Lateral	Vertical
Catenary	(lbs)	(in.)	(in.)	(in.)	(in.)	(in.)	(in.)
Gravity	15	0	0	0	0	0.00	0.00
	50.4	0	-2.875	0	-3.545	0.00	0.67
Lateral	29	1.02	-2.75	1.055	-3.594	-0.03	0.84
	56.3	2.628	-2.875	2.093	-3.747	0.54	0.87
	83.6	3.564	-3.125	2.985	-3.993	0.58	0.87
	119.6	4.596	-3.25	3.668	-4.302	0.93	1.05
					Mean =	**0.33**	**0.72**
				Standard	Deviation =	**0.40**	**0.37**

Comments	Loads	Measured	Data	Computed	Data	Absolute	difference
Test #3		Lateral	Vertical	Lateral	Vertical	Lateral	Vertical
Messenger	(lbs)	(in.)	(in.)	(in.)	(in.)	(in.)	(in.)
Gravity	15	0	0	0	0	0.00	0.00
	50.4	0	-2.5	0	-3.126	0.00	0.63
Lateral	29	-4.92	-1.875	-4.591	-2.726	-0.33	0.85
	56.3	-7.932	-1	-7.91	-1.9	-0.02	0.90
	83.6	-10.308	-0.25	-10.376	-0.984	0.07	0.73
	119.6	-12.408	0.625	-12.285	-0.127	-0.12	0.75
					Mean =	**-0.07**	**0.64**
				Standard	Deviation =	**0.14**	**0.33**

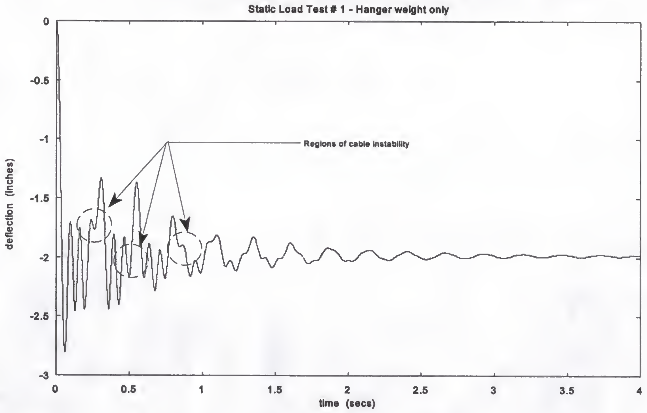

Fig. 5.6 Dynamic Structural Response at Catenary Node 6 (Test 1)

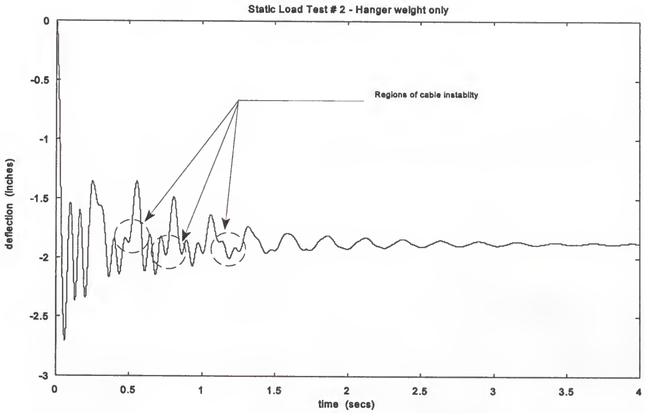

Fig. 5.7 Dynamic Structural Response of Catenary Node 6 (Test 2)

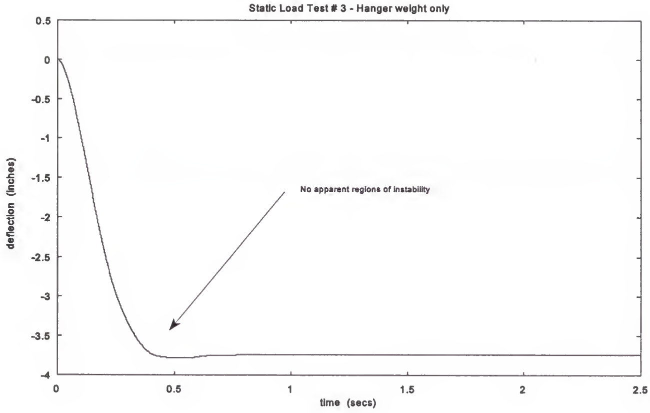

Fig. 5.8 Structural Response of Catenary Node 6 (Test 3)

CHAPTER 6
PROGRAM VERIFICATION FOR DYNAMIC LOADS

The Structure's Configuration

A full scale two-point traffic signal system was tested at the University of Florida. The span of the structure was typical of a four lane road. Details of the actual tests can be found in Ref. [31]. The system set-up and node numbering is shown in Fig. 6.1. The strain poles used were type N-V prestressed poles with concrete strength, f_c', of 6000 psi. The catenary and messenger cables were both ⅜ in. ⌀ cables. Cables were connected using strap connectors and/or 1-½ in. ⌀ steel pipes. The traffic signals mounted were 2 - 5 head light signals, 12" lens, Aluminum, no backplate and one-way bracket. The wind load applied was predominantly in the out-of-plane direction. In-plane wind forces are neglected. The devised wind loading method involved the use of air boats to create the wind fields. Wind velocity was varied between 10 mph and 100 mph to simulate gust.

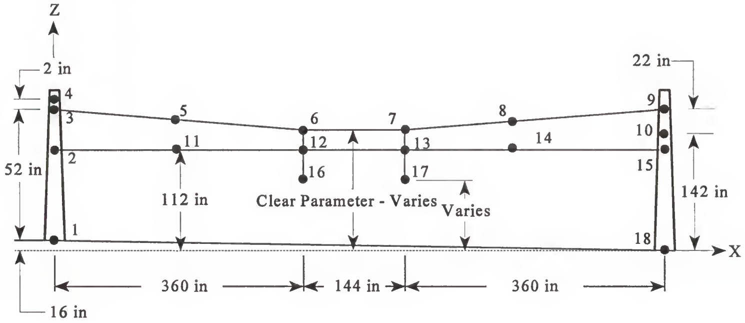

Fig. 6.1 Wind Load Test System Dimension and Node Numbering

Coordinates of Wind Load Test System Configuration:

Table 6-1 Dimensions and node coordinates for Fig. 6.1

Node	X (in)	Y (in)	Z (in)
1	0	0	16
2	0	0	112
3	0	0	164
4	0	0	166
5	180	0	c=1*
6	360	0	c=1*
7	504	0	c=1*
8	684	0	c=1*
9	864	0	164
10	864	0	142
11	180	0	112
12	360	0	112
13	504	0	112
14	684	0	112
15	864	0	112
16	360	0	112-27.3
17	504	0	112-27.3
18	864	72	0

* This initial coordinate is computed by the program.

Wind Test Set-up

The poles were tapered beams but are modeled as piece wise prismatic beam. This, of course, introduces some approximations in the analysis. It is considered, however, not to be significant. The poles were also prestressed. To adequately model this, the young modulus of the poles were selected such as to yield the 1 inch displacement at the top. Each pole was pre-loaded prior to testing to obtain the force that would produce 1 inch deflection at the top. Ignoring shear deformation, the required EI was then computed. This also accounted for possible movement in the foundation. The foundation for the poles required an embedment length of five to six feet. Back fill earthwork was used around the pole footing instead of concrete for ease of removal. The properties of the pole were chosen such that the EI value of pole 1 is 3,550,000 kip-in^2 and the EI value for pole 2 is 3,280,000 kip-in^2.

Table 6-2 Section Properties for Members shown Fig. 6.1

Section	Properties		
	Young's Modulus (ksi)	Area (in^2)	Moment of Inertia (in^4)
Poles	4000	93.4	I_2=888 I_3=888 J=484
	4000	93.4	I_2=820 I_3=820 J=484
Cables Mess. & Cat.	23000	0.079	---
Connectors 1-½ inch pipe	29000	0.799	I_2=0.310 I_3=0.310 J=0.620
strap	29000	0.5324	I_2=0.167 I_3=0.0153 J=0.500

Description of Wind Load Test

Three Wind load tests systems were considered in Ref. [31]. A two-point connection system, refer to Fig. 4.7, a one-point connection system where both the messenger and catenary cables are both connected to the same point on the poles, and a two-point connection system with drastically reduced sag. For the purpose of this dissertation only the first test system is considered. This is because the aim is to verify the theories presented in this dissertation.

Comparison of Results

For the dynamic tests, the author has chosen to concentrate only on the variation in cable tensions in relation to the variation in wind velocities. The loading pattern adopted is described next. The dead loads were applied first. The signals were hung directly from the catenary cable using disconnect boxes and hangers. The pipe hanger was used for the East signal which lie along nodes 6, 14 and 17 in Fig. 6.1. This was the only signal instrumented for lateral displacements. The strap hanger was used for the West signal along nodes 7, 15 and 18 in Fig. 6.1. Wind load was applied using the air boats at three stages: a low speed range between 33 to 46 mph, a medium speed range of 47 mph to 64 mph and a high speed range of 73 mph to 99 mph. The wind load generated on the signals were kept similar as best as possible. The range of difference of wind speeds applied to the signals vary from about 7 mph to a maximum of 11 mph. The duration of each test was 13 sec. The average wind speed for the low wind speed range is 41.684 mph (West Signal) and 38.198 mph (East Signal). The average wind speed for the medium wind speed range is 53.146 mph (West Signal) and 51.819 mph (East Signal). The average wind speed for the high wind speed range is 88.173 mph (West Signal) and 104.178 mph (East Signal).

Test Data

The initial tensions in the cables prior to application of wind loading are 843 lbs in the catenary cable and 725 lbs in the messenger cable. For Low wind speed range the data obtained from the 2 point connection test set-up is shown in Table 6-2.

Table 6-3 Wind Data for Low Wind Speed Test

Time (hr:min:sec)	Catenary Cable Tension (lb)	Messenger Cable Tension (lb)	West Air boat Wind Speed (mph)	East Air boat Wind Speed (mph)
10:52:18	741.4	993.6	38.5	38.8
10:52:19	773.6	975.4	38.7	40.7
10:52:20	750.2	1014.3	41.0	39.1
10:52:21	770.6	997.7	44.1	36.4
10:52:22	722.1	1036.6	42.1	38.0
10:52:23	762.9	1000.1	39.6	38.4
10:52:24	736.7	1033.2	41.6	39.2
10:52:25	713.8	1051.4	43.3	35.9
10:52:26	744.3	1021.8	43.2	39.6
10:52:27	712.7	1052.7	43.0	36.0
10:52:28	760.5	1005.8	41.9	39.1
10:52:29	725.5	1005.3	42.6	36.9
10:52:30	724.8	1021.7	42.4	38.5
Averages	**741.5**	**1016.1**	**41.7**	**38.2**

For medium wind speed range the data obtained from the 2 point- connection test set-up is shown in Table 6-3.

Table 6-4 Wind Data for Medium Wind Speed Test

Time (hr:min:sec)	Catenary Cable Tension (lb)	Messenger Cable Tension (lb)	West Air boat Wind Speed (mph)	East Air boat Wind Speed (mph)
10:52:49	702.3	1155.2	51.2	54.7
10:52:50	709.1	1202.6	51.4	56.6
10:52:51	734.6	1182.2	52.2	48.7
10:52:52	750.6	1174.0	52.3	53.1
10:52:53	727.6	1178.5	49.7	54.7
10:52:54	744.8	1178.1	54.2	57.3
10:52:55	735.9	1203.9	54.3	54.1
10:52:56	734.3	1196.1	52.1	54.4
10:52:57	737.0	1197.9	55.0	47.6
10:52:58	740.9	1164.6	52.4	53.1
10:52:59	734.0	1152.3	52.3	43.1
10:53:00	705.1	1168.1	55.7	44.8
10:53:01	691.9	1158.0	56.9	50.9
10:53:02	689.8	1208.6	54.3	52.7
Averages	**724.1**	**1178.0**	**53.1**	**51.8**

For high wind speed range the data obtained from the 2 point- connection test set-up is shown in Table 6-4.

Table 6-5 Wind Data for High Wind Speed Test

Time (hr:min:sec)	Catenary Cable Tension (lb)	Messenger Cable Tension (lb)	West Air boat Wind Speed (mph)	East Air boat Wind Speed (mph)
10:53:42	662.6	1540.4	88.9	107.5
10:53:43	674.8	1602.1	88.5	107.5
10:53:44	660.8	1591.4	88.7	101.4
10:53:45	656.2	1586.5	93.1	102.4
10:53:46	663.6	1595.6	86.2	103.7
10:53:47	632.5	1577.5	83.5	102.1
10:53:48	661.0	1651.6	85.4	102.6
10:53:49	670.2	1591.6	86.0	107.3
10:53:50	653.2	1625.4	92.7	103.4
10:53:51	661.5	1636.9	87.1	105.4
10:53:52	637.7	1635.2	89.3	108.7
10:53:53	671.5	1626.1	87.3	101.0
10:53:54	639.8	1620.7	89.5	101.2
Averages	**657.3**	**1606.2**	**88.2**	**104.2**

Wind Load Modeling

Comparisons are made between the test results and two simulated wind load models. It is important to note that though it could have been easier and maybe more accurate to input the entire wind history from testing into the computer program for comparison of analysis, the writer has chosen to test the wind generation routines incorporated into the program, hence only simulated wind history is used. The wind loading models are discussed in chapter 4. The first wind model is based on the averages mentioned in the preceding section held constant for the duration of the test. The second wind loading is also based on the averages but with a fluctuating component about the mean values. The average wind speed used as input in the wind analysis was the average of the averages on the East and West air boat signal heads. These values are shown in Table 6-6 below.

Table 6-6 Wind Speeds and Resulting Drag Forces Used in Dynamic Analysis

Wind Speed	**Average Input Force on Signal (lbs)**		**Input Wind Speed (mph)**		
	Constant* Velocity	Variable** Velocity	Test East/West	Constant* Velocity	Variable** Velocity
Low	45.54	40.19	38.2/41.7	39.9	40.2***
Medium	43.60	46.43	51.8/53.1	52.5	53.2***
High	108.5	97.88	104.2/88.2	88.2	88.8***

Table 6-7 Cable Tensions for Wind Load Test # 1

Wind Speed	**Catenary Cable Tensions (lbs)**			**Messenger Cable Tensions (lbs)**		
	Test	Constant* Velocity	Variable** Velocity	Test	Constant* Velocity	Variable** Velocity
Low	741	628.0	752.6	1016	964.9	670.0
Medium	724	436.0	614.2	1180	1181.0	991.0

* DYNASS Constant Wind Speed Model (See chapter 4 for details)

** DYNASS Variable Wind Speed Model (See chapter 4 for details)

*** Average velocity from fluctuating wind speed generated.

High wind ranges produced non-conclusive results due to divergence of analysis. There are many variables in dynamic wind load computation that may account for the differences between the measured and computed results. Both constant and variable speed wind models under predict the tensions in the catenary cable. The percent difference for low wind speed is 15.25% and ≈ 0% for the constant velocity and variable velocity models respectively. For the medium wind speed range the percent difference is 39.8% and 15.17%. The discrepancy in the results could be as a result of the inability to more adequately model the loading procedure. The comparisons for the messenger cable are the same with a percent difference of ≈ 0% and 34.1% respectively for the low wind range and ≈ 0% and 16.0% respectively for the medium wind range. At this time the analysis for the high wind speed range for winds of about 100 mph gives a non converging result. This is because at that wind speed the analysis predicts an overturning of the signal light head. This effect of this overturning was observed to cause drastic variations of the drag and lift forces applied at the signal heads. The range of the drag force was 300 lbs to 0 lbs. Mathematical recovery after such an overturning is being investigated and is recommended for further research. Other factors that could account for the differences in the results include discrepancies in initial tension readings between tests and an inadequate modeling of wind pressure sustained at the signal head. The low wind range, medium wind range and high wind range were tested continuously without stopping. The computer model, however, only accounts for the change in initial conditions between tests by changing the initial tension in the cables. The dynamic effects in the transition were lost and were not modeled. Both wind models developed attempts to take account of the rotation of signal head, in the wind stream, by the use of drag and lift coefficients. Inherent in the use of these coefficients is the assumption that there is an uncoupling of the along the wind response of the lights and the cross wind response. And a further assumption that the along wind response controls. Both these assumptions are presently unverifiable. The dynamic solution approach, barring the assumptions in loading, is seen to give a reasonable lower bound solution to the cable - frame problem.

CHAPTER 7
CONCLUSION

Summary

The purpose of this dissertation was to present an alternative analysis approach to the force density method used in the ATLAS program developed in the Civil Engineering Department at University of Florida. This new approach was to increase flexibility of analysis, solve the static analysis of a cable - frame assemble and be able to model true dynamic loading on the traffic signal system. The new approach espoused uses the principles of dynamic analysis. This solution approach uses finite element techniques to model the traffic signal system as made up of frame elements, cable elements, connector elements and truss elements. The elastic and inertia properties of each element in the structure is assembled to form the structures' stiffness, mass and damping properties. The nodal equations of motion for the structure are then set-up in terms of the structures' assembled global properties. These nodal equations of motion are solved using the Newmark's Beta numerical integration and Newton - Raphson iteration scheme. The analysis technique presented was compared to test results from tests performed at the University of Florida and to other analysis methods.

Review of Analysis Method Developed

A 2- node cable element was explicitly derived for the finite element analysis of the cable - frame system. Built into the formulation of this cable element are the assumptions that the element can not resist bending or compression. The cable element is hence rendered inactive when subjected to any system of compressive forces. The inertia properties of the cable element, however remain active even under compressive forces hence restoring the system and keeping the system in equilibrium. The cable element properties are derived directly in terms of the deformed global coordinates of the nodes as opposed to the classical local coordinate system with a global - local transformation. The finite element method presented is based upon the total Lagrangian version of the incremental equation of motion. Solution to the equation of motion is obtained using an improved Newmark's Beta method. The improvement is in the form of the introduction of numerical damping factor. The numerical damping uses novel manipulations of the inertia forces to stabilize an otherwise statically precarious system. This is used in addition to the conventional dissipative damping matrix. The main difference between both damping processes is that using numerical damping retains the "true" dynamic response of system, while arbitrarily increasing the conventional damping can result in over damping that can mask the "true" response of the system. The improved Newmark's Beta method reduces the nonlinear set of equations to corresponding set of linear equations that can then be solved using Newton - Raphson. A modified Newton - Raphson was presented. In addition to the regular modifications to the method to improve convergence, the author makes use of a technique of averaging the tangent stiffness of the structure in successive Newton - Raphson iterations. This is observed to curb the divergent tendencies of the algebraic equations in an unstable cable analysis.

The solution method is completed with the definition of two dynamic wind load models. The first uses a constant average wind speed but accounts for the rotation of traffic signal head by using lift and drag coefficients. The second model uses the average wind speed plus a gust component. This model also accounts for the rotation of the traffic signal head. The gust component of the second wind model is generated using auto regressive numerical filters. Both wind models generate along wind forces. Cross wind effects are ignored. The solution method presented adequately handles a nonlinear analysis with the sources of nonlinearity being large displacement in cable and connector beam elements and nonlinear wind load.

Verification of Analysis Method

A program was developed based on the solution method presented. This program, DYNASS, was applied to the traffic signal system. The computed results from this program was compared to test results of experiments done at the University of Florida. Good correlation was observed for the static load case results. For the dynamic load case, computed results are considered comparable to the measured result but with appreciable difference due assumptions in loading.

Advantages and Disadvantages of Solution Method

The solution method was verified for the traffic signal system. A major advantage of this solution technique, however, is it's flexibility. The method of analysis presented can be used for any system of cables and frames. This retains the power of the finite element technique of being valid for any structure. Another advantage of this solution approach is the additional information obtained from a typical analysis. Though this solution approach can be used for static analysis, a lot more information is gathered from the analysis than just the static solution. Since the solution method uses dynamic theories, an advantage of this solution approach is the capability to model dynamic loads.

A major disadvantage is the time it takes for a typical solution. A typical solution can be obtained in 3 sec analysis time. However, due to the nonlinearity introduced by the cables and connector elements, the solution time step required range between 0.001 and 0.0001 sec. This implies that a typical solution may require 30000 iterations. Each iteration takes about 0.01 sec. in real time. This means a typical nonlinear analysis could take as long as 50 mins.

Recommendations for Further Research

There are many ways the solution method presented could be improved. One way is the implementation of a variable time step. This would make the analysis faster. A variable time step allows for the use of a large time step in portions of the analysis not sensitive to the time step chosen. It would, however, allow for a reduction in the time step if divergence of solution is observed. Another area recommended for further research is the wind load computation. The effects of cross wind in structural building design is increasingly gaining attention. These cross wind effects are presently ignored in the analysis as is the norm. It is the author's opinion that ignoring this phenomenon under states the forces acting on the traffic signal system. A final recommendation is an implementation of other load types. Since this solution method can be applied to mooring lines, it is recommended that an additional load type be considered, i.e. hydrostatic pressure. Finally, extensions to the theory could be made to handle base excitation as would be experienced in an earthquake.

APPENDIX A
CABLE ELEMENT DERIVATION

Nonlinear 2-node cable element.

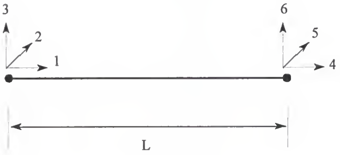

$\phi_1 = 1 - \frac{s}{L}$ $\phi_2 = 1 - \frac{s}{L}$ $\phi_3 = 1 - \frac{s}{L}$

$\phi_4 = \frac{s}{L}$ $\phi_5 = \frac{s}{L}$ $\phi_6 = \frac{s}{L}$

The above are the shape functions for the 2 node element shown.
The equation for generic displacement of any point along the element with respect to the nodal displacements can be given as shown below.

$$U = \phi_1 \cdot u_1 + \phi_4 \cdot u_2$$

$$V = \phi_2 \cdot v_1 + \phi_5 \cdot v_2$$

$$W = \phi_3 \cdot w_1 + \phi_6 \cdot w_2$$

Note that the notations and coordinate systems adopted in this appendix is as described in the chapter 3.
s is the arc length of the cable from node 1 to any generic point along the cable.
L is the initial arc length of the cable.
$\{x_1\ y_1\ z_1\ x_2\ y_2\ z_2\}$ are the nodal coordinates.
$\{u_1\ v_1\ w_1\ u_2\ v_2\ w_2\}$ are the nodal displacement vector.

$$\begin{bmatrix} 1-\frac{s}{L} & 0 & 0 \\ 0 & 1-\frac{s}{L} & 0 \\ 0 & 0 & 1-\frac{s}{L} \\ \frac{s}{L} & 0 & 0 \\ 0 & \frac{s}{L} & 0 \\ 0 & 0 & \frac{s}{L} \end{bmatrix} = N^T \qquad \begin{bmatrix} \frac{1}{L} & 0 & 0 \\ 0 & -\frac{1}{L} & 0 \\ 0 & 0 & -\frac{1}{L} \\ \frac{1}{L} & 0 & 0 \\ 0 & \frac{1}{L} & 0 \\ 0 & 0 & \frac{1}{L} \end{bmatrix} = \left(N'\right)^T$$

In matrix form, N is the above linear displacement field. N' is the first differential of the shape function with respect to s. i.e. the arc length.

To obtain the equivalent nodal loads due to the weight of the cable we have:

$$g = \int_0^L W \cdot N^T \cdot h \, ds$$

The h vector is a coordinate dependent matrix. Since the load is acting in the negative z direction to our assumed coordinate system. The h vector is as shown below.

$$\begin{bmatrix} 1-\frac{s}{L} & 0 & 0 \\ 0 & 1-\frac{s}{L} & 0 \\ 0 & 0 & 1-\frac{s}{L} \\ \frac{s}{L} & 0 & 0 \\ 0 & \frac{s}{L} & 0 \\ 0 & 0 & \frac{s}{L} \end{bmatrix} \cdot \begin{pmatrix} 0 \\ 0 \\ 1 \end{pmatrix} = N^T \cdot h$$

$$\begin{bmatrix} 0 \\ 0 \\ \frac{-(L-s)}{L} \\ 0 \\ 0 \\ \frac{-s}{L} \end{bmatrix} = N^T \cdot h \qquad g = \int_0^L W \cdot N^T \cdot h \, ds = \begin{bmatrix} 0 \\ 0 \\ \frac{1}{2} \cdot L \\ 0 \\ 0 \\ \frac{-1}{2} \cdot L \end{bmatrix} \cdot W$$

Consider the initial tension in the cable as a distributed load.

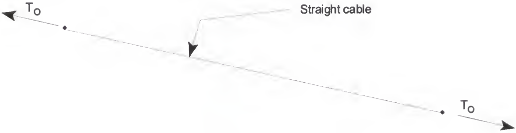

$$f_0 = \int_0^L T_0 \cdot N^T \cdot h \, ds$$

$$\begin{bmatrix} 1-\frac{s}{L} & 0 & 0 \\ 0 & 1-\frac{s}{L} & 0 \\ 0 & 0 & 1-\frac{s}{L} \\ \frac{s}{L} & 0 & 0 \\ 0 & \frac{s}{L} & 0 \\ 0 & 0 & \frac{s}{L} \end{bmatrix} \cdot \begin{pmatrix} 1 \\ 0 \\ 0 \end{pmatrix} = N^T \cdot h \qquad \begin{bmatrix} \frac{(L-s)}{L} \\ 0 \\ 0 \\ \frac{s}{L} \\ 0 \\ 0 \end{bmatrix} = N^T \cdot h$$

Note that because of the assumed tension distribution along the member this f_o is in the element local axis.

$$f_o = \int_0^L \frac{4 \cdot T_o}{L} \cdot \left(-1+\frac{2 \cdot s}{L}\right) \cdot \begin{bmatrix} \frac{(L-s)}{L} \\ 0 \\ 0 \\ \frac{s}{L} \\ 0 \\ 0 \end{bmatrix} ds = \begin{bmatrix} -\frac{2}{3} \cdot T_o \\ 0 \\ 0 \\ \frac{2}{3} \cdot T_o \\ 0 \\ 0 \end{bmatrix}$$

In structure's global axis:

$$dx = x_2 - x_1$$

$$dy = y_2 - y_1$$

$$dz = z_2 - z_1$$

$$xl = \sqrt{dx^2 + dy^2 + dz^2}$$

$$f_o = \frac{2}{3} \cdot T_o \cdot \begin{bmatrix} -\frac{dx}{xl} \\ -\frac{dy}{xl} \\ -\frac{dz}{xl} \\ \frac{dx}{xl} \\ \frac{dy}{xl} \\ \frac{dz}{xl} \end{bmatrix}$$

The mass matrix is computed from: $\int_0^L \frac{W}{g \cdot L} \cdot N^T \cdot N \, ds$

Note that W is the total weight of the element.

L is the length along the undeformed arc of the element.

g is the acceleration due to gravity. This is used to convert the weight into mass.

$$\begin{bmatrix} 1-\frac{s}{L} & 0 & 0 \\ 0 & 1-\frac{s}{L} & 0 \\ 0 & 0 & 1-\frac{s}{L} \\ \frac{s}{L} & 0 & 0 \\ 0 & \frac{s}{L} & 0 \\ 0 & 0 & \frac{s}{L} \end{bmatrix} \cdot \begin{bmatrix} 1-\frac{s}{L} & 0 & 0 & \frac{s}{L} & 0 & 0 \\ 0 & 1-\frac{s}{L} & 0 & 0 & \frac{s}{L} & 0 \\ 0 & 0 & 1-\frac{s}{L} & 0 & 0 & \frac{s}{L} \end{bmatrix} = N^T \cdot N$$

$$N^T \cdot N = \begin{bmatrix} \frac{(-L+s)^2}{L^2} & 0 & 0 & (-L+s)\cdot\frac{s}{L^2} & 0 & 0 \\ 0 & \frac{(-L+s)^2}{L^2} & 0 & 0 & (-L+s)\cdot\frac{s}{L^2} & 0 \\ 0 & 0 & \frac{(-L+s)^2}{L^2} & 0 & 0 & (-L+s)\cdot\frac{s}{L^2} \\ -(-L+s)\cdot\frac{s}{L^2} & 0 & 0 & \frac{s^2}{L^2} & 0 & 0 \\ 0 & -(-L+s)\cdot\frac{s}{L^2} & 0 & 0 & \frac{s^2}{L^2} & 0 \\ 0 & 0 & -(-L+s)\cdot\frac{s}{L^2} & 0 & 0 & \frac{s^2}{L^2} \end{bmatrix}$$

$$m=\frac{W}{6\cdot g}\cdot\begin{pmatrix}2&0&0&1&0&0\\0&2&0&0&1&0\\0&0&2&0&0&1\\1&0&0&2&0&0\\0&1&0&0&2&0\\0&0&1&0&0&2\end{pmatrix}$$

This the mass matrix in global coordinates.

From chapter 3 the elastic stiffness of the above element can be obtained from the following. Eqtns 3-10 and 3-22 give the expression for strain.

$$\varepsilon_s(t+\Delta t)=\varepsilon_s(t)+\Delta\varepsilon_s \qquad \varepsilon_s=\frac{1}{2}\cdot\left[d_n{}^T\cdot(N')^T\cdot(N')\cdot(d_n)-1\right]$$

$$\Delta\varepsilon_s=d_n{}^T\cdot(N')^T\cdot(N')\cdot(\Delta d_n)+\frac{1}{2}\cdot\left[\Delta d_n{}^T\cdot(N')^T\cdot(N')\cdot(\Delta d_n)\right] \qquad (3\text{-}16)$$

Change in strain.

$$(K_E)=\frac{A\cdot E}{2}\cdot\int_0^L (N')^T\cdot(N')\cdot\left[d_n{}^T\cdot(N')^T\cdot(N')\cdot(d_n)-1\right]ds \qquad (3\text{-}25)$$

K_E is the linear part of the cable stiffness.

$$(K_L)=A\cdot E\cdot\int_0^L \left[d_n{}^T\cdot(N')^T\cdot(N')+\Delta d_n{}^T\cdot(N')^T\cdot(N')\right]^T\cdot\left[d_n{}^T\cdot(N')^T\cdot(N')+\frac{1}{2}\cdot\left[\Delta d_n{}^T\cdot(N')^T\cdot(N')\right]\right]ds \qquad (3\text{-}26)$$

K_L is the non-linear part of the cable stiffness formulation.
Substituting the shape functions into the above expressions for K_E we have the following.

Compute the term: $d_n^T \cdot (N')^T \cdot (N') \cdot (d_n) - 1$

$$\begin{bmatrix} \frac{-1}{L} & 0 & 0 \\ 0 & \frac{-1}{L} & 0 \\ 0 & 0 & \frac{-1}{L} \\ \frac{1}{L} & 0 & 0 \\ 0 & \frac{1}{L} & 0 \\ 0 & 0 & \frac{1}{L} \end{bmatrix} \cdot \begin{bmatrix} \frac{-1}{L} & 0 & 0 & \frac{1}{L} & 0 & 0 \\ 0 & \frac{-1}{L} & 0 & 0 & \frac{1}{L} & 0 \\ 0 & 0 & \frac{-1}{L} & 0 & 0 & \frac{1}{L} \end{bmatrix} = (N')^T \cdot (N')$$

$$\begin{bmatrix} \frac{1}{L^2} & 0 & 0 & \frac{-1}{L^2} & 0 & 0 \\ 0 & \frac{1}{L^2} & 0 & 0 & \frac{-1}{L^2} & 0 \\ 0 & 0 & \frac{1}{L^2} & 0 & 0 & \frac{-1}{L^2} \\ \frac{-1}{L^2} & 0 & 0 & \frac{1}{L^2} & 0 & 0 \\ 0 & \frac{-1}{L^2} & 0 & 0 & \frac{1}{L^2} & 0 \\ 0 & 0 & \frac{-1}{L^2} & 0 & 0 & \frac{1}{L^2} \end{bmatrix} = (N')^T \cdot (N')$$

$$\begin{pmatrix} x_1 & y_1 & z_1 & x_2 & y_2 & z_2 \end{pmatrix} \cdot \begin{bmatrix} \frac{1}{L^2} & 0 & 0 & \frac{-1}{L^2} & 0 & 0 \\ 0 & \frac{1}{L^2} & 0 & 0 & \frac{-1}{L^2} & 0 \\ 0 & 0 & \frac{1}{L^2} & 0 & 0 & \frac{-1}{L^2} \\ \frac{-1}{L^2} & 0 & 0 & \frac{1}{L^2} & 0 & 0 \\ 0 & \frac{-1}{L^2} & 0 & 0 & \frac{1}{L^2} & 0 \\ 0 & 0 & \frac{-1}{L^2} & 0 & 0 & \frac{1}{L^2} \end{bmatrix} \cdot \begin{bmatrix} x_1 \\ y_1 \\ z_1 \\ x_2 \\ y_2 \\ z_2 \end{bmatrix} = d_n^T \cdot \left(N'\right)^T \cdot \left(N'\right) \cdot \left(d_n\right)$$

$$\left[\frac{\left(-2 \cdot x_1 \cdot x_2 - 2 \cdot y_1 \cdot y_2 + x_1^2 + y_1^2 + z_1^2 - 2 \cdot z_1 \cdot z_2 + x_2^2 + y_2^2 + z_2^2\right)}{L^2} \right] = d_n^T \cdot \left(N'\right)^T \cdot \left(N'\right) \cdot \left(d_n\right)$$

$$\frac{\left(-2 \cdot x_1 \cdot x_2 - 2 \cdot y_1 \cdot y_2 + x_1^2 + y_1^2 + z_1^2 - 2 \cdot z_1 \cdot z_2 + x_2^2 + y_2^2 + z_2^2\right)}{L^2} - 1 = d_n^T \cdot \left(N'\right)^T \cdot \left(N'\right) \cdot \left(d_n\right) - 1$$

$$\int_0^L \left[\frac{\left(-2 \cdot x_1 \cdot x_2 - 2 \cdot y_1 \cdot y_2 + x_1^2 + y_1^2 + z_1^2 - 2 \cdot z_1 \cdot z_2 + x_2^2 + y_2^2 + z_2^2\right)}{L^2} - 1 \right] \cdot \left(N'\right)^T \cdot \left(N'\right) \, ds$$

Multiply the above equation with each term in the N^TN matrix and factor expression we have the following:

$$\int_0^L \left[\frac{\left(-2\cdot x_1\cdot x_2-2\cdot y_1\cdot y_2+x_1^2+y_1^2+z_1^2-2\cdot z_1\cdot z_2+x_2^2+y_2^2+z_2^2\right)}{L^2}-1\right]\cdot\frac{1}{L^2}\,ds$$

Note that x, y, and z coodinates are for any time (t).

$$K_{11}=\frac{1}{2\cdot L^3}\cdot\left[\left(x_1-x_2\right)^2+\left(y_1-y_2\right)^2+\left(z_1-z_2\right)^2-L^2\right]$$

$$K_{22}=\frac{1}{2\cdot L^3}\cdot\left[\left(x_1-x_2\right)^2+\left(y_1-y_2\right)^2+\left(z_1-z_2\right)^2-L^2\right]$$

$$K_{33}=\frac{1}{2\cdot L^3}\cdot\left[\left(x_1-x_2\right)^2+\left(y_1-y_2\right)^2+\left(z_1-z_2\right)^2-L^2\right]$$

$$K_{44}=\frac{1}{2\cdot L^3}\cdot\left[\left(x_1-x_2\right)^2+\left(y_1-y_2\right)^2+\left(z_1-z_2\right)^2-L^2\right]$$

$$K_{55}=\frac{1}{2\cdot L^3}\cdot\left[\left(x_1-x_2\right)^2+\left(y_1-y_2\right)^2+\left(z_1-z_2\right)^2-L^2\right]$$

$$K_{66}=\frac{1}{2\cdot L^3}\cdot\left[\left(x_1-x_2\right)^2+\left(y_1-y_2\right)^2+\left(z_1-z_2\right)^2-L^2\right]$$

$$K_{14}=\frac{-1}{2\cdot L^3}\cdot\left[\left(x_1-x_2\right)^2+\left(y_1-y_2\right)^2+\left(z_1-z_2\right)^2-L^2\right]$$

$$K_{25}=\frac{-1}{2\cdot L^3}\cdot\left[\left(x_1-x_2\right)^2+\left(y_1-y_2\right)^2+\left(z_1-z_2\right)^2-L^2\right]$$

$$K_{36}=\frac{-1}{2\cdot L^3}\cdot\left[\left(x_1-x_2\right)^2+\left(y_1-y_2\right)^2+\left(z_1-z_2\right)^2-L^2\right]$$

$$K_{41}=\frac{-1}{2\cdot L^3}\cdot\left[\left(x_1-x_2\right)^2+\left(y_1-y_2\right)^2+\left(z_1-z_2\right)^2-L^2\right]$$

$$K_{52}=\frac{-1}{2\cdot L^3}\cdot\left[\left(x_1-x_2\right)^2+\left(y_1-y_2\right)^2+\left(z_1-z_2\right)^2-L^2\right]$$

$$K_{63}=\frac{1}{2\cdot L^3}\cdot\left[\left(x_1-x_2\right)^2+\left(y_1-y_2\right)^2+\left(z_1-z_2\right)^2-L^2\right]$$

$$K_E = A\cdot E\cdot\begin{bmatrix} K_{11} & 0 & 0 & K_{14} & 0 & 0 \\ 0 & K_{22} & 0 & 0 & K_{25} & 0 \\ 0 & 0 & K_{33} & 0 & 0 & K_{36} \\ K_{41} & 0 & 0 & K_{44} & 0 & 0 \\ 0 & K_{52} & 0 & 0 & K_{55} & 0 \\ 0 & 0 & K_{63} & 0 & 0 & K_{66} \end{bmatrix}$$

K_E is referred t as the initial stress matrix. It is computed at the beginning of each time step. It is remains constant within the time step.

$$K_E = \frac{A\cdot E}{2\cdot L^3}\cdot\left[\left(x_1 - x_2\right)^2 + \left(y_1 - y_2\right)^2 + \left(z_1 - z_2\right)^2 - L^2\right]\cdot\begin{bmatrix} 1 & 0 & 0 & -1 & 0 & 0 \\ 0 & 1 & 0 & 0 & -1 & 0 \\ 0 & 0 & 1 & 0 & 0 & -1 \\ 1 & 0 & 0 & 1 & 0 & 0 \\ 0 & 1 & 0 & 0 & 1 & 0 \\ 0 & 0 & -1 & 0 & 0 & 1 \end{bmatrix}$$

Note that the tension in the cable at time t is :

$$T_t = \frac{A\cdot E}{L^2}\cdot\left[\left(x_1 - x_2\right)^2 + \left(y_1 - y_2\right)^2 + \left(z_1 - z_2\right)^2 - L^2\right]$$

It is more convenient to cast this tension expression in terms of incremental strain in order to account for pre-tension. In which case this expression becomes:

$T_t = T_{t-\Delta t} + A\cdot E\cdot\Delta\varepsilon$ Change in strain can be computed using Eqn. 3-16.

The initial tension is taken from either a given value or computed from the slack configuration.

$$\Delta T = E\cdot A\cdot\left[d_n^{T}\cdot\left(N'\right)^{T}\cdot N' + \frac{1}{2}\cdot\left[\Delta d_n^{T}\cdot\left(N'\right)^{T}\cdot N'\right]\right]\cdot\left(\Delta d_n\right)$$

Compute the R_E as shown in Eqn. 3-27.

$$\left(R_E\right) = \frac{A\cdot E}{2}\cdot\int_0^L \left(N'\right)^T\cdot\left(N'\right)\cdot\left[d_n^{T}\cdot\left(N'\right)^T\cdot\left(N'\right)\cdot\left(d_n\right) - 1\right]\cdot d_n\, ds$$

The coresponding nodal force vector for the stress at any time t is as follows.

$$\frac{A\cdot E}{2}\cdot\begin{bmatrix} K_{11} & 0 & 0 & K_{14} & 0 & 0 \\ 0 & K_{22} & 0 & 0 & K_{25} & 0 \\ 0 & 0 & K_{33} & 0 & 0 & K_{36} \\ K_{41} & 0 & 0 & K_{44} & 0 & 0 \\ 0 & K_{52} & 0 & 0 & K_{55} & 0 \\ 0 & 0 & K_{63} & 0 & 0 & K_{66} \end{bmatrix}\cdot\begin{bmatrix} x_1 \\ y_1 \\ z_1 \\ x_2 \\ y_2 \\ z_2 \end{bmatrix} = \frac{A\cdot E}{2\cdot L^3}\cdot\begin{bmatrix} K_{11}\cdot x_1 + K_{14}\cdot x_2 \\ K_{22}\cdot y_1 + K_{25}\cdot y_2 \\ K_{33}\cdot z_1 + K_{36}\cdot z_2 \\ K_{41}\cdot x_1 + K_{44}\cdot x_2 \\ K_{52}\cdot y_1 + K_{55}\cdot y_2 \\ K_{63}\cdot z_1 + K_{66}\cdot z_2 \end{bmatrix} = R_E$$

$$R_E = \frac{A\cdot E}{2\cdot L^3}\cdot\left[\left(x_1 - x_2\right)^2 + \left(y_1 - y_2\right)^2 + \left(z_1 - z_2\right)^2 - L^2\right]\cdot\begin{bmatrix} x_1 - x_2 \\ y_1 - y_2 \\ z_1 - z_2 \\ x_2 - x_1 \\ y_2 - y_1 \\ z_2 - z_1 \end{bmatrix}$$

Or alternatively,

$$R_E = \frac{T_{t-\Delta t} + \frac{A\cdot E}{2\cdot L^2}\cdot\Delta\varepsilon}{L}\cdot\begin{bmatrix} x_1 - x_2 \\ y_1 - y_2 \\ z_1 - z_2 \\ x_2 - x_1 \\ y_2 - y_1 \\ z_2 - z_1 \end{bmatrix}$$

Similarly we can compute the K_L matrix as follows.

$$\left(K_L\right) = A\cdot E\cdot\int_0^L \left[d_n^T\cdot\left(N'\right)^T\cdot\left(N'\right) + \Delta d_n^T\cdot\left(N'\right)^T\cdot\left(N'\right)\right]^T\cdot\left[d_n^T\cdot\left(N'\right)^T\cdot\left(N'\right) + \frac{1}{2}\cdot\left[\Delta d_n^T\cdot\left(N'\right)^T\cdot\left(N'\right)\right]\right] ds$$

The term $d_n^T \cdot (N')^T \cdot (N')$ is equal to the following.

$$\begin{pmatrix} x_1 & y_1 & z_1 & x_2 & y_2 & z_2 \end{pmatrix} \cdot \begin{bmatrix} \frac{1}{L^2} & 0 & 0 & \frac{-1}{L^2} & 0 & 0 \\ 0 & \frac{1}{L^2} & 0 & 0 & \frac{-1}{L^2} & 0 \\ 0 & 0 & \frac{1}{L^2} & 0 & 0 & \frac{-1}{L^2} \\ \frac{-1}{L^2} & 0 & 0 & \frac{1}{L^2} & 0 & 0 \\ 0 & \frac{-1}{L^2} & 0 & 0 & \frac{1}{L^2} & 0 \\ 0 & 0 & \frac{-1}{L^2} & 0 & 0 & \frac{1}{L^2} \end{bmatrix} = d_n^T \cdot (N')^T \cdot (N')$$

$$\begin{bmatrix} \frac{(x_1 - x_2)}{L^2} & \frac{(y_1 - y_2)}{L^2} & \frac{(z_1 - z_2)}{L^2} & \frac{-(x_1 - x_2)}{L^2} & \frac{(y_1 - y_2)}{L^2} & \frac{-(z_1 - z_2)}{L^2} \end{bmatrix} = d_n^T \cdot (N')^T \cdot (N')$$

The term $\Delta d_n^T \cdot (N')^T \cdot (N')$ is nonlinear and dependent on Δd_n. Note that Δd_n is unknown at the start of an analysis. Therefore, we replace the above expression for K_L with K_A as an initial approximation.

$$K_A = A \cdot E \cdot \int_0^L \left[d_n^T \cdot (N')^T \cdot (N') \right]^T \cdot \left[d_n^T \cdot (N')^T \cdot (N') \right] ds \qquad (3\text{-}28)$$

This expression is used at the beginning of the time step analysis. Within each time step, i.e. during the Newton-Raphson iteration, the true expression will be used.

Compute K_A: Let $Q = \left[d_n^T \cdot (N')^T \cdot (N')\right]^T \cdot \left[d_n^T \cdot (N')^T \cdot (N')\right]$

$$\begin{bmatrix} \frac{(x_1 - x_2)}{L^2} \\ \frac{(y_1 - y_2)}{L^2} \\ \frac{(z_1 - z_2)}{L^2} \\ \frac{(-x_1 + x_2)}{L^2} \\ \frac{(-y_1 + y_2)}{L^2} \\ \frac{(-z_1 + z_2)}{L^2} \end{bmatrix} \cdot \begin{bmatrix} \frac{(x_1 - x_2)}{L^2} & \frac{(y_1 - y_2)}{L^2} & \frac{(z_1 - z_2)}{L^2} & \frac{(x_1 \quad x_2)}{L^2} & \frac{(y_1 - y_2)}{L^2} & \frac{-(z_1 - z_2)}{L^2} \end{bmatrix} = Q$$

For convenience, let the above expressions be replaced as follows.

$$\begin{bmatrix} \frac{(x_1 - x_2)}{L^2} & \frac{(y_1 - y_2)}{L^2} & \frac{(z_1 - z_2)}{L^2} & \frac{(x_1 - x_2)}{L^2} & \frac{(y_1 - y_2)}{L^2} & \frac{-(z_1 - z_2)}{L^2} \end{bmatrix} = \frac{1}{L^2} \cdot (-dx \quad -dy \quad -dz \quad dx \quad dy \quad dz)$$

$$\begin{bmatrix} \frac{(u_1 - u_2)}{L^2} & \frac{(v_1 - v_2)}{L^2} & \frac{(w_1 - w_2)}{L^2} & \frac{-(u_1 - u_2)}{L^2} & \frac{-(v_1 - v_2)}{L^2} & \frac{-(w_1 - w_2)}{L^2} \end{bmatrix} = \frac{1}{L^2} \cdot (-du \quad -dv \quad -dw \quad du \quad dv \quad dw)$$

The matrix K_A is therefore as given below:

$$K_A = \frac{A \cdot E}{L^3} \cdot \begin{bmatrix} (-dx)^2 & (-dx)\cdot(-dy) & (-dx)\cdot(-dz) & -(-dx)^2 & (-dy)\cdot(dx) & (-dz)\cdot(dx) \\ (-dx)\cdot(-dy) & (-dy)^2 & (-dy)\cdot(-dz) & (-dy)\cdot(dx) & -(-dy)^2 & (dy)\cdot(-dz) \\ (-dx)\cdot(-dz) & (-dy)\cdot(-dz) & (-dz)^2 & (-dz)\cdot(dx) & (dy)\cdot(-dz) & -(-dz)^2 \\ -(-dx)^2 & (-dy)\cdot(dx) & (dz)\cdot(dx) & (-dx)^2 & (-dx)\cdot(-dy) & (-dx)\cdot(-dz) \\ (-dy)\cdot(dx) & -(-dy)^2 & (dy)\cdot(-dz) & (dx)\cdot(dy) & (-dy)^2 & (-dy)\cdot(-dz) \\ (-dz)\cdot(dx) & (dy)\cdot(-dz) & -(-dz)^2 & (-dx)\cdot(-dz) & (-dy)\cdot(-dz) & (-dz)^2 \end{bmatrix}$$

The above expression for K_A is used at the beginning of the time step. Within the time step the following derived K_L is used.

$$\begin{pmatrix} u_1 & v_1 & w_1 & u_2 & v_2 & w_2 \end{pmatrix} \cdot \begin{bmatrix} \frac{1}{L^2} & 0 & 0 & \frac{-1}{L^2} & 0 & 0 \\ 0 & \frac{1}{L^2} & 0 & 0 & \frac{-1}{L^2} & 0 \\ 0 & 0 & \frac{1}{L^2} & 0 & 0 & \frac{-1}{L^2} \\ \frac{-1}{L^2} & 0 & 0 & \frac{1}{L^2} & 0 & 0 \\ 0 & \frac{-1}{L^2} & 0 & 0 & \frac{1}{L^2} & 0 \\ 0 & 0 & \frac{-1}{L^2} & 0 & 0 & \frac{1}{L^2} \end{bmatrix} = \Delta d_n^T \cdot (N')^T \cdot N'$$

$$\begin{bmatrix} \frac{(u_1 - u_2)}{L^2} & \frac{(v_1 - v_2)}{L^2} & \frac{(w_1 - w_2)}{L^2} & \frac{-(u_1 - u_2)}{L^2} & \frac{(v_1 - v_2)}{L^2} & \frac{-(w_1 - w_2)}{L^2} \end{bmatrix} = \Delta d_n^T \cdot (N')^T \cdot N'$$

$$\frac{1}{2} \cdot \begin{bmatrix} \frac{(u_1 - u_2)}{L^2} & \frac{(v_1 - v_2)}{L^2} & \frac{(w_1 - w_2)}{L^2} & \frac{(u_1 - u_2)}{L^2} & \frac{-(v_1 - v_2)}{L^2} & \frac{-(w_1 - w_2)}{L^2} \end{bmatrix} = \frac{1}{2} \cdot \left[\Delta d_n^T \cdot (N')^T \cdot N' \right]$$

$$(K_L) = A \cdot E \cdot \int_0^L \left[d_n^T \cdot (N')^T \cdot (N') + \Delta d_n^T \cdot (N')^T \cdot (N') \right]^T \cdot \left[d_n^T \cdot (N')^T \cdot (N') + \frac{1}{2} \cdot \left[\Delta d_n^T \cdot (N')^T \cdot (N') \right] \right] ds$$

$$d_n^T \cdot (N')^T \cdot (N') + \Delta d_n^T \cdot (N')^T \cdot (N') = \frac{1}{L^2} \cdot \begin{pmatrix} -dx & -dy & -dz & dx & dy & dz \end{pmatrix} + \frac{1}{L^2} \cdot \begin{pmatrix} -du & -dv & -dw & du & dv & dw \end{pmatrix}$$

$$d_n^T \cdot (N')^T \cdot (N') + \frac{1}{2} \cdot \left[\Delta d_n^T \cdot (N')^T \cdot (N') \right] = \frac{1}{L^2} \cdot \begin{pmatrix} -dx & -dy & -dz & dx & dy & dz \end{pmatrix} + \frac{1}{2 \cdot L^2} \cdot \begin{pmatrix} -du & -dv & -dw & du & dv & dw \end{pmatrix}$$

The term in the integral therefore becomes the following.

$$\begin{bmatrix} -dx - du \\ -dy - dv \\ dz - dw \\ dx + du \\ dy + dv \\ dz + dw \end{bmatrix} \cdot \begin{pmatrix} -dx - \frac{1}{2} \cdot du & -dy - \frac{1}{2} \cdot dv & -dz - \frac{1}{2} \cdot dw & dx + \frac{1}{2} \cdot du & dy + \frac{1}{2} \cdot dv & dz + \frac{1}{2} \cdot dw \end{pmatrix}$$

See the next page for the K_L matrix.

At the beginning of the time step analysis: $K = K_E + K_A$

For the rest of the analysis: $K = K_E + K_L$

$$[K_L] = \frac{AE}{2L^3}\begin{bmatrix} (dx+du)(2dx+du) & (dx+du)(2dy+dv) & (dx+du)(2dz+dw) & -(dx+du)(2dx+du) & -(dx+du)(2dy+dv) & -(dx+du)(2dz+dw) \\ (dy+dv)(2dx+du) & (dy+dv)(2dy+dv) & (dy+dv)(2dz+dw) & -(dy+dv)(2dx+du) & -(dy+dv)(2dy+dv) & -(dy+dv)(2dz+dw) \\ (dz+dw)(2dx+du) & (dz+dw)(2dy+dv) & (dz+dw)(2dz+dw) & -(dz+dw)(2dx+du) & -(dz+dw)(2dy+dv) & -(dz+dw)(2dz+dw) \\ -(dx+du)(2dx+du) & -(dx+du)(2dy+dv) & -(dx+du)(2dz+dw) & (dx+du)(2dx+du) & (dx+du)(2dy+dv) & (dx+du)(2dz+dw) \\ -(dy+dv)(2dx+du) & -(dy+dv)(2dy+dv) & -(dy+dv)(2dz+dw) & (dy+dv)(2dx+du) & (dy+dv)(2dy+dv) & (dy+dv)(2dz+dw) \\ -(dz+dw)(2dx+du) & -(dz+dw)(2dy+dv) & -(dz+dw)(2dz+dw) & (dz+dw)(2dx+du) & (dz+dw)(2dy+dv) & (dz+dw)(2dz+dw) \end{bmatrix} \tag{3-32}$$

APPENDIX B

USER'S MANUAL FOR DYNASS

DYNASS USER'S GUIDE

INTRODUCTION

DYNASS is a dynamic analysis program, it does a nonlinear analysis of a cable structure including but not limited to the traffic signal systems. The method of analysis used is the implicit numerical integration of a piece-wise linear equation of motion. The default implicit numerical scheme is the Newmark's Beta method. The program can, however, simulate other numeric integration schemes e.g. central difference, backward difference and Euler integration method. For the Newmark's Beta method, the program provides a numerical damping feature called the alpha modification. This enables a faster die-down of the structure's vibration while still maintaining the true dynamic properties of the system. Table B-1 shows the factors to used for the different methods.

Table B-1 Integration constants for use in DYNASS

Method of Analysis	α	β	γ
Newmark's Beta method			
Constant acceleration	0	0.25	0.5
Linear acceleration	0	0.167	0.5
Variable acceleration	0	0.125	0.5
Alpha Modification			
Option 1	0.1	0.3025	0.6
Option 2	-0.1	0.5	0.6
Option 3*	-0.1	0.3025	0.6
Central Difference method	0	0.5	0.5
Backward Difference method	0	1	0.5
Euler Integration method	0	0	0.5

* This option is suggested for traffic signal system analysis.

To run DYNASS it is required that the user prepare an input file, the following section discusses the terminology in use for an adequate input to the program and the general form of the input file. The program requires that the file serving as input to the program be called INPUT. The results from the program is written to a file called OUTPUT. In-addition, two plot files are generated by the program. The first is the time - displacement history for previously chosen nodal points. The second is time-velocity listing for the wind loading generated by the program. The first plot file is called PLOT and the second is SVEL. These can be plotted by regular plotting routine. A plotting routine is currently not included in the latest version of DYNASS. The terminology used in the input file refers to the traffic signal cable structure as shown in Fig. B.1.

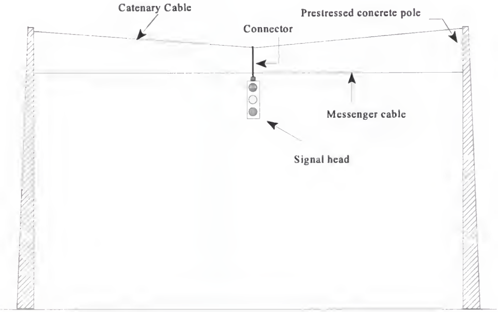

Fig. B.1 Definition of terms used in the INPUT file

NOMENCLATURE

CATENARY- This indicates the primary dead load supporting cable. The word catenary is derived from the root word “catenate” which implies to link or tie strings together. The initial configuration for this cable is assumed as a parabolic shape when there is no pre-tension.

MESSENGER - This indicates the lower cable. It’s name was derived from the electrical messenger wires that it supports.

BEAMS - This refers to the support strain poles at each end of the span. In the case of the traffic signal system, these are prestressed concrete poles.

CONNECTOR - This refers to the element connecting the catenary cable, the messenger cable and, often times, a traffic signal head or auxiliary sign or some other cladding or load attachment.

INITIAL SAG - This is the sag in the cable due only to cable self weight and tension. Sag due to signal lights is not included. This is used as a starting position for the solution procedure.

WIND - This refers to wind loads acting on the signal light, accessories, cables, and poles. This load is specified by providing an average wind speed and the direction of wind. To model gust the length of wind record and the sampling interval for the wind data must be provided.

LOADS - This refers to the additional gravity and lateral loads acting on the signal light and is used in combination with the wind loads.

SIGNAL - This is used to complete the wind load definition. A detailed description of the signal or sign gives the area impacted by the wind pressure and the gravity load of the signal light.

NONLINEAR - The nonlinear parameters pertaining to the cable geometric properties are the tension in the cable and the original sag in the catenary cable.

DYNAMICS - The die-down tolerance and the integration constants given in Table B-1 are part of the dynamic parameters used by the program. Other parameters specified as dynamic parameters are discussed later in this section.

INPUT FILE SYNTAX

The following is syntax rules that should observed when attempting to write the input for the DYNASS program. The input file is free-format hence only blank spaces or commas are needed to separate data. The following are the conventions used for input:

1. A "C" in column 1 of any line will cause the line to be echoed as a comment on the console.

2. A back slash "\" at the end of information on the first line will allow the next line to be interpreted as a continuation of the first line: therefore, a 160 character record is possible.

3. A colon ":" indicates the end of information on a line. Any information entered to the right of the colon is ignored by the program. This space can be used to provide additional comments within the input file.

4. If a blank identifier is specified, the data string is assumed to be the first data string of the record.

5. If fewer data exist than are specified, the values returned will be either a zero or blank according to the type of data expected.

6. Real numbers do not require decimal points: E formats with + or - exponents are accepted.

7. Simple arithmetic statements may be used within the input. The functions that can be used are +,-,*,/. The order of evaluation is sequential, not hierarchical as in the FORTRAN language.

INPUT DATA

The following is a guide to the user for preparing an INPUT file. The data, as shown below, is entered in sections. Each section has a designation and is separated from the others by a colon ":". The first two lines have no apparent section designation but is referred to as the control section. The first line is the 80 character title line. The second line contains the general information parameters. The positioning of the first two lines is critical to the running of the program and hence can not be omitted or repositioned. The order of the rest of the sections is arbitrary. It is not necessary to separate the first two control lines from the next section with the colon mentioned above.

The information necessary in the second line control section are

1. The number of nodes in the structure. The syntax for this is nodes= #. Where the # sign is a numeric value. Note that there should not be any white space between the letter 's' and '='.
2. The number of elements types in the structure. DYNASS is capable of handling only

   beam, truss, cable and connector elements. The syntax for this is elem_no= #. Or simply, No= #.
3. The number of cables in the structure must be specified next. The syntax for this is cable= #. If no cable present. This could be omitted or set to zero.
4. The final control section parameter is the istat. This is used to identify the kind of analysis to run. The program is capable of three types of analysis depending on the wind load model selected.
   - A) Wind load applied as a lateral load not altered in the time step solution. For this istat=0. The computation of the lateral load is left to the user. The lateral load must be entered in the section designated as loads.
   - B) Variable area wind model. Since the wind is impacting a free-swinging traffic signal. The rotation of the traffic signal in the along-wind direction is taken into consideration in the computation of the wind force. The non-fluctuating average wind speed based on the ASCE 7, 3 sec wind gust criteria is used for the computation of wind pressure. For this istat=1.
   - C) Variable velocity wind model. The fluctuating part of wind

velocity is generated in the program using auto-regressive numerical filters. The fluctuating portion of the wind velocity is added to the average wind velocity similar to that in paragraph B above to compute the required wind pressure. See chapter 4 for details of the different wind models and the equations used in wind load computation. For this istat=-1.

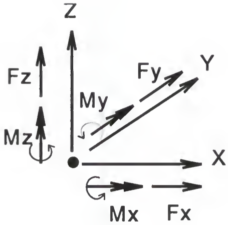

Fig B.2 Coordinate system used in DYNASS

Using the above coordinate system. A typical input could be generated for a traffic signal system using the following sequence of section definitions. It is important to note that the default plane for a structure in DYNASS is the x-z plane. For a 3-D structure, the z direction as the elevation of the poles must be maintained. For a structure defined in the x- y plane an error statement of not finding the structure's plane will be printed and the program terminated.

NON-LINEAR PARAMETERS

This section describes the nonlinear cable elements. The syntax rules are as follows:

NONLINEAR - (Section Designation)

NND ND= $N_1, N_2, N_3, \ldots, N_{NND}$ SG= S1 TEN= T1 W= W1 P= P1

NND = Number of nodes in the cable being specified. When cables are connected to poles, this number includes the nodes at the cable-pole supports. This number must be greater or equal to 3.
The more elements per cable used, the better the accuracy of the solution.

N_1 = First node in the cable. Preferably the left cable-pole node.

N_2 = Second node in the cable, moving from left to right.

N_3 = Third node in the cable and so on

N_{nnd} = Last node in the cable. Preferably the right cable-pole node.

S1 = The original sag in the catenary cable.

T1 = The pretension in the catenary cable. This is optional. If none is specified, pre-tensioning is done due to self weight of the cable only.
If one is specified. The value must be specified in kips.

W1 = weight of the cable (lbs/ft). This must be specified. Note the units. Weight must be specified in lbs/ft.

P1 = This is the type of cable. P= 0 indicates a catenary cable. P= 1 indicates a messenger cable. This also must be specified. This Information is used for accurate printing of results.

NOTE: The prefix ND=, SG=, TEN=, W= and P= must precede the specification of the numerical values mentioned above. This command line is specified for each cable in the structure. Both messenger and catenary cables are specified separately if both present in the structure.

This section MUST end with a blank line.

DYNAMIC PARAMETERS

This section describes the dynamic parameters necessary for analysis.

DYNAMICS - (Section Designation)

TOL A= ALPHA B= BETA G= GAMMA P= P1 N= N1

TOL = This is the die-down criteria. This must always be less than or equal to 0.001. The smaller the value the better the equivalent static solution. The only caveat is that the smaller the tolerance value the longer the program runs to achieve die-down.

ALPHA = This is the alpha term selected from Table B-1.

BETA = This is the beta term selected from Table B-1.

GAMMA= This is the gamma term selected from Table B-1.

P1 = In order to be sure of die-down, the structure's response of a critical node must be plotted. The node to be plotted is P1.

N1 = The displacement degree of freedom (dof) for the node to be plotted must also be specified. X dof=1. Y dof=2. Z dof=3.

This section MUST end with a blank line.

JOINT COORDINATE DATA

This section defines the nodal coordinates in a positive Cartesian coordinate system. The following lines will define the coordinates;

COORDINATES - (Section Designation)

ND X=X_1 Y=Y_1 Z=Z_1 or C=C_1

ND = Node number for the given coordinates,

X_1 = X coordinate for the node ND,

Y_1 = Y coordinate for node ND,

Z_1 = Z coordinate for node ND,

C_1 = Cable number that the node belongs.

NOTE: Any node that is not specified will default to the origin.

This section MUST end with a blank line.

BOUNDARY CONDITION DATA

This section defines the active degrees freedom for the structure to be analyzed. All the degrees of freedom must be specified as fixed or released, according to the boundary conditions and the types of elements connected to the node. The following lines of input describe the state of the DOF.

BOUNDARY - (Section Designation)

NF,NL,NI DOF=F_1,F_2,F_3,F_4,F_5,F_6

NF = First node in a generation sequence for which the degree of freedom is specified.

NL = Last node in a generation sequence for which the degree of freedom is specified.

NI = Increment for generating node numbers between NF and NL for which the DOF specification is used. NL and NI can be left blank if no generation is desired.

F_i = State of the i-th DOF, either fixed or released. Therefore F_i can have ONLY the two following values; F_i = F is for fixed or F_i = R is for released.

The boundary specification line may be repeated as many times as is necessary to define the boundary conditions of all the nodes. Any node that is not defined will default to the fully fixed condition.

This section MUST end with a blank line.

WIND PARAMETERS

This section defines the wind loading parameters. The syntax rules are as follows:

WIND - (Section Designation)

SPEED= S1 DIRECTION= D1 GUST= G1,G2 K=K1 S=STD

S1 = Average wind speed (mph).

D1 = Wind approach angle. If wind impact angle is perpendicular to the default x-z plane, D1= 90°. See Fig. B3.

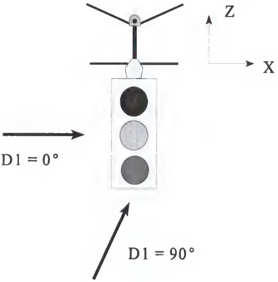

Fig. B-3 Wind Impact Angle

G1 = If istat is specified as -1 in the control section then the gust parameters must be specified. Otherwise this must be omitted. G1 is the duration of the wind data to generate. Duration could range from 3 seconds to 90 seconds. There is a default limit of 90 seconds incorporated into the program.

G2 = Sampling interval for the gust wind generation. This must not be less than 0.1 seconds. The numerical filters used to generate the wind load tends to be divergent if G2 is less than 0.1. Note also that G2 can not be greater than G1.

K1 = roughness factor. This is depended on the environment surrounding the structure. K1 values can be obtained from chapter four.

STD = This the standard deviation from the mean velocity desired in the random velocity component. If omitted, a default value is computed based on the spectral density distribution in chapter 4. If the default STD value is not desired a value of one implies standard deviation is ignored.

This section MUST end with a blank line.

ELEMENT DATA

One section each must be supplied for the different element types that makes up the structure. The units of element properties unless otherwise specified must be in kips and inches.

CABLE - (Section Designation)

NM,NP

NM = Number of cable members.

NP = Number of material properties.

Material Property Lines - NP lines

MID A=A E=E D=D

MID = Material property set number.

A = Cross sectional area, A.

E = Modulus of elasticity, E.

D = Damping ratio, D.

Cable Element Lines - NM lines

NN,NI,NJ M=MP C=C_1

NN = Member identification number.

NI = Joint number I (Starting node).

NJ = Joint number j (Ending node).

MP = Material property number.

C_1 = Number of cable that the element belongs.

This section MUST be terminated with a blank line.

TRUSS - (Section Designation)

NM,NS

NM = Number of truss members.
NS = Number of material properties.

Material property lines - (NS lines).

MID A=A E=E D=D M=M

MID = Material property set number.
A = Cross Sectional Area, A.
E = Modulus of elasticity, E.
D = Damping ratio
M = mass density of material. (lbs/ft^3).

TRUSS element lines - NM lines

NN,NI,NJ M=MP

NN = Member identification number.
NI = Joint number I (Starting node).
NJ = Joint number J (Ending node).
MP = Material property number.

This section MUST be terminated with a blank line.

THREE DIMENSIONAL BEAM, AND CONNECTOR ELEMENTS

There are two types of three dimensional beam elements used in DYNASS. Both types of beam elements are used to model members which have bending stiffness about the two principal axes and axial stiffness. Shearing deformations are neglected for both elements. The members are prismatic and connected to nodes i and j. A dummy node, k, is used to specify the direction of the principal bending axis. Axis 1 is the i-j direction; Axis 3 is normal to axis 1 and is in the i-j-k plane; Axis 2 is normal to the plane 3 formed by the 1 and 3 axes and completes the right hand rule. The orientation of the axes is shown in Fig. B.3.

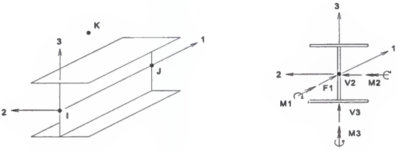

Fig. B.3 Axis Orientation

The information for each type must be supplied in a separate block. The Beam element is a full 3-D beam which serves as a pole in the structure. The Connector element is a large displacement 3-D beam element and it connects the catenary cable with the messenger cable and the signal light or sign.

BEAM - (Section Designation)

NM,NP

NM = Number of beam members.

NP = Number of material types.

Material Property Lines - NP lines

MID I=I_2,I_3 J=J A=A E=E G=G T=TYPE M=M D=D

MID = Material property number.

A = Cross sectional area.

J = Torsional moment of inertia about the 1 axis.

I_2 = Moment of inertia about the 2 axis, I_{22}. Strong Axis.

I_3 = Moment of inertia about the 3 axis, I_{33}. Weak Axis.

E = Modulus of elasticity (Young's Modulus), E.

G = Shear Modulus, G, only used to calculate the torsional stiffness.

TYPE = 1 (beam used as part of the strain pole). 2 (other beam usage excluding connector. Necessary for other types of structures.)

D = Damping ratio.

M = Mass density of the beam material (lbs/ft^3).

Beam element Connectivity - NM lines

NN,NI,NJ,NK,NPL M=MP

NN = Member number.

NI = Node number I (Staring node).

NJ = Node number j (Ending node).

NK = Node number k (Dummy node for orientation).

NPL = Pole number to which the beam belongs.
If T=2, this value must be omitted.

MP = Material property for this member. (DEFAULT= previous).

This section MUST be terminated with a blank line.

CONNECTOR - (Section Designation)

NM,NP

NM = Number of connector members.

NP = Number of material types.

Material Property Lines - NP lines

MID I=I_2,I_3 J=J A=A E=E M=M D=D

MID = Material property number.

A = Cross Sectional area.

I_2 = Moment of inertia about the 2 axis, I_{22}.

I_3 = Moment of inertia about the 3 axis, I_{33}.

E = Modulus of elasticity (Young's Modulus), E.

J = Torsional moment of inertia about the 1 axis.

M = Mass density of the connector material. (lbs/ft^3).
Default=490 lbs/ft^3.

D = Damping ratio.

Connector element Connectivity - NM lines

NN,NI,NJ,NK M=MP

NN = Member number.

NI = Node number I.

NJ = Node number J.

NK = Node number K.

MP = Material property set for this member.
(DEFAULT= previous).

This section MUST be terminated with a blank line.

SIGNAL/SIGN ELEMENTS

These two elements are not like the other elements because their stiffness properties are never calculated. The signals and sign are specified to compute wind loading. If the typical signal heads or auxiliary signs are used [appendix C, ref 19] the program is equipped to compute the necessary areas and weights. If a new atypical cladding is used, the sign type OTHER should be selected.

SIGNAL - (Section Designation)

NM,NP

NM = Number of signals and /or signs nodes.

NP = Number of different signal or sign specification.

Property Specification Lines - NP lines

MID S=S D=D_1,..,D_S E=E_1,...,E_S L=L_1,...,L_S G=G_1,...,G_S

or

MID N=N A=A

MID = Material property number.

S = Type of bracket. S=1 indicates a one-way bracket hence one signal head attached to the node. S=4 is the largest number of signal heads that can be attached to any one node.
This indicates a 4-way light.

D_i = Diameter of the lens. There are only two choices. 8" or 12" lens. A choice of lens diameter should be specified for each face of light depending on the value of S specified. I=1..S

E_i = Border preference for the signal light. The choices are without, WO, with 5" border backplate, W5, and with 8" border backplate, W8..

L_i = Material type for the signals. There are only two choices, Aluminum, AL, or Poly Carbonate, PC.

G_i = Geometry of the signal face. See ref [19] and Table B-4 for details. The order the signal faces must be specified is clock-wise starting from the face parallel to the x-z plane. So if Fig. B-3 is referred to. The face first specified corresponds to the wind impact angle D1 of 90°, the next face corresponds to an impact angle D1 of 0° and the next to an impact angle of 270° and finally the face corresponding to an impact angle of 180°. If the structure exist in the y-z plane, i.e. facing the impact wind direction of 0°, a zero specification (e.g. $D = 0, D_2$) must precede the lens diameter list for a single bracket light.

Alternatively an auxiliary sign could be specified.

N = Typical Auxiliary sign notation. See ref [19] for details. If N=OTHER is specified. Then specify area.

A = Surface area of the sign or atypical signal. Note this is only specified in conjunction with the sign type OTHER.

Table B-4 Light face arrangement for G specification

Geometry Denotation	Light Configuration	Description
G=1	1 section light	Used as blinking caution light
G=2	2 linear section Commonly at railway crossing.	
G=3	3 linear section	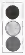
G=4	4 linear section	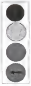
G=5	5 linear section	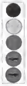
G=6	5 special (dog house type)	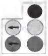
G=7	5T special	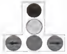

Signal/Sign Node Assignment - NM lines

NN,NM M= MP

NN = Signal or Sign number.

NM = Signal or Sign node.

MP = Signal Light or Traffic Sign type to assign to the node.

This section MUST be terminated with a blank line.

LOADS - (Section Designation)

NF F=F_X, F_Y, F_Z

NF = Node on which the load will act.

F_X = Load corresponding to the X transnational degree of freedom.

F_Y = Load corresponding to the Y transnational degree of freedom.

F_Z = Load corresponding to the Z transnational degree of freedom.

The load line specification line may be repeated as many times as is necessary to define all the loads acting on the structure. Any loads not specified will default to zero.
This section MUST end with a blank line.

MEMORY MANAGEMENT AND SPECIAL FEATURES IN DYNASS

It is necessary to discuss special features in the program. One of such feature is tied to the dynamic memory management employed in the program. For a more efficient memory management the program uses the profile equation solver. The profile form of the mass, stiffness and damping matrices are stored because of the skyline form and the sparseness of these matrices. The inverse of the assembled mass and effective stiffness matrices was required at various stages in the analysis process, matrix inversion was performed using a typical inversion technique. The commonly used algorithms used to perform a matrix inversion include the Gauss elimination, standard Cholesky ($A=LL^T$) and the modified Cholesky ($A=LDL^T$). The modified Cholesky is adopted in this program. The profile solver programmed into DYNASS is a based on Carlos Fellipa's Profile solver given in ref [33]. The Algorithm for matrix inversion is simply;

$Ax = b;$	***A is the n × n matrix, x is the unknown displacement vector, b is the force vector.***
$A = LDU;$	***Factorize A. L is the unit lower triangular matrix, D is a non-singular diagonal matrix, U is the transpose of L.***
$Lz = b;$	***Forward substitution.***
$y = z / D;$	***Scaling.***
$Ux = y;$	***Back substitution.***

The above procedure is typical of all modified Cholesky solution procedure. What is not typical is the storage of the coefficients of matrix [A]. If [A] is defined below a 9 x 9 matrix with zero terms.

$$A=\begin{bmatrix}
a_{11} & a_{12} & & & a_{15} & & & & \\
 & a_{22} & a_{23} & & 0 & & & a_{28} & \\
 & & a_{33} & a_{34} & a_{35} & & & a_{38} & \\
 & & & a_{44} & a_{45} & a_{46} & a_{47} & a_{48} & \\
 & & & & a_{55} & a_{56} & 0 & a_{58} & a_{59} \\
 & & & & & a_{66} & a_{67} & 0 & a_{69} \\
 & \mathit{SYMM.} & & & & & a_{77} & a_{78} & a_{79} \\
 & & & & & & & a_{88} & 0 \\
 & & & & & & & & a_{99}
\end{bmatrix}$$

Matrix A has a skyline profile. The profile matrix stored is as shown below.

$$A=\left\{\begin{matrix}
a_{11} & a_{12} & a_{22} & a_{23} & a_{33} & a_{34} & a_{44} & a_{15} & 0 & a_{35} \\
a_{45} & a_{55} & a_{46} & a_{56} & a_{66} & a_{47} & 0 & a_{67} & a_{77} & a_{28} \\
a_{38} & a_{48} & a_{58} & 0 & a_{78} & a_{88} & a_{59} & a_{69} & a_{79} & 0 & a_{99}
\end{matrix}\right\}$$

A pointer array was developed to accurately store and recover the above profile matrix. The pointer array, referred to as the NA array in the program, for the above matrix is therefore

$$NA = \{1 \quad 3 \quad 5 \quad 7 \quad 12 \quad 15 \quad 19 \quad 26 \quad 31\}$$

This locates the terms along the diagonal of the original [A] matrix. To conform with Carlos Fellipa's profile solver [33]. There is a negative unit regressive shift of the above pointers, such that the pointer now pointing to the first diagonal term in the [A] matrix is zero. The equivalent Fellipa's NA is

$$NA = \{0 \quad 2 \quad 4 \quad 6 \quad 11 \quad 14 \quad 18 \quad 25 \quad 30\}$$

One of the limitations in the program has to do with the maximum size of the NA array. The default maximum permissible size is 2000. The above example has an NA size of 9, corresponding to the number of degrees of freedom. Another memory restriction is the size of the profile matrix. For the above example the profile matrix size is 31. For the DYNASS program the default maximum profile size is 6000. Any attempt to exceed these limits results in a memory restriction error to be printed and an abrupt termination of the program. Included is a sample INPUT and OUTPUT files.

SAMPLE INPUT AND OUTPUT FILES FOR DYNASS

The sample input file included is for the wind load test #1 discussed in chapter 6. All coordinates, member properties and connectivity information related to Fig. 6.1. The modified Newmark's Beta method is adopted for analysis with a tolerance of 0.000133 and numerical parameters of -0.1 for alpha, 0.3025 for beta and 0.6 for gamma. he average wind speed is 39.941 and wind model 2 (i.e. istat= -1) is used. The wind is generated for 2.5 sec, same as for total time of analysis. Time step of analysis is 0.0003 but time step for wind speed generation is 0.1. Dynamic response for node 16, y direction is printed as output plot file SVEL.

```
First Wind Test -- Low Wind Speed load test
nodes=18, elem_no=3, cable=2, istat=-1
nonlinear
6 nd=3,5,6,7,8,9 sg=5.00 ten=0.6 w=0.27 p=0
6 nd=2,11,12,13,14,15 ten=0.829 w=0.27 p=1
:
dynamics
t=0.000133 a=-0.1 b=0.3025 g=0.6 time=2.5,0.0003 p=16 n=2
:
wind
speed=39.941 direction=90 gust=2.5 ,0.1 k=0.05 s=1
:
coordinates
1   x= 0     y= 0.000  z= 16
2   x= 0     y= 0.000  z= 112
3   x= 0     y= 0.000  z= 164
4   x= 0     y= 0.000  z= 166
5   x= 15*12 y= 0.000  z= 145.28
6   x= 30*12 y= 0.000  z= 126.55
7   x= 42*12 y= 0.000  z= 126.55
8   x= 57*12 y= 0.000  z= 145.28
9   x= 72*12 y= 0.000  z= 164
10  x= 72*12 y= 0.000  z= 142
11  x= 15*12 y= 0.000  z= 112
12  x= 30*12 y= 0.000  z= 112
```

```
13  x= 42*12 y= 0.000  z= 112
14  x= 57*12 y= 0.000  z= 112
15  x= 72*12 y= 0.000  z= 112
16  x= 30*12 y= 0.000  z= 112-27.3
17  x= 42*12 y= 0.000  z= 112-27.3
18  x= 72*12 y= 0.000  z= 0
:
boundary
1,18,1 dof=r r r r r r
1   dof=f f f f f f
5   dof=r r r f f f
8   dof=r r r f f f
11  dof=r r r f f f
14  dof=r r r f f f
18  dof=f f f f f f
:
Cable
10,1
1  A=0.079 E=23000 D=0.05
1  3,5  M=1 C=1
2  5,6  M=1 C=1
3  6,7  M=1 C=1
4  7,8  M=1 C=1
5  8,9  M=1 C=1
6  2,11 M=1 C=2
7  11,12 M=1 C=2
8  12,13 M=1 C=2
9  13,14 M=1 C=2
10  14,15 M=1 C=2
:
beam
6,2
1 A=93.4 I=888,888  J=484 E=4000   M=195.0 T=1   D=0.05   :EI = 3 550 000
2 A=93.4 I=820,820  J=484 E=4000   M=195.0 T=1   D=0.05   :EI = 3 280 000
1   1,2,18,1  M=1
2   2,3,18,1  M=1
3   3,4,18,1  M=1
4   9,10,1,2  M=2
5   10,15,1,2  M=2
6   15,18,1,2  M=2
```

```
:
connector
4,2
1 A=0.799 I=0.310,0.310 J=0.620 E=29000 M=490.2 D=0.05 : pipe connector

2 A=0.5324 I=0.167,0.01534 J=0.50 E=29000 M=490.2 D=0.05 : strap
1  6,12,18  M=1 P=0.07140
2  12,16,18  M=1 P=0.07140
3  7,13,18  M=2 P=0.07140
4  13,17,18  M=2 P=0.07140
:
signal
2,1
1 R=1.5 S=1 D=12 E=WO L=AL G=6
1 16 m=1
2 17 m=1
:
loads
12 F=0,0,-8.15/1000,0,0,0
13 F=0,0,-8.15/1000,0,0,0
6 F=0,0,-4.35/1000,0,0,0
7 F=0,0,-4.35/1000,0,0,0
:
```

The corresponding OUTPUT file for the previous INPUT file is given next. Note the units used as output is kips and inches unless otherwise stated. The OUTPUT includes an echo of the input parameters and the results of computations. There also two different output generated by the program, a displacement plot in the file PLOT and the wind generation information given in the plot file SVEL. The header for the PLOT file is time, nodal displacement, nodal velocity and nodal acceleration. The header for the SVEL file is time, wind speed, nodal wind drag force, tension in the catenary cable(s) and finally the tension in the messenger cable(s).

```
++++++++++++++++++++++++++++++++++++++++++++++++++++++
+   #####    #   #  #    #    ##     ####    ####    +
+   #    #    # #   ##   #   #  #   #       #        +
+   #    #     #    # #  #  #    #   ####    ####    +
+   #    #     #    #  # #  ######       #       #   +
+   #    #     #    #   ##  #    #  #    #  #    #   +
+   #####      #    #    #  #    #   ####    ####    +
+                                                    +
+             *---------------------------*          +
+             |                           |          +
+             |          Developed        |          +
+             |             By            |          +
+             |                           |          +
+             |   Dr. Adeola K. Adediran  |          +
+             |                           |          +
+             |        In Conjuction      |          +
+             |            With           |          +
+             |                           |          +
+             |     Dr. Marc Hoit         |          +
+             |     Dr. Ronald Cook       |          +
+             |     Dr. Petros Christou   |          +
+             |                           |          +
+             *---------------------------*          +
+                                                    +
+                                                    +
++++++++++++++++++++++++++++++++++++++++++++++++++++++
```

Title and General Information

```
First Wind Test -- Low Wind Speed load test


 Number of joints                     =        18

 Number of element types              =         3

 Number of cables                     =         2


 Units are in Kips and Inches unless otherwise stated


ECHO OF INPUT DATA


A. Boundary conditions                  B. Input nodal point coordinates


  Node  X    Y    Z   XX   YY   ZZ            X            Y            Z


   1    F    F    F    F    F    F        0.000        0.000       16.000
   2    R    R    R    R    R    R        0.000        0.000      112.000
   3    R    R    R    R    R    R        0.000        0.000      164.000
   4    R    R    R    R    R    R        0.000        0.000      166.000
   5    R    R    R    F    F    F      180.000        0.000      145.280
   6    R    R    R    R    R    R      360.000        0.000      126.550
   7    R    R    R    R    R    R      504.000        0.000      126.550
   8    R    R    R    F    F    F      684.000        0.000      145.280
   9    R    R    R    R    R    R      864.000        0.000      164.000
  10    R    R    R    R    R    R      864.000        0.000      142.000
  11    R    R    R    F    F    F      180.000        0.000      112.000
  12    R    R    R    R    R    R      360.000        0.000      112.000
  13    R    R    R    R    R    R      504.000        0.000      112.000
  14    R    R    R    F    F    F      684.000        0.000      112.000
  15    R    R    R    R    R    R      864.000        0.000      112.000
  16    R    R    R    R    R    R      360.000        0.000       84.700
  17    R    R    R    R    R    R      504.000        0.000       84.700
  18    F    F    F    F    F    F      864.000         0.000         0.000


C. Element information



Beam Element information


    Property Number        =   1
    Modulus of Elasticity             =    4000.00
    Area                              =  93.400000
    Moment of Inertia (Strong axis)= 888.000000
    Moment of Inertia (Weak   axis)= 888.000000
    Torsional Moment of Inertia    =   484.0000
    Shear Modulus                     =    1739.13
    Damping Ratio                     =   0.050000
    Material density                  = 195.000000  lbs/ft^3

    Property Number        =   2
    Modulus of Elasticity             =    4000.00
    Area                              =  93.400000
    Moment of Inertia (Strong axis)= 820.000000
    Moment of Inertia (Weak   axis)= 820.000000
    Torsional Moment of Inertia    =   484.0000
    Shear Modulus                     =    1739.13
    Damping Ratio                     =   0.050000
    Material density                  = 195.000000  lbs/ft^3

  - Number of Elements =   6

    Member #   Beam Type   Node I   Node J   Node K   Material #
       1           1          1        2       18         1
    2            1        2        3        18        1

    3            1        3        4        18        1

    4            1        9       10         1        2

    5            1       10       15         1        2

    6            1       15       18         1        2


   Beam type 1 - Pole

   Beam type 2 - Other Beam Usage



Cable element information


  Property Number        =   1

  Modulus of Elasticity =   23000.00

  Area                   =   0.079000

  Damping Ratio          =   0.050000


Number of Elements =  10


Member #   Node I   Node J   Material #   Cable #    Initial Tension (kips)
       1        3        5            1         1          0.652482
       2        5        6            1         1          0.652018
       3        6        7            1         1          0.648627
       4        7        8            1         1          0.652018
       5        8        9            1         1          0.652482
       6        2       11            1         2          0.829000
       7       11       12            1         2          0.829000
       8       12       13            1         2          0.829000
       9       13       14            1         2          0.829000
      10       14       15            1         2          0.829000
```

```
Cable initial sag


Cable  1:  0.050000

Cable  2:  0.000000



Connector Element information


   Property Number      =   1

   Modulus of Elasticity          =   29000.00

   Area                           =   0.799000

   Moment of Inertia (Strong axis)=   0.310000

   Moment of Inertia (Weak   axis)=   0.310000

   Torsional Moment of Inertia    =       0.62

   Shear Modulus                  =   11153.85

   Damping Ratio                  =   0.050000

   Material density               = 490.200000 lb/ft^3


   Property Number      =   2

   Modulus of Elasticity          =   29000.00

   Area                           =   0.532400

   Moment of Inertia (Strong axis)=   0.167000

   Moment of Inertia (Weak   axis)=   0.015340

   Torsional Moment of Inertia    =       0.50

   Shear Modulus                  =   11153.85

   Damping Ratio                  =   0.050000

   Material density               = 490.200000 lb/ft^3


   Number of Elements =   4


   Member #   Node I   Node J   Node K   Material #
```

```
          1        6        12        18            1
          2       12        16        18            1
          3        7        13        18            2
          4       13        17        18            2
M= 1 Single Light   D=12 E=  WO L= G=**


     Signal and Sign information
     Sign(al) #   Node #   Material #   Weight (kips)   Area (in^2; 1-3, 1-2
planes)
          1      16       1            0.71E-01        0.11E+04        0.00E+00
          2      17       1            0.71E-01        0.11E+04        0.00E+00


 *** Load Analysis Started ***




 G. Concentrated Nodal Loads

  Node  Load        x         y         z        xx        yy        zz
    12     1  0.00E+00  0.00E+00 -0.82E-02  0.00E+00  0.00E+00  0.00E+00
    13     1  0.00E+00  0.00E+00 -0.82E-02  0.00E+00  0.00E+00  0.00E+00
     6     1  0.00E+00  0.00E+00 -0.43E-02  0.00E+00  0.00E+00  0.00E+00
     7     1  0.00E+00  0.00E+00 -0.43E-02  0.00E+00  0.00E+00  0.00E+00


 *** Formation of Stiffness Matrix ***


 E. Time Step Analysis:
  Time Step Interval  =    0.000300 secs.

  Max. Time Allowed   =   90.000000 secs.



F. Displacements After Die-Down


   Node            X            Y            Z           XX           YY           ZZ

      1 0.00000E+00 0.00000E+00 0.00000E+00 0.00000E+00 0.00000E+00 0.00000E+00

      2 0.16734E+00 0.43437E-02-0.18611E-04-0.70688E-04 0.28118E-02 0.00000E+00

      3 0.32096E+00 0.81251E-02-0.28003E-04-0.73741E-04 0.30254E-02 0.00000E+00

      4 0.32701E+00 0.82726E-02-0.28003E-04-0.73741E-04 0.30254E-02 0.00000E+00

      5 0.38091E-01 0.25155E+01-0.22159E+01 0.00000E+00 0.00000E+00 0.00000E+00

      6-0.84318E-01 0.50543E+01-0.30377E+01 0.61937E+00-0.13009E-02-0.96823E-03

      7-0.92674E-01 0.51359E+01-0.29750E+01 0.61044E+00-0.37933E-02 0.72197E-04

      8-0.21992E+00 0.26392E+01-0.21046E+01 0.00000E+00 0.00000E+00 0.00000E+00

      9-0.49211E+00 0.12680E-01-0.30868E-04-0.10466E-03-0.41988E-02 0.00000E+00

     10-0.40003E+00 0.10382E-01-0.26925E-04-0.10406E-03-0.41575E-02 0.00000E+00

     11 0.52082E-01 0.67560E+01-0.52327E+00 0.00000E+00 0.00000E+00 0.00000E+00

     12-0.60736E-01 0.13502E+02-0.33418E+00 0.61966E+00-0.12998E-02-0.96690E-03

     13-0.48410E-01 0.13499E+02-0.33101E+00 0.61621E+00-0.37534E-02 0.12170E-03

     14-0.16262E+00 0.67573E+01-0.50794E+00 0.00000E+00 0.00000E+00 0.00000E+00

     15-0.27777E+00 0.72958E-02-0.21548E-04-0.10130E-03-0.39682E-02 0.00000E+00

     16-0.16572E-01 0.29365E+02 0.47473E+01 0.62021E+00-0.12980E-02-0.96452E-03

     17 0.30688E-01 0.29437E+02 0.48043E+01 0.62699E+00-0.36755E-02 0.21618E-03

     18 0.00000E+00 0.00000E+00 0.00000E+00 0.00000E+00 0.00000E+00 0.00000E+00



H. Final Displaced Configuration


   Node            X            Y            Z

      1        0.000        0.000       16.000
      2       0.167       0.004     112.000
      3       0.321       0.008     164.000
      4       0.327       0.008     166.000
      5     180.038       2.516     143.064
      6     359.916       5.054     123.512
      7     503.907       5.136     123.575
      8     683.780       2.639     143.175
      9     863.508       0.013     164.000
     10     863.600       0.010     142.000
     11     180.052       6.756     111.477
     12     359.939      13.502     111.666
     13     503.952      13.499     111.669
     14     683.837       6.757     111.492
     15     863.722       0.007     112.000
     16     359.983      29.365      89.447
     17     504.031      29.437      89.504
     18     864.000       0.000       0.000


*** Force Recovery Started ***




I. Element Forces

 1. Primary(Catenary) cables

  - Cable Member Forces

    Cable      Member      Force      Stress
```

```
      1          1  0.5648E+00  0.7149E+01

                 2  0.5643E+00  0.7143E+01

                 3  0.5608E+00  0.7098E+01

                 4  0.5637E+00  0.7136E+01

                 5  0.5642E+00  0.7141E+01


2. Secondary(Messenger) cables


 - Cable Member Forces


   Cable      Member       Force       Stress


      2          6  0.9992E+00  0.1265E+02

                 7  0.9991E+00  0.1265E+02

                 8  0.9986E+00  0.1264E+02

                 9  0.9997E+00  0.1265E+02

                10  0.9997E+00  0.1265E+02


Beam Member Forces



                          1-2 Plane                1-3 Plane
   Member Node       Moment         Shear       Moment         Shear     Axial Force


      1    1    0.1789E+03  0.4580E-01  0.4814E+01  -.1560E+01     0.7243E-01
           2    -.2918E+02  -.4580E-01  -.4170E+00  0.1560E+01     -.7243E-01
                                                 Axial Torque =  0.00000E+00


      2    2    0.2918E+02  0.7972E-02  0.4158E+00  -.5611E+00     0.6748E-01
           3    0.4148E-03  -.7972E-02  -.1288E-02  0.5611E+00     -.6748E-01
                                                 Axial Torque =  0.00000E+00
```

```
         3     3   0.3470E-05  0.6444E-05  0.1571E-04  -.1175E-04     0.4226E-07
               4   0.2003E-04  -.6444E-05  -.2825E-05  0.1175E-04     -.4226E-07
                                                Axial Torque =  0.00000E+00


         4     9   -.1937E-02  -.8211E-02  -.2193E-03  0.5600E+00     0.6696E-01
              10   -.1232E+02  0.8211E-02  -.1804E+00  -.5600E+00     -.6696E-01
                                                Axial Torque =  0.00000E+00


         5    10   0.1232E+02  -.8089E-02  0.1803E+00  0.5590E+00     0.6696E-01
              15   -.2909E+02  0.8089E-02  -.4230E+00  -.5590E+00     -.6696E-01
                                                Axial Torque =  0.00000E+00


         6    15   0.2906E+02  -.4547E-01  0.4205E+00  0.1556E+01     0.7188E-01
              18   -.2034E+03  0.4547E-01  -.5513E+01  -.1556E+01     -.7188E-01
                                                Axial Torque =  0.00000E+00



Connector (Hanger) Forces



                         1-2 Plane                1-3 Plane
   Member Node       Moment       Shear       Moment       Shear    Axial Force


         1     6   -.7777E-05  0.2472E-01  0.2399E-05  -.1774E-03     -.4768E-01
              12   0.2588E-02  -.2472E-01  0.3597E+00  0.1774E-03     0.4768E-01
                                                Axial Torque =  0.15738E-06


         2    12   -.2532E-02  -.1317E-01  -.3597E+00  0.9571E-04     -.5883E-01
              16   -.8104E-04  0.1317E-01  0.1136E-03  -.9571E-04     0.5883E-01
                                                Axial Torque =  0.14089E-06
```

```
 3    7   0.1534E-03  0.2419E-01  -.2255E-03  -.5635E-04      -.4790E-01

     13   0.6665E-03  -.2419E-01  0.3522E+00  0.5635E-04      0.4790E-01

                                          Axial Torque =  0.19264E-05


 4   13   -.2507E-03  -.1291E-01  -.3519E+00  0.8344E-05      -.5920E-01

     17   0.2288E-04  0.1291E-01  -.5080E-03  -.8344E-05      0.5920E-01

                                          Axial Torque =  0.40491E-05
```

LIST OF REFERENCES

1. Schek, J. H. (1974), "The Force Density Method for Finding and Computation of General Networks," Computer Methods in Applied Mechanics, North Holand Publishing Co.

2. Norris, H. C. and Wilbur, J. B. (1976), Elementary Structural Analysis, McGraw-Hill, New York, Third Edition.

3. Folwer, D. (1986), Private Treatise and Class Notes for ARE 388, Civil Engineering Department, University of Texas at Austin.

4. Irvine, H. M., and Caughey, T. K. (1974), "The Linear Theory of Free Vibrations of a Suspended Cable," Proceeding, Royal Society of London, London, England, Series A Vol. 341, pp 299-315.

5. Starossek, Uwe (1991), "Dynamic Stiffness Matrix of Sagging Cable," Journal of Engineering Mechanics, ASCE, Vol 117 (12), pp 2815 - 2829.

6. Veletos, A. S., and Darbre, G. R. (1983), "Free Vibration of Parabolic Cables," Journal of Structural Engineering, ASCE, Vol 109 (2), pp 503 - 519.

7. Leonard, J. W. (1988), Tension Structures - Behavior and Analysis, McGraw-Hill, New York.

8. Fertis, D. G. (1973), Dynamics and Vibration of Structures, Wiley, New York.

9. Tuma, J. J. (1987), Handbook of Structural and Mechanical Matrices, McGraw-Hill, New York.

10. Hays, C. (1990), Private Treatise and Class Notes for CES 6106, Civil Engineering Department, University of Florida at Gainesville.

11. Chen, Z. Q., and Agar, J. A. (1992), "Geometric Nonlinear Analysis of Flexible Spatial Beam Structures," Computers and Structures, Vol 49 (6) pp 1083 - 1094.

12. Bathe K. J., and Bolourchi, S. (1978), "Large Displacement Analysis of Three - Dimensional Beam Structures," International Journal of Numerical Methods in Engineering, Vol 14 (4), pp 961 - 986.

13. Argyris, J.H., Dunne, P. C., and Scharpf, D. W., (1978), "On Large Displacement - Small Strain Analysis of Structures with Rotational Degrees of Freedom." Computer Methods in Applied Mechanics and Engineering, Vol 14-15, pp 401 - 451..

14. Chopra A. K. (1995), Dynamics of Structures, Theory and Application to Earthquake Engineering, Prentice Hall.

15. Krishna, P. (1978), Cable Suspended Roofs, McGraw-Hill Book Company, New York.

16. Hengold W. M., and Russell J. J. (1976), "Equilibrium and Natural Frequencies of Cable Structures (A Non-linear Finite Element Approach)," Computers and Structures, Vol 6 pp 267 - 271.

17. Haritos N., and He, D. T. (1990), "A Finite Element Formulation for Cables suitable for Dynamic Modelling," Mathematics and Computers in Simulation, Vol 32, pp 179 - 184.

18. Burnett, D. S., (1987), Finite Element Analysis From Concepts to Application, Addison Wesley Publishing.

19. Weaver, W. Jr., and Gere, J. M. (1990), Matrix Analysis of Framed Structures, Third Edition, Van Nostrand Reinhold.

20. Wood, W. L., Bossak, M., and Zienkiewicz, O. C. (1980), "An Alpha Modification of Newmark's Method," International Journal of Numerical

Methods in Engineering, Vol 15 (10), pp 1562 - 1566.

21. Hoit, M. I., Cook, R. A., Christou, P. M., and Adediran A. K. (1994), "Computer Aided Design Program for Signal Pole and Span Wire Assemblies with Two Point Connection System," Research Report, Civil Engineering Department.

22. Cohen, E., and Perrin, H. (1957), "Design of Multi-level Guyed Towers: Wind Loading," Journal of Structural Division, ASCE, Vol 83 (5), pp 1355-1 - 1355-29.

23. Christou, P. M. (1996), An Integrated Technique for the Analysis of Frame and Cable Structures, Ph. D. Thesis, University of Florida.

24. Davenport, A. G. (1961), "The Application of Statistical Concepts to the Wind Loading of Structures," Proceeding, Institute of Civil Engineers, London, England, Vol 19, pp 449 - 472.

25. Chen, Yu., and Ahmadi, G. (1992), "Wind Effects on Base - Isolated Structure," Journal of Engineering Mechanics, ASCE, Vol 118 (8) pp 1708 - 1727.

26. Iannuzzi, A., and Spinelli, P. (1987), "Artificial Wind Generation and Structural Response," Journal of Structural Engineering, ASCE, Vol 113 (12), pp 2382 - 2397.

27. Giovanni, S. (1993), "Gust Buffeting II: Dynamic Along-wind Response," Journal of Structural Engineering, ASCE, Vol 119 (2), pp 383 -398.

28. Giovanni, S. (1988), "Equivalent Wind Spectrum Technique Theory and Applications," Journal of Structural Engineering, ASCE, Vol 114 (6) pp 1303 - 1321.

29. Haritos, N. (1988), "The Excitation of Cable-Stayed Masts by Turbulent Wind," Mathematics and Computers in Simulation, Vol 30, pp 81-86.

30. Leva, J. L. (1992), "A fast Normal Random Number Generator," ACM Transactions on Mathematical Software, Vol 18 (4), pp 449 - 453.

31. Wajek, S. L. (1994), Static and Dynamic Tests on Dual Cable Supported Traffic Signal Systems, Masters Report, Civil Engineering, University of Florida.

32. Baron, F., and Vendatesan, M. S., (1971), "Non-linear Analysis of Cable and Truss Structures," Journal of the Structural Division, ASCE, Vol 97 (2), pp 679-710.

33. Felippa, C. A. (1974), "Solution of Linear Equations with Skyline-Stored Symmetric Matrix," Computers and Structures, Vol 5 pp 13 - 29.

BIOGRAPHICAL SKETCH

Adeola Kehinde Adediran is one of seven kids born to her parents. She was born on Feburary 17, 1966 in Nigeria. She is also one of a pair of identical twins. Her undergraduate work was conducted at Nigeria's premiere university, the University of Ibadan, Oyo state, Nigeria. She graduated with honors and proceeded to an obligatory one-year military training and youth service to her country. In Nigeria, she worked as consulting engineer for two years. Working on various projects, notably the 17-storey Federal Mortgage bank building, Marina, Lagos State and the Nigerian Council for Women Socities Headquarters in Abuja, Nigeria.

She was admitted into the master's program at the University of Tennessee, Fall of 1989 and graduated with a master's degree Summer of 1991. She then proceeded to a doctoral program at the University of Florida in Spring of 1992. She is currently completing all requirements for the degree, to be issued Spring 1997.

She is a member of the American Concrete Institute, the Society of Women Engineers and the International Federation of University Women. Ms. Adeola Adediran joined the design team of Walter P. Moore and Associates at their Houston head office as a structural engineer on the 20th of January 1997.

I certify that I have read this study and that in my opinion it conforms to acceptable standards of scholarly presentation and is fully adequate, in scope and quality, as a dissertation for the degree of Doctor of Philosophy.

Marc I. Hoit, Chair
Associate Professor of Civil
Engineering

I certify that I have read this study and that in my opinion it conforms to acceptable standards of scholarly presentation and is fully adequate, in scope and quality, as a dissertation for the degree of Doctor of Philosophy.

Ronald A. Cook, Cochair
Associate Professor of Civil
Engineering

I certify that I have read this study and that in my opinion it conforms to acceptable standards of scholarly presentation and is fully adequate, in scope and quality, as a dissertation for the degree of Doctor of Philosophy.

Fernando Fagundo
Professor of Civil Engineering

I certify that I have read this study and that in my opinion it conforms to acceptable standards of scholarly presentation and is fully adequate, in scope and quality, as a dissertation for the degree of Doctor of Philosophy.

John M Lybas

John Lybas
Associate Professor of Civil
Engineering

I certify that I have read this study and that in my opinion it conforms to acceptable standards of scholarly presentation and is fully adequate, in scope and quality, as a dissertation for the degree of Doctor of Philosophy.

James P. Hobert
Assistant Professor of Statistics

This dissertation was submitted to the Graduate Faculty of the College of Engineering and to the Graduate School and was accepted as partial fulfillment of the requirements for the degree of Doctor of Philosophy.

May, 1997

Winfred M. Phillips
Dean, College of
Engineering

Karen A. Holbrook
Dean, Graduate School

LD
1780
1997 .A228

UNIVERSITY OF FLORIDA
3 1262 08555 0571